

Master Thesis

Humans in the Loop: Model Predictive
Control for Thermal Conditioning of
Buildings using On-line Learning from
Occupant Feedback

Thomas Stesco
October 26th, 2018

Advisors

Dr. Annika Eichler

Prof. Dr. John Lygeros

Abstract

A novel building thermal conditioning model predictive control (MPC) framework is developed to consider human-in-the-loop feedback of thermal preference votes from occupants by updating individualized Bayesian thermal preference models in real-time using on-line learning methods. On-line presence (or occupancy) models are also developed and an aggregation mechanism using an approximated expectation function is proposed to simplify the stage cost function. A toolchain to construct compatible resistance-capacitance building models, run the MPC loop, perform on-line Bayesian learning, and solve the resulting optimization problem is implemented. Finally simulation experiments are performed as a proof of concept using real thermal preference data from the RP-884 database. The framework shows potential in exploiting combined variance in thermal preferences and presence between different occupants to reduce energy consumption and improve overall thermal comfort.

Contents

List of Figures	7
List of Tables	8
1 Introduction	1
1.1 Thermal Comfort Standards	1
1.2 Thermal Conditioning of Buildings	2
1.3 Building Energy Management Systems	4
1.4 Integrating Occupant Behavior	6
1.5 Research Contributions	7
2 Occupant Behavior	10
2.1 Thermal Comfort	11
2.2 Occupancy	13
2.3 Occupant Internal Heat Gains	14
3 Thermal Comfort Prediction	16
3.1 Hierarchical Bayesian Model	17
3.2 Heat Load Function	18
3.3 On-line Bayesian Parameter Estimation	19
3.4 Algorithm Implementation	21
3.5 Simulation Analysis	21
4 Occupancy Prediction	25
4.1 Inhomogeneous Markov Chains	26
4.2 Change Point Detection	26
4.3 Algorithm Implementation	27
4.3.1 Initialization	28
4.3.2 Exponentially Weighted Daily Occupancy Profile	28
4.3.3 RuLSIF Change Point Detection	29
4.3.4 Fitting Markov Transition Probabilities	29
4.4 Simulation Analysis	32
5 Controller Optimization	35
5.1 Discrete MPC formulation	35
5.2 MPC Cost Function	36
5.3 Optimization Framework	40
6 Building Simulation	41
6.1 Resistance Capacitance Building Model	42

6.2	Parameters of Building Model for Simulation Experiments	43
7	Simulation Experiments	45
7.1	Simulation Setup	45
7.2	Simulation Results	46
7.3	Conclusions	50
	Bibliography	51
A	Thermal Comfort Methods	63
A.1	Steady-State Heat Balance	63
A.2	Adaptive Thermal Comfort	63
B	Building Simulation	65
B.1	Building Simulation Software	65
B.2	Whole Building Simulation Software	65
B.3	Building Component Models	66
B.4	Hierarchical Simulation Environments	67
B.5	Discussion of Building Modelling Platforms	68
B.6	Building Material Properties	70
C	Additional Simulation Results	71

List of Figures

1.1	Schematic diagram of implemented building energy management system (BEMS) control loop with human-in-the-loop feedback.	8
2.1	Diagram of extended adaptive thermal heat balance (ATHB) model, figure adapted from [87].	12
3.1	Mean absolute error (MAE) of three thermal preference classes (want warmer, no change, want cooler) for each prediction in sequence from on-line learned model during simulation of building with 15 occupants. Each colored line represents the MAE for an individual occupant model.	23
3.2	On-line learning of thermal preference model for specific occupant from sampling of the true model d) at the simulated thermal states. Each faint colored line represents one particle and the black line the selected maximum likelihood particle. a) the initial prior from other occupant data in the same building, b) the first update given an observation from the occupant, c) the fourteenth such update, and d) the true model that was being sampled from to generate the observations used to update the model.	24
4.1	Input (top) and output of occupancy prediction model (bottom) showing exponentially weighted moving average daily occupancy profile (second from top) and changepoint scoring and detection (third from top).	28
4.2	Occupancy n-step ahead prediction mean absolute error (MAE) for different offset time steps	32
4.3	Occupancy n-step ahead prediction root mean squared error (RMSE) for different offset time steps	33
4.4	Occupancy prediction daily (24 time step) moving average log loss, 12-step offset	33
4.5	Occupancy prediction weekly (168 time step) moving average log loss, 12-step offset	34
5.1	Expected zone thermal preference function (black lines) given the individual occupant preference functions conditional on their occupancy (grey lines). Also showing approximation with exponential functions (red and blue lines) and respective errors (dashed lines).	38
6.1	Building RC model exterior wall component showing boundary conditions and RC elements.	42
6.2	Building RC model exterior wall component showing boundary conditions and RC elements.	44

7.1	Simulation results with disturbances to building controlled with MPC using $l_c = l_w = 10$ with (a) on-line learning, (b) perfect information, and (c) standard comfort temperature (21°C) with schedule based occupancy, all for first zone of three zone building	48
7.2	Pareto front of different model types with varied weighting of thermal preference (comfort). Standard models labeled with occupancy model (scheduled or perfect information) because they do not have a weighting and only track difference from 21°C	49
7.3	Cumulative cost (CHF) of energy and thermal preferences over first 20 days of simulation experiments for $l_c = l_w = 5$ with different thermal preference (TP) and occupancy (O) models.	50
C.1	Simulation results with on-line learned occupancy and thermal preference models for 15 occupants in three zone building, $l_c = l_w = 10$. From top to bottom zone 1, zone 2, and zone 3.	72
C.2	Simulation results with perfect occupancy and thermal preference models for 15 occupants in three zone building, $l_c = l_w = 10$. From top to bottom zone 1, zone 2, and zone 3.	73
C.3	Simulation results with constant 21°C comfort temperature and schedule based occupancy model for 15 occupants in three zone building. From top to bottom zone 1, zone 2, and zone 3.	74
C.4	Simulation results with constant 21°C comfort temperature and perfect occupancy model for 15 occupants in three zone building. From top to bottom zone 1, zone 2, and zone 3.	75

List of Tables

A.1 EN15251 standard categories of acceptable temperature ranges in free-running mode, from [110].	64
B.1 Whole building simulation software packages	66
B.2 List of building component models	67
B.3 List of available simulation environments	69
B.4 Building model thermal properties, material layers listed outer surface to inner surface. Thermal properties from ISO-10456[23].	70

Chapter 1

Introduction

Buildings are heated and cooled to achieve thermal comfort for the occupants inside them. It has long been intuited and now shown with mounting empirical evidence that achieving thermal comfort increases productivity and health [41, 82, 84, 148]. These productivity increases can be due to reduced sick leave or break time in addition to actual increases in the speed with which work can be done [52]. Thermal comfort is therefore crucial in developed regions where people spend well over 90% of their lives indoors [141]. At the same time, buildings consume 20% to 40% of total energy in these developed regions, with approximately half dedicated to thermal conditioning [123]. In cool climates this portion can be even higher, for example in Switzerland from 2000 to 2016 buildings consumed on average 45% of total energy. Space heating alone consumed 34% of total Swiss energy over this 17 year period [47]. The Intergovernmental Panel on Climate Change (IPCC) has also listed building energy reduction as the largest and most cost effective mitigation measure to reduce global atmospheric carbon [98]. For these reasons the thermal conditioning of buildings carries considerable social, economic, and environmental impact. In this chapter an account of existing practices of thermal conditioning and a case for considering individualized thermal comfort to enhance performance is developed.

1.1 Thermal Comfort Standards

The original definition of thermal comfort from the ISO 7730 standard is given as “that condition of mind which expresses satisfaction with the thermal environment” [70]. This definition is based entirely on a subjective individual expectation and experience. It is clear that a large psychological and physiological variance between people exists in their experience of the same thermal environment [176]. The implementation within thermal comfort standards commonly adopted in practice has however been based on an average experienced sensation of large populations. In particular the widely implemented predicted mean vote (PMV) and percentage people dissatisfied (PPD) method developed by Fanger in 1970 [51, 131]. The basis of this method is a regression between a non-linear heat load balance on the human body and the surveyed thermal sensation of individuals under different conditions within a climate controlled chamber. This method then predicts the mean vote of a large population on a thermal comfort scale under steady-state conditions (i.e. after being in the space for some time to reach near thermal equilibrium). The dominant ASHRAE 55 [10] and EN 15251 standards, which were based on the EN ISO 7730 standard, also implement the PMV method by default [32]. This steady-state method is commonly used by practitioners to prescribe a static temperature set-point for a building given design values for typical situations [147]. A critical comparison of existing physics based ther-

mal models of humans is given in [74]. The Fanger heat load balance is proposed for extension within this work because of its success in empirical studies and wide scale implementation as the physical basis of the PMV.

In contrast to the steady-state approach the adaptive method assumes people can adapt to a wide range of thermal environments given sufficient opportunity [131]. It has been only in roughly the last two decades that adaptive methods have gained popularity, and only recently that they have been added as alternative standard methods for naturally ventilated buildings [38, 39]. These methods are implemented in standards as linear regression between outdoor temperature and the indoor set-point temperature from field data of large populations. A key distinction between the steady-state methods being the use of field data of office workers in numerous buildings instead of climate controlled chambers and experiment participants. The two landmark field data sets used in standards being the RP-884 database for the ASHRAE 55-2010 [39] and SCATs database for the EN 15251 [95, 110].

In practice both widely accepted thermal comfort standard implementations are based on regression over a large population which is intended to satisfy a theoretical average occupant. While these implementations are useful for achieving guidelines they are not able to incorporate the variance between individuals and therefore cannot be used to predict the underlying phenomena of individualized sensation or preference [176]. Even extrapolation to averages of different populations (e.g. in different climates, cultures, or building types) has been shown inaccurate [16, 117]. This is not surprising given the goal of the standards as guideline documents and the limitations of data acquisition and analysis at the time the standards were initially developed. However it has been proposed that even typically acceptable thermal and air quality conditions can reduce cognitive performance significantly and thus greater attention is required [160]. There have also been substantial improvements in data acquisition infrastructure with the proliferation of inexpensive sensors in recent years. These factors motivate the development of individual models for thermal conditioning that directly account for the variance between individuals.

1.2 Thermal Conditioning of Buildings

Asserting static temperature bounds invariant to the seasons or outdoor conditions, even if conservative and carefully derived, has long been observed to be “neither necessary nor desirable” [111, 130]. This can lead to frustrating cases of expending energy to reduce thermal comfort. In a recent study of four large Canadian office buildings (comprising 650 thermal zones) the majority of temperature set-point change requests made to building operators were either to increase the temperature set-points during the cooling season or to decrease them during the heating season [57]. In the same study when occupants were given direct control over the thermostat, set-point changes were 24 times more frequent. Interestingly it was also noted that the building operators tended to make larger magnitude set-point changes upon hot and cold complaints than the occupants did.

Giving occupants direct control of thermostat set-points in shared offices is however problematic due to multiple and conflicting temperature preferences. This has been observed in a recent study of a large newly constructed high performance building in Budapest, Hungary [17]. Occupants were able to change the thermostat set-point +/- 3 °C from the default set-points. During a walk-through audit the researchers found 48% of thermal zones were in heating mode and 52% in cooling, with large variance in set-points from 19 to 28 °C. In this extreme case occupants had adversarial feedback with and used increasingly inefficient methods to restore their personal comfort, such as: personal electric heaters, covering air vents, or opening windows during heating

periods. This in part caused both high energy costs and occupant discomfort with 42% of all office workers being unsatisfied with thermal comfort or air quality in the study.

While centrally controlled systems can reduce perceived control of occupants they alleviate many other problems and are in many cases preferred by occupants. For example in a field study of 313 occupants within cellular (single person) and open-plan offices it was observed that 80% of people in open plan offices preferred a centrally operated thermal conditioning, as opposed to only 10% in cellular offices [142]. In interviews the main reason communicated by occupants was that setting a temperature that satisfies everyone is difficult, causing arguments and social tension. Without additional colleagues in the same thermal zone most occupants would then prefer to have control. A minority of occupants reported that they would prefer not to think about the temperature in any case and simply focus on their work. Although, every occupant interviewed expressed a desire to have some control if they were uncomfortable. Similar results are found in another survey study from 1160 occupants on university campuses in three regions of Italy [41]. They find that control over the indoor environment is over 80% of the time shared within occupants in the same zone. The same survey indicates that thermostats are the control action occupants find most challenging (least ease and least knowledge) largely because of required discussions with other occupants to make a change. The authors also note a general dissatisfaction by occupants with the shared control of thermostat settings. Additionally observed in their study is the correlation between thermal comfort and both workplace satisfaction and self-assessed productivity.

From a strictly economic perspective (neglecting any social or other benefits) it is understood that the personnel costs in an office are over two orders of magnitude higher than energy costs and the thermal comfort of occupants is prioritized over energy savings [38, 160]. Given current estimates of the effect of thermal comfort on productivity this is completely justified. For example a recent longitudinal within-subjects study of the effects of environmental stressors (thermal discomfort, lighting discomfort, and noise) on office worker productivity finds a productivity decrease in the range of 2.4 to 14.6% given one, two, or three environmental stressors [82]. The authors note a range consistent with the order of magnitude range typically found in literature for one or two stressors of 0.5% to 5%. The main finding of the study is however that the combined effect of multiple environmental stressors is most detrimental to office productivity (i.e. if an occupant is both too cold and annoyed by noise they become much more distracted). Potentially the true productivity benefit of achieving thermal comfort for a given individual is from avoiding situations with multiple environmental stressors, not simply avoiding the single stressor of thermal discomfort independently. Furthermore while thermal discomfort on its own does not have a large average decrease in their study, there is a large variance between individuals.

This change in the effect between individuals is also seen in a study measuring the effect of temperature on office worker productivity and correlating it also with electroencephalography (EEG) brain signal measurements [107]. The authors have a small population of seven participants, each performing an addition task and a typing task at 22.2 °C and at 30 °C. Notably the performance between participants and tasks shows completely different correlations with temperature, even in different directions. As mentioned in a recent review [131], the different methods used to assess productivity and different field environments requires more attention before drawing conclusions on the effect of thermal comfort on work place productivity for whole populations. It is however quite clear that the high inter-personal variance observed within many studies indicates a complex and individual relationship.

1.3 Building Energy Management Systems

The complexity of building energy management systems (BEMS or sometimes BMS) has been growing steadily in recent decades as new energy distribution, storage, and generation technologies are being deployed. Generally a BEMS can be considered a high-level automation layer providing holistic system logic above the field layer that performs equipment level sensory measurements and actuation in the building with relays, valves, or by setting references (set-points) for local equipment controllers [108]. In pursuit of greater efficiency additional complexity also comes from sharing energy generation, storage, and load between multiple buildings in an energy hub [33, 35, 94]. MPC methods have been extensively researched for BEMS, including control of HVAC, lighting, and appliances, as well as energy storage and generation [1, 108, 143, 150]. Additional techniques such as robust MPC [34, 149] and stochastic MPC [121] have also been shown capable of accounting for uncertainty in predictive models.

Shaikh et al. [143] find that MPC is the most popular control method with researchers as it can deal directly with constraints on multi-output control actuation and exploit knowledge of both system dynamics and disturbances. Other control methods such as fuzzy logic controllers and agent systems are also mentioned in [143]. In [1] the advantages of MPC are explained in light of their applications to HVAC. The authors compare MPC with other hard control methods, as well as other classes of control methods, such as classical control (ON/OFF and PID), soft control (fuzzy logic and neural networks). They conclude from both simulation and field experimental results that MPC offers significant advantages in handling varied or slow dynamics with delays, constraints of physical actuation, and time-varying exogenous disturbances. MPC has also been proposed for the integration of occupants, individual buildings, and energy hubs to the energy grid at large to yield energy savings [42, 78, 102].

MPC has been demonstrated to exploit predictive information about system disturbances such as weather [116], energy price [101, 128], and building occupancy [54, 115]. Disturbances in the dynamic sense being any exogenous input to the system that cannot be influenced by the control actuation. Lighting and appliance control generally cannot make use of anything but extremely short-term predictive information as the demand cannot be stored within the building as thermal energy can be. Therefore the majority of building predictive control research focuses on HVAC, and in particular buildings with longer thermal response times [108]. Occupancy predictions usage in building MPC has been field tested in [2] and [122] where 30% and 7-52% energy savings are reported as compared to scheduled cooling operations respectively. It has been a result of some studies in [115] and [54] that long-term predictive occupancy information does not significantly improve controller energy savings. These results could be due to modeling of all occupants with a single model and not considering variance in the thermal preferences of occupants in these studies. Though in all simulation and field studies mentioned using at least real-time occupancy detection does yield significant savings.

Sturzenegger et al. [146] presents a review of MPC building control field experiments and a cost benefit analysis which indicates that building MPC is near commercial viability. They determine that while technical performance and energy savings have been proven, engineering costs related to the model and software development are still prohibitive. This is because in many cases the sensor hardware exists already in low level control loops so adding the high level MPC may only require additional software interfaces over a network. The model development cost has been estimated at 75% for such a project [129]. Towards reducing the development effort Sturzenegger et al. propose three strategies for further work: 1) a control framework to create and solve the optimization problem and interface with low level controllers, 2) a Model generation frame work to aide in development of building models that are both accurate and suitable for optimization,

and 3) training of engineers and technicians.

The authors in [129] note that the typical linear system models used for thermal dynamics need extension to equipment dynamics, which may require control actuation for example by setting a flow rate instead of a heat flux. This combined equipment model is then likely to be non-linear if the heating system is not electric resistance but something more complex such as a heat pump coupled with a radiator or fan coil unit. Linearization of non-linear dynamics in the region of operation is a potential solution, however non-linear optimization methods are also possible. As result more research into non-linear systems which may have non-convex optimization problems is required. In a similar fashion research into the formulation of the objective function is required such that the goal of globally optimal control is meaningful. Despite these open areas of research the authors in [129] propose MPC as a strong candidate to supersede current rule-based building control practices.

Killian and Kozek in [78] ask if there is any “silver bullet” for developing the building dynamics model. They explore the model-structures of white-box (physics-based), grey-box (parameter estimation) and black-box (data driven). White-box models are common in engineering analysis and use domain knowledge combined with underlying physics to impose the structure and parameters of the system model. While appealing in theoretical study these model can be costly to deploy in real world systems due to the reliance on domain knowledge of the specific system and manual calibration. Black-box methods, also called machine learning methods, instead use data from the real system to fit a (typically non-linear) function for the combined structure and parameters of the model. This can reduce the model complexity and cost however comes with the bias-variance trade-off (or over-fitting and under-fitting problem), which is the trade-off between a complex (high variance) and approximate (high bias) model [72]. The complex model will contain additional structure for variance in the training dataset that may be unrelated to the model output. Alternatively, the approximate model will be biased towards some structures in the dataset, neglecting others that may be relevant to the model output. This issue is crucial because buildings will likely have limited excitation during normal operating conditions [146]. Finally there is also reduced interpretability of the model where the parameters and structure no longer have a physical meaning.

Grey-box methods are hybrids in that the structure of the model in whole or in part can be taken from domain knowledge of the system. The parameters of the model can then be estimated using system identification techniques or optimization. This method allows for the exploitation of domain knowledge of the specific system where existing and data driven fitting of otherwise difficult to model parts. The authors in [78] note the ability to directly encode structure for the building thermal zones as a key benefit for grey-box building models. They also mention that expert engagement should be part of building MPC projects. Including this domain knowledge where possible is a good way to improve both accuracy and interpretability of the building model. For these reasons grey-box methods are chosen for development of the occupant predictive models as discussed in later sections.

Each extension of the MPC optimization problem with information about disturbances can provide more accurate predictions for the objective function can improve overall system performance. For example considering time varying energy prices (hourly, time of use, and real-time) yielded up to 42% lower electricity costs in simulation [101]. Many building MPC studies reviewed in [103] consider occupancy comfort in the objective cost, however it is typically only a post-calculated variable from the Fanger PMV method, deviation from a constant temperature set-point [172], or simply being within static upper and lower temperature bounds. This treatment of thermal comfort in MPC, and building operations more broadly, is in need of incorporating thermal comfort as experienced by occupants, and ideally through direct occupant feedback.

1.4 Integrating Occupant Behavior

The recently concluded five year International Energy Agency (IEA) Energy in Buildings and Communities (EBC) Annex 66 Definition and Simulation of Occupant Behavior in Buildings research programme final report underscores occupant behaviour as a significant factor to both energy use and occupant comfort [169, 170]. The authors also indicate that data collection is fundamental to modelling behavior because of the diversity in both occupants and building contexts, which includes psychological and sociological factors as well as physical. Therefore detailed physics-based approaches alone do not always outperform simple deterministic models if important factors are neglected or measured inaccurately. For this reason they propose that grey-box methods (also called inverse modelling, machine learning, or system identification) should be considered for developing scalable models for different buildings and occupants. The Annex 66 authors further propose model predictive control (MPC) for integrating occupant behavior into BEMS to achieve higher levels of comfort, operational cost reductions, and energy savings.

In a recent international survey of 274 building performance simulation practitioners the majority of participants agreed that occupants use more energy in reality than what they normally assume in simulation models [113]. Additionally, 75% agreed that simulation tools need more occupancy features. Occupancy behavior modeling is a key issue in current literature, with modeling of average occupants and disregarding their individual variance named as a source for the so-called performance gap [60]. Many other operational issues linked to occupants are addressed in [76], such as: lack of occupancy monitoring, lack of occupant knowledge of energy efficiency and building operation, and mismatch between idealized assumptions and actual occupant behavior patterns.

It can be seen that the impact of occupant interaction and feedback during building operations is not well described in models used for design of buildings and design of control systems. If for example an occupant prefers to be warmer in the summer, and decides to open the window to a warmer outdoor temperature (if perhaps because they are not able to adjust the thermostat), a static set-point controller will increase its effort to cool the room and waste more energy. This creates adversarial feedback between the occupant and the controller where the occupant seeks to override the controller but cannot, both infuriating the occupants and causing energy inefficient behavior [56, 84]. The psychological component of occupant feedback with regards to perceived control should not be neglected. For this reason it is a common practice to install placebo thermostats that are not connected to anything solely to improve the occupants perceived control [56].

In a survey of 248 low income households on energy saving intentions perceived control is one of the most important factors [27]. It is intuitive that those who feel they cannot control their building energy consumption having diminished intention to do so. Their findings also show cost as the most frequently sited reason for energy saving, and comfort for energy usage as one may expect. One potential method to reduce occupant energy usage is through eco-feedback systems which encourage energy saving behavior through positive feedback or incentives. [118] reviews the current state of eco-feedback systems that guided behavior change to energy conservation, concluding that their longterm efficacy is still an open question and possible conflicts between energy goals of the system and comfort of occupants may erode benefits. They posit the interesting question: How can the building control system for energy and comfort interact with and adapt to occupant preferences? Based on review of existing research in [174], accounting for actual occupancy behavior could yield energy savings in the range of 5% to 30% for commercial buildings and 10% to 25% for residential buildings. MPC has the potential to achieve these

energy savings through multi-objective optimization of cost, energy, and comfort while handling system constraints while providing a transparent feedback interface for occupants. Interpretable integration of occupant feedback could additionally improve perceived control and incentivize energy saving behavior which could further increase energy savings.

Eichler et al. in [45] proposes human-in-the-loop feedback through a game between occupant agents and the BEMS. The BEMS is able to give occupants a small payment to deviate from fixed temperature bounds in order to save energy costs, and the occupant agents (or potentially occupant directly if feedback timing issues could be resolved) can accept this payment or reject it. A generalized Nash equilibrium problem is then formulated to minimize system energy costs and temperature deviations (in degrees per hour). This feedback mechanism aggregates occupant preferences for different temperatures (as reported by the agents) at the thermal zone level and uses distributed optimization to solve for the equilibrium in a receding horizon. They additionally note that the occupant agent models could be learned so that occupants do not need to give frequent feedback. The method allows for black box modeling of the occupant agents so a wide range of techniques are available for implementation.

1.5 Research Contributions

The concept of a *thermobile*, which changes the temperature to adapt to the current thermal environment and demands (as opposed to a *thermostat*) has been written about in various forms for some time by thermal comfort researchers [111]. As inspired by Eichler et al. [45], this work proposes the use of occupant feedback, processed into continuously updated machine learning models (on-line learning), as a component of the feedback control loop. In this way the controller is continuously learning its cost function based on feedback from occupants within the building system it controls. This could also be viewed as the function generating comfort temperature bounds being formulated as a high-latency interactive feedback loop with the occupant directly. This concept is implemented using MPC because of its well documented success in BEMS controls (as previously discussed), and especially in exploiting a wide range of predictive models in a reliable, interpretable, and optimal way. The implemented control loop investigated in simulation is shown schematically in Figure 1.1 below.

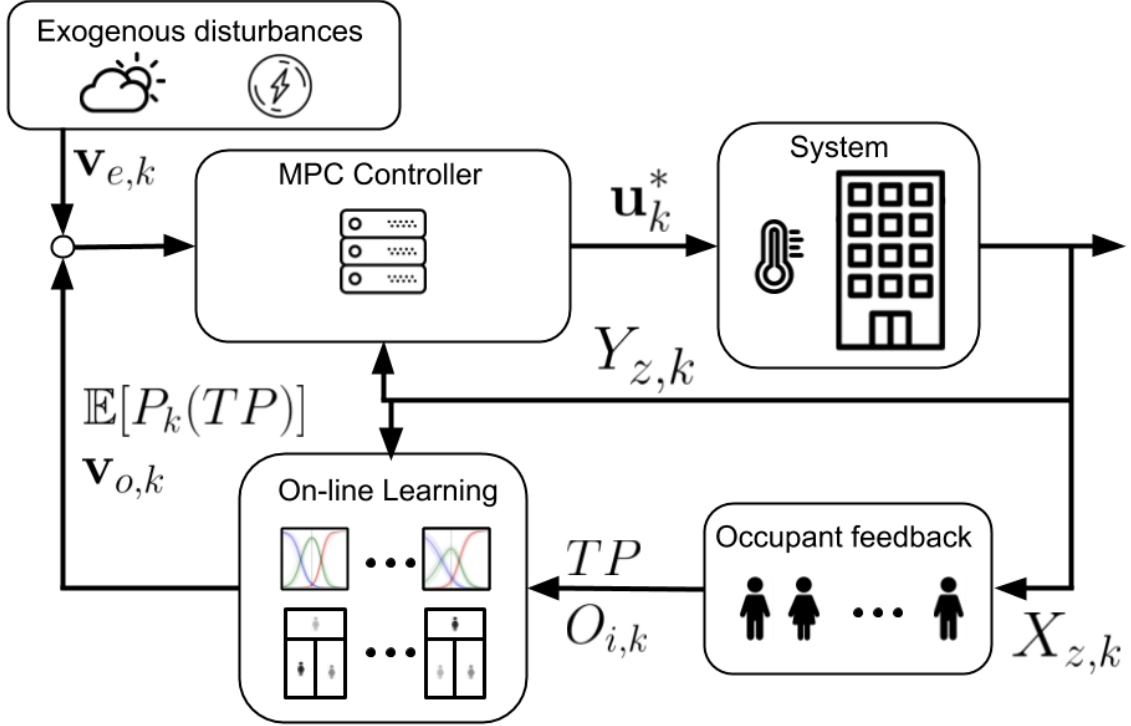


Figure 1.1: Schematic diagram of implemented building energy management system (BEMS) control loop with human-in-the-loop feedback.

The thermal state is denoted by $X_{z,k}$ for zone z at time k (chosen to denote discrete time steps), this state includes the dry bulb temperature, humidity, and running mean outdoor temperature. Occupant feedback is given in the form of thermal preferences, TP , which can be one of either *want warmer*, *want no change*, or *want cooler* for any time step. The benefits of this feedback stemming from unambiguity and simplicity are further explained in section 2.1.

The thermal preference data is directly given by occupants and could be collected through a simple smart phone app. The occupant presence (occupancy) $O_{i,k}$ of each occupant i could be measured with minimal sensing equipment, for example as in Konis et al. [81] using radio data from occupant smart phones. The next step in the control loop is the on-line learning of an individualized predictive model of thermal preference and occupancy for each occupant based on their feedback and the measured thermal state $Y_{z,k}$. On-line learning model here refers to a model that is updated within the control loop by each new observed data point. For the thermal preference model this feedback is simply the preference vote of the occupants. In the occupancy model feedback is the passively measured presence of each occupant. To simplify the experiments the thermal state measurements are assumed perfectly accurate, though additional consideration of measurement error through state estimation could be incorporated. The output is a probabilistic function for each possible thermal preference conditional on the thermal state, for example $P(TP = \text{warmer} \parallel X_{z,k})$. This function is also conditional on the occupancy, which itself is only conditional on time. The expected value of preferences of each type is used to aggregate the individual predictive models at the thermal zone level as detailed in Section 5.2. This expectation function, $E[P_k(TP)]$, is then part of the stage cost function of the resulting discrete finite time MPC optimization problem. Also considered are occupancy related disturbances $v_{o,k}$ such as metabolic heat gains ($v_{o,k}$ here refers to the occupancy as opposed to exogenous disturbances denoted by $v_{e,k}$).

The MPC minimizes energy consumption and the expectation of occupants preferring to be

warmer or cooler (see Section 5.2). This optimization output is the optimal control sequence \mathbf{u}_k^* , the first input of which is applied to the building system then the control loop repeated in typical MPC fashion. The building system is emulated with the same thermal dynamics as the MPC model to avoid modeling errors, the reduction of which is not the focus of this work. The research contributions of this work are in developing this probabilistic multi-objective control loop, outlining an upper bound on system performance with perfect information, and finally by characterizing how on-line learning models approach ground truth in simulation.

Our approach is similar in spirit to the multi-agent approach in [171], however we perform centralized optimization at the building level for each thermal zone with predictive models of thermal preferences and occupancy for a receding horizon MPC approach. The use of these on-line learned models has been proposed as a future research area in [143] and [1] to decrease feedback latency with grey-box models and allow for direct use in a feedback loop. The on-line learning of these individual preference and occupancy models is integrated in the control loop. Similar also to the aggregation of predictive models for different loads at the building level with energy hubs in [35], this work proposes aggregation of predictive models of different occupants within the same thermal zone. The combined variance of the preferences of each occupant and their occupancy patterns may provide sufficient deviation from a static optimal temperature to demonstrate the flexibility of the MPC system and achieve both energy savings and improved comfort. This approach is also similar to the human-in-the-loop feedback proposed by Eichler et al. [45] but differs from the distributed optimization method by 1) considering only preference as the observed variable instead of temperatures and 2) by directly learning each individual occupant’s thermal preference functions and sharing them with the centralized optimization through cumulative expectation functions at the thermal zone level.

It should also be noted that formulation of thermal comfort as an individualized probabilistic function has benefits in the design stage of buildings. Explicitly representing the provisions a building has for occupants to adapt and attain personal comfort can offer greater flexibility to building designers and improved performance simulation if adopted in standard practices [111]. This could help shift to a descriptive rather than prescriptive implementation in standards. The question of interest is then how implemented on-line learning predictive models can track the theoretical limits of MPC with perfect predictive models. In this work both an on-line thermal comfort prediction and occupancy prediction algorithm are implemented based on recent methods proposed in literature and simulation experiments of a small multi-occupant office are conducted to answer this question.

Chapter 2

Occupant Behavior

The theory of occupant behavior from a building energy performance perspective has been widely addressed within the recent IEA-EBC Annex 66 project [169]. The bulk of the development effort within the annex 66 project is towards simulation of occupants, i.e. generating time-series occupant data from a stochastic model that has similar statistics as measured data sets. The purpose of this is largely for more accurate building performance simulation (i.e. to estimate how a given building performs in possible scenarios) to inform decision making during building design. One such result for simulation being a co-simulation tool called the obFMU [65, 67], a review of which can be found in [31]. Each occupant behavior can be measured and simulated to have similar statistics as measured longitudinal data sets, for example with the obFMU or methods presented in [60]. The researchers within this project show that the occupant behaviors effecting energy usage are:

- Leaving and entering thermal zones.
- Adjustment of thermostats set-points.
- Switching lights on and off.
- Switching appliances or equipment on and off.
- Opening and closing of windows.
- Opening and closing of window shading.

The interdisciplinary work within the Annex 66 shows new research directions and advances toward better consideration of occupant behavior [64, 68]. However, these methods are geared toward building performance simulation and additional work is required to develop predictive models for optimization within an MPC framework. Predictive models are developed to accurately predict a specific time-series with minimal error compared to ground truth measured data. Predictive models can then be used for operations in an MPC framework in three ways, 1) using receding horizon predictions for disturbances, 2) directly using a predictive model in the cost function, and 3) using a predictive model for the state dynamics. Both 1) and 2) are investigated through individualized predictive models of occupants, which are the focus of this work. When considering use within the cost function or state dynamics there must be additional constraints on models, such as being twice differentiable or having no time dependent control flows. Crucially, these individualized occupant models consider both inter-occupant and intra-occupant variance which can be quite large [59].

Each behavior can be seen as an adaptive measure taken by occupants to restore some type of

comfort (thermal, visual, or aural). Thermostat adjustment is related solely to thermal comfort, though it has a complex social aspect when considering spaces shared by multiple occupants as previously discussed. Window opening/closing and shading adjustment are complex because they could be due to any type of comfort. For example a window could be opened to make the space more visually appealing and then closed due to unwanted noise from outside. In particular lighting levels and glare are important for shading adjustment [56]. Existing predictive models for window opening/closing and shading adjustment are not highly accurate as assessed by Dong et al. in [43]. These and other predictive models, for example of door opening, require additional development before they would be beneficial to building MPC implementation when considering the added complexity. Lighting and appliance usage (plug-loads) can contribute significant heat to the space, but with the introduction of LED lighting and energy efficient appliances their contribution is increasingly reduced. Lighting and plug load models are also extremely dependent on occupancy and there is no pre-operation or load-shifting opportunities for lighting and most appliances (i.e. an occupant only wants the lighting or appliance to be on when they want to use it and not before or after). This makes predictive models of lighting and plug-loads less helpful for MPC as underlying occupancy models, however combining these models could increase accuracy of electrical demand predictions for grid-scale optimization.

Occupant presence remains the core of the occupant behavior, in that occupants can only exhibit physical behavior if they are physically present, yet Dong et al. [43] also note that models for different behaviors are purpose built and typically not interconnected. For these reasons this work focuses on implementing an individualized on-line learning predictive occupant presence model which can be extended to predict more detailed behavior conditional on occupant presence. Occupant thermal preference, as observed proxy for thermal comfort, is then implemented in this way. A brief treatment of the theoretical basis for observed behaviors of thermal comfort and occupancy are given in the following sections. In the following chapters the predictive model implementations are detailed.

2.1 Thermal Comfort

Recent reviews of thermal comfort point to the increasing support of the adaptive thermal comfort theory [38, 104, 131]. It is however important to note that adaptive comfort approach is not applicable in buildings that provide no way for occupants to adapt to different thermal states. The reasons for this can be social factors such as uniform or dress policies as well as not having physical means such as operable windows. These conditions are similar to the controlled experiments performed for derivation of the steady state methods, therefore making them more applicable. However air-conditioned buildings can provide adaptive measures just as free-running (naturally ventilated) buildings [104]. Observed adaptive measures are evaluated in [104] based on availability and use. A framework for evaluating observed adaptive measures based on effectiveness, ease of use, and economy is proposed in [104] for understanding how occupants evaluate different adaptive behavior opportunities and plan their actions. This becomes exceedingly complex if cultural norms and past personal experience are considered. Another more general ontological framework considering the drivers, needs, actions, and systems (DNAS) occupants utilize to achieve thermal comfort is proposed in [66].

Halawa and van Hoof mention that the push to investigate the adaptive methods has however led to not considering important findings of the heat balance methods [58]. The adaptive thermal heat balance (ATHB) framework proposed by Schweicker et al. in [138] merges the steady-state heat balance and adaptive methods. The core of this method is the same heat load balance on the occupant as the PMV, but including adaptive regression coefficients accounting for the effect

of the outdoor temperature on clothing and metabolic rate. We propose a further extension to this framework by estimating additional parameters of radiant temperature and air velocity to further reduce the data acquisition burden, leaving only the easiest two of the six typical factors of the typical steady state heat balance to be measured, plus measuring additionally the outdoor temperature which is also inexpensive. This is similar to the successful work by Burrati et al. [24] in using air temperature and relative humidity to estimate the PMV. A schematic showing these observed and estimated variables is shown in Figure 2.1 below.

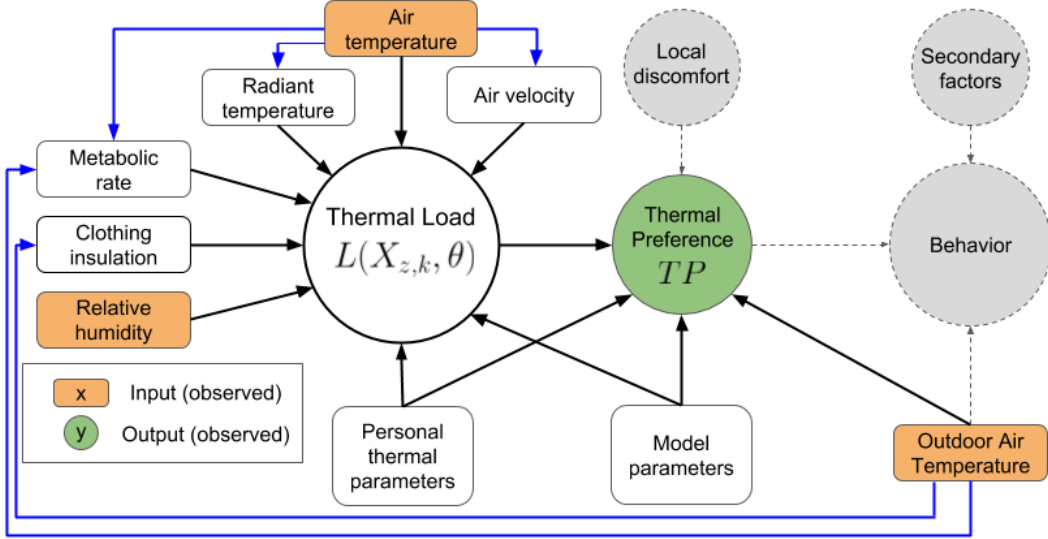


Figure 2.1: Diagram of extended adaptive thermal heat balance (ATHB) model, figure adapted from [87].

The heat load balance yields the thermal load, $L(X_{z,k}, \theta)$, which is a function of the thermal state $X_{z,k}$ and the regression parameters θ . This heat load has a physical interpretation as being the amount of heat that is being transferred (in Watts) to or from the occupant to the thermal environment via convection and radiation. Conduction is negligible in typical indoor settings. Thermal preferences, TP , of either: *want warmer*, *want no change*, or *want cooler* are the observed variable for thermal comfort used in this work. This feedback is typically referred to as the McIntyre index [96] and has been used similarly in the thermal preference prediction method developed by Lee et al. [87]. Kim et al. [79] note that thermal sensation, thermal acceptability, thermal preference, and thermal satisfaction are possible thermal comfort feedback variables, with thermal preference being the closest to measuring what the ideal conditions are, and therefore best suited to HVAC control. There is growing consensus that thermal comfort scales and thermal sensation votes are inadequate in predicting or characterizing thermal comfort [140]. This is largely due to the fact they were intended to represent averages of large populations not individual occupants [124]. There are additional issues with interpretation of common thermal comfort indices for continuous occupant feedback. For example the thermal sensation vote (TSV) or seven point ASHRAE comfort scale (3 being *cold*, 0 being *neutral*, and 3 being *hot*), which is used for the PMV, does not mean the same thing to different people, especially in different languages, climates, or cultures. The implicit assumption in this scale is that all occupants want to feel thermally neutral (vote of 0) which has been proven invalid. In a survey presented by Humphreys et al. [69] 57% of respondents preferred a sensation other than *neutral* with preferred sensations ranging from *cool* to *hot*. For these reasons thermal preference is used as the direct feedback mechanism from each occupant on the thermal preference scale or MCI to avoid ambiguity.

It should also be noted that this model does not take into account the localized effects such as

drafts (which could not be accurately measured by an inexpensive sensor) or other psychological phenomena such as visual satisfaction (e.g. due to lighting or colors). The actual occupant behavior (i.e. detailed information of what activity the occupant is doing within the space) is also not considered within this model, aside from expression of thermal preferences and physical presence. It is assumed that the occupants have unknown personal goals independent of the thermal state, therefore unobserved and unmodeled secondary factors dominate their unobserved behavior. Alternatively, detailed physics based thermal comfort models for transient and asymmetrical environments (e.g. the UC Berkeley model) rely on computational fluid dynamics (CFD) simulation for non-uniform air movement which greatly increase complexity and makes implementation intractable for use within an optimization problem [28, 32]. Another limitation of these detailed models is that they are not combined with thermoregulation and behavioral models. For these reasons the extended ATHB model is used for further development and simulation experiments.

Rupp et al. mention that personalized conditioning represents “probably the best ways to increase user acceptability with the thermal environment” [131]. This is because setting a single thermal state for multiple occupants has the inherent limitations of not being able to satisfy any one occupant fully (unless by chance they happen to prefer exactly the thermal state that least upsets all other occupants). Of course the reality is that no thermal zone is completely homogeneous, so exploiting this within a personalized conditioning framework could create heterogeneous thermal micro-zones around each occupant to achieve greatest thermal comfort. This is important when considering personal fans, or convective cooling with supply air, which can help achieve comfort when the cooling set-point is increased. A review of personal comfort field studies in [152] shows energy savings from cooling set point increases in the range of 4-51% when the cooling set-point is increased by 2.5-6 °C. Similarly, personal radiant heating has shown promising results in allowing heating set-point decreases, though more testing is required to separate its effect from other variables. Interestingly, this energy savings is from simply increasing the dead-band range and not considering predictive controls, so further energy savings and comfort improvements could be realized doing so.

The on-line individualized comfort models developed within this work are in spirit to the framework proposed by Kim et al. for continuous learning of personalized comfort models [79]. Kim et al. further investigates the use of a personal comfort system implemented in a heated chair that occupants can control with their thermal preference responses and a personal comfort is learned [80]. One potential issue with these personal comfort models is that the size of the data set available for each person is limited by their feedback frequency and may be small. Aggregating data between occupants or using this as prior data could help alleviate this problem. The authors also mention that batch learning using all available data is computationally intensive and makes continuously updating the models difficult. For this they recommend on-line learning methods which are investigated within this work. Further work into personal comfort systems through modeling and actuation appears to be an emerging research area with high potential for improving comfort and energy savings.

2.2 Occupancy

It is tautological that an occupant can only exhibit behavior or preferences if they are physically present in a building zone. For this reason occupancy models are considered the core of any holistic occupant behaviour model [25]. Generally there are two types of occupancy prediction models: presence and occupancy level (or simply occupancy). Presence refers to if there is at least one person in the zone, and occupancy level refers to the number of occupants within the

zone. In the case of individualized prediction models the occupancy presence and level of a single occupant are equivalent. Models developed for either purpose are related and often similar but some approaches are more suited to one or the other. Occupancy is typically considered dependent on only time and current occupancy (often using the Markov property). Often it is assumed that occupancy has a diurnal and weekly cycle. Additional information from specific occupants, such as their calendar appointments, could also be useful for improving individualized models though this raises privacy concerns. Some methods also target simulation rather than prediction, for example the queuing method in [73] with adaptive breakpoint selection seeks to recreate key average statistics of the occupancy level in simulation and thus do not use the current occupancy state as an input.

In a recent review Dong et al. show that occupancy models have applications in: energy performance analysis, architectural design analysis, safety design analysis, and building operation (including BEMS) [43]. Dong et al. also score the popular methods for applications in building operation, including Markov process, random sampling, agent-base, and machine learning methods. Markov process methods are the most widely implemented with the lowest model complexity and data requirement. Additionally they have roughly the same accuracy as higher complexity models making them attractive for implementation. Dong et al. [43] conclude that issues with validation and scalability are holding back adoption of predictive models into practice. By this they mean that a specific model cannot be manually developed and validated by experts for each BEMS economically. This outcome means machine learning methods are increasingly important for achieving valid models for each building in a scalable way. Though machine learning methods have only recently been investigated and are not widely implemented. Another barrier to validation is lack of standard data sets and data availability. Current field data sets are typically short in duration or have small sample sizes, they may also use different ground truth measurement technologies.

Occupancy detection has recently seen improvements in sensing technologies, such as deep learning video feed occupant counting and passive radio-based techniques using mobile phones (WiFi, Bluetooth, GPS, etc). These are in addition to the commonly deployed method of passive infrared (PIR) motion sensing [154]. From these sensing developments Wang et al. [157] present several state of the art real-time occupant spatial tracking methods and their own k-Nearest-Neighbors based classification algorithm to spatially resolve an occupancy distribution within a specific building zone using measurements on a Bluetooth Low Energy (BLE) network of occupant mobile phones and a unique media access control address (MAC address) as an identifier. From this work it can be seen that high resolution real time individualized occupancy data is attainable with a low cost sensing network and without the privacy concerns of image based sensing. These breakthroughs in economical individualized occupancy sensing make the use of individualized occupancy models possible in practice once a scalable model and sensing framework can be validated.

2.3 Occupant Internal Heat Gains

The heat given off by each occupant due to their metabolism can be quite large in densely occupied zones. Ahmed et al. [3] gives a figure for office buildings of 118 W per person from field data, which is broken down into 44.1 W convective heat 38.7 W radiant heat 25.9 W latent heat and 9.7 W from sweating. This is close to the standard values for office buildings reached by multiplying a typical metabolic rate of 1.2 (58.15 W/m²) by the average Dubois body surface area of 1.80 m²) to get 125 W/person. Considering just the sensible heat in our building model gives an average value of approximately 83 W/person. This constant value can be used as a

coefficient to the occupancy for each occupant because the contribution to the zone heating is only large when many occupants are in a zone and thus the average accuracy is more important. The value could in theory be modelled and estimated for each occupant individually in a similar way to the on-line methods for estimating occupancy or thermal preference. The uncertainty would however be large due to uncertainty in activity and the relative impact would be low, i.e. a difference on the order of 100 W in heat gains for an office thermal zone with several occupants. This model may be useful in more advanced applications such as diagnosing faults in the heating system, but an implementation would likely be difficult and should only be attempted after reducing uncertainty in more impactful areas, such as the building construction. Consideration of the occupant internal gains in this work is largely to demonstrate a predictive model of a disturbance that is directly interlinked to the individual on-line occupancy models, in this case with a simple constant scalar of 83 W/person.

Chapter 3

Thermal Comfort Prediction

The predictive thermal comfort models surveyed in [48] typically predict based on the PMV or a modified version of the PMV (e.g. adaptive PMV [36] and extended Predicted Mean Vote [50]). To avoid the issues mentioned in Section 2.1 thermal comfort in this work is considered through thermal preference and in a probabilistic sense. In particular the probability of an occupant having a thermal preference (TP) to be warmer, $P(TP = \text{warmer})$, or cooler $P(TP = \text{cooler})$. This is taken to be a function of thermal state $X_{z,k}$ in some zone z at some time step k . The goal of this prediction is to add on-line estimates of $P(TP = \text{warmer} \parallel X_{z,k})$ and $P(TP = \text{cooler} \parallel X_{z,k})$ into the objective cost function of the MPC controller as discussed in Section 5.2. The benefit being increased accuracy in approximating the relative cost of a given thermal state to the comfort of the occupants within a given building zone for all given time steps.

The on-line learning problem is quite different from conventional off-line parameter estimation (also called machine learning) in that both inference of the model and forward prediction run continuously within a feedback loop. Newly observed data is used to update the model in real-time for the prediction at the next time step. The algorithm developed within this section is for an on-line implementation which is proposed to improve feedback latency compared to off-line models which would need to be retrained (for example with the neural network models mentioned in [48]) as part of a separate process running at a much lower frequency than the controller. The other benefit of on-line models is continuous learning in constant time and constant (or-near constant) memory and storage. Again as compared to off-line models which (in most cases) require the full history of observations to be stored and retrained upon at each iteration. The use of a Bayesian model is desirable here because it allows for explicitly 1) encoding a specific model structure from theoretical understanding of the problem, 2) exploiting model parameters prior distributions from existing experimental data, and 3) updating of the model parameters when new observations are made. This is an intuitive way to incrementally improve the accuracy of the predicted posterior distribution of the model as more measurements are made, and in our case as more occupant feedback is given. Also called Bayesian inverse modelling (for modeling the model parameters given the observed output), this follows directly from Bayes theorem where given observed data Y , model M , and parameters Θ

$$P(\Theta \parallel Y, M) = \frac{P(Y \parallel \Theta, M)P(\Theta \parallel M)}{P(Y \parallel M)} \quad (3.1)$$

When considering Bayesian inference methods for approximating otherwise intractable probability distributions there are generally considered to be two families of methods, variational inference and Markov chain Monte Carlo (MCMC). Variational inference is an optimization

based approach that is well suited for large data sets [20]. MCMC on the other hand is better suited for small data sets and has been a foundational numerical tool in statistics since the work of Metropolis et al. [97] and the famous Metropolis-Hastings algorithm [61, 62]. In our case the data sets are actual human thermal preference votes which will always be small for any given individual occupant, on the order of 100 to 1000 votes (assuming on average 1 to 5 votes per week and a conservative lifetime of 20 years). In reality a lower number of thermal votes per occupant can be expected because as the system improves each occupant would be less incentivized to provide feedback and correct the model. Due to the limited data for a specific occupant leveraging prior information is required to generate accurate individual models. Collective learning approaches as in [63] show potential but an on-line implementation does not appear practical due to increased model updating burden. A method to cross-update occupant models based on-line feedback from other occupants is a promising area of future work. Here the construction of the starting prior distribution for each occupant model is simply considered from pre-existing data from the same building.

3.1 Hierarchical Bayesian Model

Hierarchical Bayesian models are prevalent in learning with small data, for example in recommender systems [175]. In previous work (Semester Arbeit) it has been shown that hierarchical Bayesian models are promising methods for learning theoretically motivated thermal preference models for existing data sets of specific occupants. This was done by extending the fully Bayesian approach proposed by Lee et al. [87] for inferring the thermal preference of an individual using as a combination of several common cluster models. This method uses a Linear Discriminant Analysis (LDA) or multinomial logistic regression on a modified PMV occupant heat balance. They add underlying additional parameters to the PMV heat balance (see Appendix A.1) for inter-personal physiological and psychological differences. The LDA then estimates the mutually exclusive probabilities of the occupant having each possible thermal preference (TP). The TP being a categorical dependent variable y , and the heat load $L(X_{z,k}, \boldsymbol{\theta})$ being the class parameter, where $X_{z,k}$ is the observed independent variables (thermal state), $\boldsymbol{\theta}$ are the heat balance parameters, while μ and σ are model parameters for classification, representing each class (TP) mean heat load on the occupant and standard deviation respectively. The LDA can then be rewritten as

$$P(y_i = TP | X_{z,k}, \boldsymbol{\theta}, \boldsymbol{\mu}, \sigma) = \frac{\exp\left(-\frac{1}{2\sigma^2} (L(X_{z,k}, \boldsymbol{\theta}) - \mu_{TP})^2\right)}{\sum_{c=1}^3 \exp\left(-\frac{1}{2\sigma^2} (L(X_{z,k}, \boldsymbol{\theta}) - \mu_c)^2\right)} \quad (3.2)$$

It should be noted that the underlying PMV heat load function is non-linear which complicates the implementation. The hierarchical Bayesian model can then be conditioned on the observed data with MCMC to approximate the probability distribution of each model parameter. Lee et al. [87] implement a combination of shared cluster models for certain model parameters instead of learning a model for each occupant independently. In this work we choose to investigate independent models for each occupant instead and use a different heat load function, the ATHB, which has been developed specifically to account for the physiological and psychological differences between occupants. Recent work by Lee et al. extends application of these thermal preference models with approximate dynamic programming (ADP, also referred to as reinforcement learning) [85] and simulation analysis [86].

3.2 Heat Load Function

The heat load function $L(X_{z,k}, \boldsymbol{\theta})$ has the physical interpretation as is an estimate of the thermal energy flow across the skin of an occupant to the thermal zone they are in. This base function is the steady state heat balance from the PMV method and is described in greater detail in Appendix A.1. The main components are the internally produced body heat (metabolic rate, M) and heat loss ($h_{loss}(X_{z,k}, \boldsymbol{\theta})$) to the environment through all heat transfer modes. The mechanical work (W) done by a person in an office is typically negligible.

$$\begin{aligned} L &= (M - W) - h_{loss}(X_{z,k}, \boldsymbol{\theta}) \\ h_{loss} &= h_{radiation} + h_{convection} + h_{exvaporation} + h_{respiration} + h_{sweat} \end{aligned} \quad (3.3)$$

For our predictive thermal preference model this function is extended using the ATHB framework developed by Schweiker et al. [138] as described in Section 2.1. The key difference being that the original ATHB uses the measured metabolic rate, operative temperature, and air velocity. The extension in this work uses regression of both clothing and metabolic rate as adapted parameters to further simplify the implementation. The adapted clothing is simply a linear function of the outdoor running mean temperature T_{rm} ,

$$CLO_{adapted} = \theta_1 + \theta_2 T_{rm} \quad (3.4)$$

While the adapted metabolic rate is a function of the running mean outdoor temperature and the current indoor temperature,

$$MET_{adapted} = \theta_3 T_{rm} + \theta_4 T_{in} + \theta_5 \quad (3.5)$$

This gives a linear regression model for clothing and metabolic rate with each parameter (θ) having a physical interpretation. All model parameters in Equation 3.2 (expect σ) are assumed to be Gaussian distributed with mean values following from [138] and [139]. An inverse gamma distribution is assumed as prior for σ and a normal distribution for μ with class means taken to be at 3.5, 0, and -3.5 respectively, with an almost fixed no-change mean at 0 as proposed in [87]. The priors are given relatively large standard deviations, on the same order of magnitude as the mean, because uncertainty is high and to allow MCMC to explore the posterior more easily. The prior distributions for each parameter are given below.

$$\begin{aligned} P(\theta_1) &\sim \mathcal{N}(1.25, 0.1) \\ P(\theta_2) &\sim \mathcal{N}(-0.03, 0.03) \\ P(\theta_3) &\sim \mathcal{N}(-0.0178, 0.02) \\ P(\theta_4) &\sim \mathcal{N}(0.0032, 0.003) \\ P(\theta_5) &\sim \mathcal{N}(0.283, 0.3) \\ P(\mu_0) &\sim \mathcal{N}(3.5, 1) \\ P(\mu_1) &\sim \mathcal{N}(0, 0.01) \\ P(\mu_2) &\sim \mathcal{N}(-3.5, 1) \\ P(\sigma) &\sim InvGamma(2, 0.5) \end{aligned} \quad (3.6)$$

While these priors may seem quite restrictive they will have a declining effect as they are conditioned on the observed data.

3.3 On-line Bayesian Parameter Estimation

A drawback of using a conventional MCMC approach, or any off-line inference method, is that the model must be retrained with all observed data in order to incorporate information from new observations. The number of observations being potentially unbounded for long-running systems this becomes quite problematic for run time and storage with even efficient algorithms running in $\mathcal{O}(N)$. On-line inference differs from typical off-line methods by iteratively inferring the sequence of posterior distributions given each new observation Y_k in the same ordered sequence. A more efficient approach with a recursive Sequential Monte Carlo (SMC) or particle filtering implementation is explored in this section. Doucet et al.[44] frames this problem using Bayes theorem as a formulation of the posterior distribution of the model parameters for Markovian, nonlinear, non-Gaussian state-space models. Considering $Y_k = TP_k$ as the observation (being implicitly conditional on the thermal state X_k), and taking the Bayesian model parameters $\{\theta_k, \sigma_k, \mu_k\}$ to be simply Θ_k . The notation for indexed sequences such as $\{Y_0, Y_1, \dots, Y_k\}$ can then be denoted by $Y_{0:k}$. One can now use the formulation introduced by Doucet et al. to express this problem conditional on all observed data as

$$p(\Theta_{0:k} \parallel Y_{0:k}) = \frac{p(Y_{0:k} \parallel \Theta_{0:k})p(\Theta_{0:k})}{\int p(Y_{0:k} \parallel \Theta_{0:k})p(\Theta_{0:k})d\Theta_{0:k}} \quad (3.7)$$

6

The integral in the denominator (normalization factor) is intractable analytically but can be approximated numerically using MCMC. The recursive formulation for the probability of the model parameters given the next ($k+1$) observed state uses the Markov property that $p(Y_{k+1} \parallel Y_{1:k}) = p(Y_{k+1} \parallel Y_k)$ and is

$$p(\Theta_{0:k+1} \parallel Y_{1:k+1}) = p(\Theta_{0:k} \parallel Y_{1:k}) \frac{p(Y_{k+1} \parallel \Theta_{k+1})p(\Theta_{k+1} \parallel \Theta_k)}{p(Y_{k+1} \parallel Y_k)} \quad (3.8)$$

If the posterior density of model parameters at every time step, $p(\Theta_k \parallel Y_{1:k})$, is Gaussian, then it can be shown analytically that a Kalman filter is the optimal algorithm [9, 44]. However, for this to be true the transition sequence $\Theta_k = f_k(\Theta_{k-1}, V_{k-1})$, and its measurement function, must be known linear functions and the i.i.d process noise V_{k-1} must be Gaussian. Unfortunately there is no reason for these to be generally true in the case of thermal preferences. It can be seen from the Monte Carlo estimates of the model parameters that some parameters exhibit multi-modal and skewed behavior, which are not generally well approximated by Gaussian distributions [9]. Alternatively considered in [9] are grid search methods. These are optimal for cases with a discrete and finite state space, which again is not the case with thermal preference. However a bounded discretization could be implemented as an approximate grid-based method. Other suboptimal algorithms such as extended Kalman filter (EKF), unscented Kalman filter (UKF), and particle filters will work in general non-linear case. The EKF locally approximates non-linearities with Taylor expansion while the UKF uses the non-linear function, but the resulting density function is still approximated by a Gaussian. Particle filtering techniques, also known as SMC, do not approximate the resulting posterior with a Gaussian and are the family of methods focused on in the remainder of this section.

Kantas et al. [77] give a review of off-line and on-line particle filtering methods for state estimation, giving methods for on-line maximum likelihood parameter estimation and Bayesian parameter estimation. They also address particle degeneracy as the key issue with on-line methods of Bayesian parameter estimation. This is due to the accumulation of relative weighting by likely particles after each successive generation leading to effectively only one particle remaining (also called sample impoverishment in [8]). One potential way to by-pass this issue is through fixed lag particle sampling (i.e. only incorporating particles in a sliding window). Another less restrictive method is MCMC steps between particle iterations, which is later employed in the implementation.

Kantas et al. denotes the sequence of posterior distributions of the model parameters as $\{p_\Theta(X_{0:k}, \theta \parallel Y_{0:k})\}_{k \geq 0}$ [77]. This notation follows the convention that $p_\Theta(z) = p(z \parallel \Theta)$ is the marginal density of some stochastic variable z conditional on Θ . They propose using an auxiliary particle filter to approximate the k^{th} iterate of the sequence by sampling particles $\{\Theta_k^i\}$ distributed by

$$p(\Theta \parallel Y_{0:k}) \propto p(X_{0:k-1}, \Theta \parallel Y_{0:k-1}) q_\Theta(X_k, Y_k \parallel X_{k-1}) \quad (3.9)$$

For the recursive formulation $p(X_{0:k-1}, \Theta \parallel Y_{0:k-1})$ is approximated by the previous iteration particles. MCMC can then be used to combat particle degeneracy by moving all the particles in the parameter space proportional to the posterior and increasing diversity. The SMC² algorithm proposed in [30] for example uses MCMC steps and importance resampling for steps in the Θ_k dimension, while internally using similar particle filters in the state space.

Minson et al. [100] propose a similar algorithm for Bayesian inference of model parameters called cascading adaptive transitional Metropolis in parallel (CATMIP). This algorithm combines, 1) importance resampling, 2) MCMC, and 3) transitional MCMC [29]. The CATMIP algorithm has been developed in particular to handle multi-modal distributions and additionally can compute a likelihood estimate for each particle which makes it quite attractive for implementation. As mentioned previously the importance resampling and MCMC steps between particle filtering steps are to treat particle degeneracy. Transitional MCMC additionally uses a simulated annealing approach to improve MCMC sampling efficiency [29]. This is done by slowly increasing the difference between the prior and sampled transitional distribution (instead of directly sampling the posterior) during MCMC. The transitional distribution is annealed exponentially in m steps towards the target posterior with $f(\Theta \parallel Y, \beta_m) \propto p(\Theta)p(Y \parallel \Theta)^{\beta_m}$. Where β_m is the annealing factor that is calculated adaptively to keep the difference between $f(\Theta \parallel Y, \beta_m)$ and $f(\Theta \parallel Y, \beta_{m+1})$ small.

This allows for the MCMC sampling to progress much more efficiently by rejecting far fewer samples. The transition time required is proportional to how informative the new data is, and thus how different the posterior and prior are. In the case of on-line learning the transition allows for faster MCMC sampling, typically in few transitional steps (less than 10). This CATMIP algorithm has been used in other Bayesian inference applications for planetary surfaces [83] and building seismic assessment [49]. The CATMIP algorithm has been grouped within the family of sequential tempered MCMC (STMCMC) algorithms in [26], while the authors there note it appears to still have some issue with sample degeneracy and propose an incremental improvement.

3.4 Algorithm Implementation

The thermal preference on-line learning algorithm is implemented in Python using the probabilistic programming framework PyMC3 [132]. The steps are detailed in Algorithm 1 below and explained in this section. The initialization step starts with preprocessing by extracting all data from a given building excluding a specific occupant. The RP-884 database [37] is used for the simulation experiments. A prior model is generated by conditioning the hierarchical Bayesian model (described in Section 3.1) using the CATMIP [100] algorithm (which is also used for on-line learning). Metropolis-Hastings MCMC was tested for generating the prior model though there was no improvement in performance and the computation time was much longer so the results reported are for the case using CATMIP. In the case that the prior model is generated using the Metropolis-Hastings MCMC sampling or a different technique that does not yield n particles (not the case when using the CATMIP), it is sampled n times to generate n particles as mentioned in [8, 9, 100]. Another possible initialization technique being model parameter mean averaging from a large data set as described in [173].

The current thermal state and occupancy state for each occupant is then polled. If the occupant is currently in the building then their true preference model is polled for an observed TP . If $TP = \text{no change}$ then the thermal preference and state are stored in a buffer (Y_{buf}, X_{buf}) and no update occurs until a change is preferred (i.e. $TP \neq \text{no change}$). This is a simple way to make it so the system does not update the model and cause a change if the occupant responds that they prefer no change. Only updating the model on-line when a change is preferred also reduces the computational workload significantly. It is also anticipated that $TP = \text{no change}$ could be encoded for a time step in which no feedback is given. The on-line update then runs on all states and temperature preferences in the buffer and afterwards the buffer emptied. Interestingly, because the on-line algorithm only requires storage of the current particle states, the observation data can be deleted from memory entirely after exiting the update buffer. The first step of the on-line update is to take a kernel density estimate of the previous iteration particles $K(\Theta \parallel \{\tilde{\Theta}\}_{i,k-1})$. The density estimate is only used as the starting transitional distribution (a MCMC proposal distribution) within the CATMIP algorithm. The previous iteration particles, $\{\tilde{\Theta}\}_{i,k-1}$, become the samples of the Bayesian prior instead of sampling from a prior distribution. The rest of the CATMIP algorithm follows as described by Minson et al. in Table 1 of [100]. The number of particles was set to 100, more and less particles were tested though the error was not improved and using a relatively low number of particles keeps computation time low. Running the CATMIP algorithm also produces a likelihood estimate for the updated particles, the maximum likelihood estimate is then selected to be the updated model parameters. The on-line thermal preference prediction model uses this set of parameters until a new preference from the occupant is observed and the the on-line model inference algorithm runs again.

3.5 Simulation Analysis

Models for 15 emulated occupants are learned on-line as described in the previous section within simulation experiments for a three zone building being controlled by MPC minimizing the probability that occupants have a thermal preference (i.e. $TP \neq \text{no change}$). The details of the simulation experiments can be found in Section 7.1. The mean absolute error (MAE) convergence of on-line learned models to the ground truth model in simulation can be seen in Figure 3.1 below. In this figure each line represents the MAE in prediction of the three thermal preference classes ($TP = \text{want warmer}$, $TP = \text{no change}$, $TP = \text{want cooler}$) for an individual occupant thermal preference model.

Algorithm 1 On-line Thermal Preference Model Inference

```
1:  $ns \leftarrow$  number of particle samples
2:  $np \leftarrow$  number of occupants
3:  $X_{RP884}, Y_{RP884} \leftarrow$  load preprocessed RP884 database
4:  $p(\Theta) \leftarrow$  prior parameter distributions from section 3.2
5:  $k \leftarrow 0$ 
6: for  $i$  in  $1:np$  do
7:    $X_{i,0} \leftarrow$  state data for same building minus occupant  $i$  data
8:    $Y_{i,0} \leftarrow$  thermal preference vote data for same building minus occupant  $i$  data
9:    $\{\tilde{\Theta}\}_{i,0} \leftarrow \hat{p}_{i,0}(\Theta \parallel X_{i,0}, Y_{i,0}) \propto p(\Theta)p(X_{i,0}, Y_{i,0} \parallel \Theta)$  from [100]
10:   $\Theta_{i,0}^* \leftarrow \underset{\Theta}{\operatorname{argmax}} \log p(\{\tilde{\Theta}\}_{i,0})$ 
11: end for
12: while on-line do
13:    $k \leftarrow k + 1$ 
14:   for  $i$  in  $1:np$  do
15:      $X_{i,k} \leftarrow$  current thermal state
16:      $O_{i,k} \leftarrow$  current occupancy state
17:     if  $O_{i,k}$  is in building then
18:        $Y_{i,k} \leftarrow$  poll occupant preference
19:        $Y_{buf} \leftarrow (Y_{buf}, Y_{i,k})$ 
20:        $X_{buf} \leftarrow (X_{buf}, X_{i,k})$ 
21:       if  $Y_{k,i} \neq$  no-change then
22:          $q(\Theta)_{i,k-1} \leftarrow K(\Theta \parallel \{\tilde{\Theta}\}_{i,k-1})$ 
23:          $\{\tilde{\Theta}\}_{i,k} \leftarrow \hat{p}(\Theta \parallel X_{buf}, Y_{buf})_{i,k} \propto \hat{p}(\{\tilde{\Theta}\}_{i,k-1}) \cdot q_\Theta(X_{buf}, Y_{buf} \parallel X_{k-1})$  from [100]
24:          $\Theta_{i,k}^* \leftarrow \underset{\Theta}{\operatorname{argmax}} \log \hat{p}(\{\tilde{\Theta}\}_{i,k})$ 
25:          $Y_{buf} \leftarrow \emptyset$ 
26:          $X_{buf} \leftarrow \emptyset$ 
27:       end if
28:     end if
29:   end for
30: end while
```

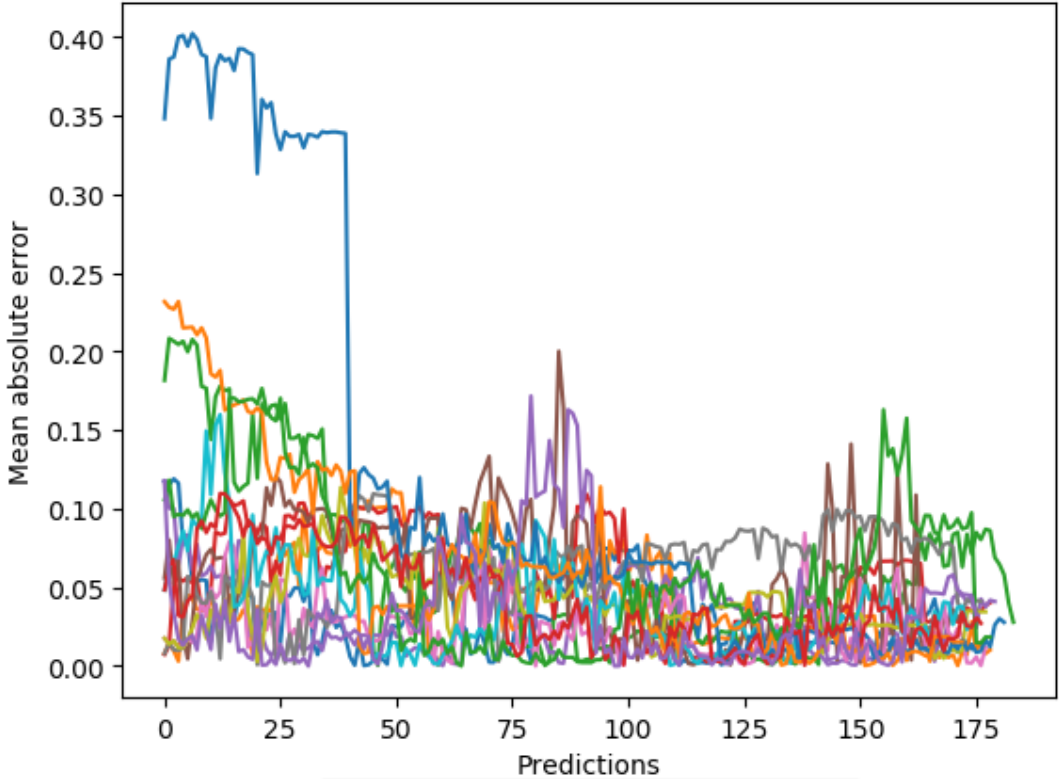


Figure 3.1: Mean absolute error (MAE) of three thermal preference classes (want warmer, no change, want cooler) for each prediction in sequence from on-line learned model during simulation of building with 15 occupants. Each colored line represents the MAE for an individual occupant model.

Models with high initial MAE quickly reach lower MAE, however MAE may increase from one prediction-observation-update iteration to the next. This is in part due to the sampling of observed preferences from the ground truth distribution, which may give unlikely preferences for a single observation and cause a shift in the wrong direction to the model parameters. Additionally there is the problem of non-persistent excitation, in that the observed thermal states and observed preferences are biased towards near the maximum of $TP = \text{want no change}$. This is because the controller keeps the thermal state within this region, causing occupants to have the majority of observations for $TP = \text{want no change}$ and one of the two other preference classes (i.e. either $TP = \text{want warmer}$ or $TP = \text{want cooler}$). Reducing the error for the third class cannot be accomplished because it is effectively never observed. The convergence of the on-line models can be seen to converge more qualitatively for each class in cases such as in Figure 3.2 below. The mutually exclusive probability of each temperature preference class given a fixed relative humidity and running mean outdoor temperature (50%, and 10.0 °C respectively) is shown in these figures. Blue represents $TP = \text{want warmer}$, green is $TP = \text{want no change}$, and red is $TP = \text{want cooler}$. Each class is represented by a colored line. The initial prior, Figure 3.2a, based on existing data from other occupants in the same building is updated once to the model in Figure 3.2b, then several more times to reach Figure 3.2c. This model is close to the ground truth model Figure 3.2d assumed in the simulation. However not all models converge in simulation to near the true model due to the bias in sampling as previously mentioned.

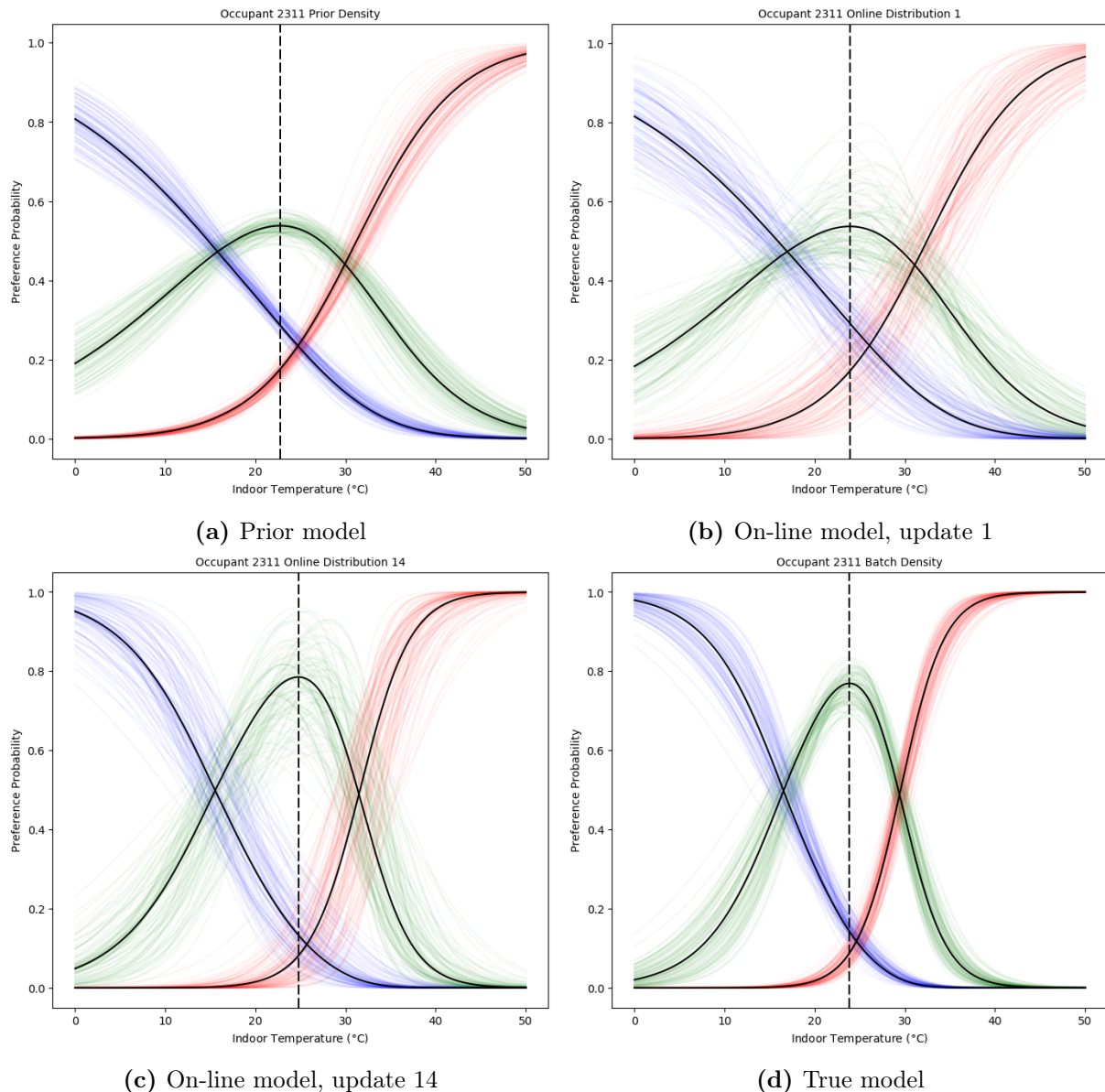


Figure 3.2: On-line learning of thermal preference model for specific occupant from sampling of the true model d) at the simulated thermal states. Each faint colored line represents one particle and the black line the selected maximum likelihood particle. a) the initial prior from other occupant data in the same building, b) the first update given an observation from the occupant, c) the fourteenth such update, and d) the true model that was being sampled from to generate the observations used to update the model.

Chapter 4

Occupancy Prediction

In this section an on-line learning algorithm is developed to treat the issue of scalability for occupancy modeling outlined by Dong et al. in [43]. Providing a scalable algorithm to creating an occupant and building specific model being the goal. This on-line learning method can start from a conservative prior, for example a schedule in agreement with general occupancy modelling practices, and continuously update into an increasingly specific model as occupancy data is logged for each occupant for the building in question. Off-line models have been demonstrated to be successful towards similar goals, such as the Markov based feedback recurrent neural network (M-FRNN) proposed by Wang et al. [158]. Their implementation predicts occupancy level in a single zone using WiFi and is compared with a classic Markov and CO₂ based method. The classic Markov model has transfer probabilities fit on data of the zone occupancy with observed conditional probabilities. The M-FRNN additionally uses temporal feedback and predicts a unique Markov transition probability matrix for each occupant (identified by mobile phone MAC address). They conduct real world experiments with video based ground-truth data and report mean absolute percentage error in occupancy level (in step-ahead prediction) of 33.5% for the Markov and 36.0 % for the M-FRNN. In this work a different Markov transition matrix fitting approach is considered.

Li and Dong have developed the UTSA Markov model [88, 89] for short term prediction of both presence and occupancy level in residential and commercial buildings with direct applications in MPC. In [89] the authors validate their method using experimental data from four offices and additionally compare the prediction performance to existing methods of: inhomogeneous Markov chains, hierarchical probability sampling, ANN (artificial neural networks), and support vector regressions (SVR). They compare model the correctness of the model in prediction modes of one step ahead (15 minutes, 30 minutes, and 1 hour) and one day ahead (24 hours in steps of 15 minutes and 1 hour). Their one-step ahead prediction results show their UTSA Markov model to outperform the existing models with correctness for each office ranging from 68.0% to 87.6%, with an average correctness of 79.6%. This model is also reported to have the lowest RMSE and MAE in step-ahead prediction of the occupancy level. The authors also compare models with respect to their ability to predict the key statistics of first arrival, last departure, occupancy duration, and inter-departure time of occupants.

The UTSA Markov model is chosen for implementation in this work because the experimental results in [89] show it as most performant in step-ahead prediction, which is most important for MPC, and additionally because it can accurately reproduce statistics found in experimental data. In this work the UTSA model is extended for use in predicting the occupancy pattern of individual occupants in a building with multiple zones and in an on-line learning implementation. The

difference between zone occupancy level prediction and individual occupant presence prediction is that data is not aggregated at the zone level and the occupancy of each occupant is predicted independently. This has some advantages and disadvantages normally associated with agent based models. In the case that not many unconsidered visitors enter the building, occupant conservation (enforcing that each occupant can only be in one zone at a time) can help short-term predictions. However, this may be unable to account for periods of high occupancy such as meetings or events without incorporating correlations between occupants, as considered in [158].

4.1 Inhomogeneous Markov Chains

Markov processes are inhomogeneous if the transition probabilities vary over time. Wang et al. present this method for occupancy simulation in [155]. The formulation used within this work is for discrete occupancy states $O_{i,k}$ of occupant i at time step k . Thus the probability of occupant i transitioning from current state $O_{i,k} = l$ to next state $O_{i,k+1} = j$ for a first order Markov chain using the Markov property is given by

$$P(O_{i,k+1} = j \parallel O_{i,k} = l, O_{i,k-1}, \dots, O_{i,0}) = P_{lj}^i(k) \quad (4.1)$$

Where $P_{lj}^i(k)$ is the state transition matrix for time step k . This method is proposed for simulation as extension to widely used Markov methods and has been implemented in the obXML toolset [65]. Interestingly, using such a time varying sequence of Markov transition matrices for each individual occupant yields something closer to an agent-based model. Inhomogeneous Markov chains allows for the use of absorbing states, which have no transition from them to other states [155]. These are simple ways to account for first arrival and last departure behavior which is most important for pre-heating and cooling of buildings. Similarly, changes in behavior such as leaving ones office during lunch time or for meetings in other offices. These changes are similarly discretized to occur at a specific time step.

For a given building we define z possible occupancy states to be each of the building thermal zones and taking the $z = 0$ to be anywhere outside the building. The occupancy prediction at time step $k + 1$ for an occupant i is the product of the current state at k and the current Markov transition probability matrix $P_{lj}^i(k)$, which has following structure

$$P_{lj}^i(k) = \begin{bmatrix} p_{00} & p_{01} & \dots & p_{0z} \\ p_{10} & p_{11} & \dots & p_{1z} \\ \vdots & \vdots & \ddots & \vdots \\ p_{z0} & p_{z1} & \dots & p_{zz} \end{bmatrix} \in \mathcal{R}^{z+1 \times z+1} \quad (4.2)$$

Each additional time step can be predicted by successive matrix multiplication by the Markov transition probability matrix for that time step. The UTSA Markov method is an algorithm to fit an inhomogeneous Markov chain to occupancy data using a fixed lag time frame. In order to determine at which time steps the Markov transition matrices change for each occupant, which is central to the method design, a change point detection algorithm is employed.

4.2 Change Point Detection

Li and Hong [89] propose the use of the Relative unconstrained Least Squares Importance Fitting (RuLSIF) change point detecting method introduced in [90]. The core of RuLSIF is estimating

the relative density ratio of two density functions using a Gaussian kernel (fit with least squares minimization) [168]. These two probability density functions for our application are from a daily occupancy profile (see 4.3.2) $k - n$ steps backwards, $P_{k-n:k}$, and $k + n$ steps forward, $P_{k:k+n}$, from the current step k . A maximum divergence between these two density functions therefore indicates a change point, i.e. the point at which the densities with forward data diverge the most from densities with backward data. A symmetric divergence score called the alpha-relative Pearson (PE) divergence defined as $PE_\alpha(P_{k-n:k} \parallel P_{k:k+n}) + PE_\alpha(P_{k:k+n} \parallel P_{k-n:k})$ is used as proposed in [90]. This incorporates a linear combination of the divergence in either directions with coefficient α , and additionally bounds the density ratio from above by $1/\alpha$ (in the case of $P_{k:k+n} = 0$) [90]. This produces a change point score for each point which is itself computed in a sliding window over the time series. The change points are taken to be the local minima and maxima of the approximated symmetrized PE divergence curve as in [89]. An example of the change point score with the minima and maxima highlighted is shown in the third chart from the top (second from the bottom) in Figure 4.1.

4.3 Algorithm Implementation

In this study the synthetic simulation data is generated with a similarly structured inhomogeneous Markov chain with absorbing states and inter-zone transition probabilities which is predetermined for each occupant and then learned using the UTSA Markov model previously mentioned [89]. The occupancy prediction on-line learning algorithm is implemented in Python code. An example of the input and output from this algorithm is given below in figure 4.1 and described in detail in this section. The structure of the algorithm is defined by the following steps: 1) Initialization, 2) Exponentially weighted daily profile, 3) RuLSIF change point detection, and 4) Fitting Markov transition probabilities. Each step is described in the following subsections. A pseudo-code implementation is presented in Algorithm 2.

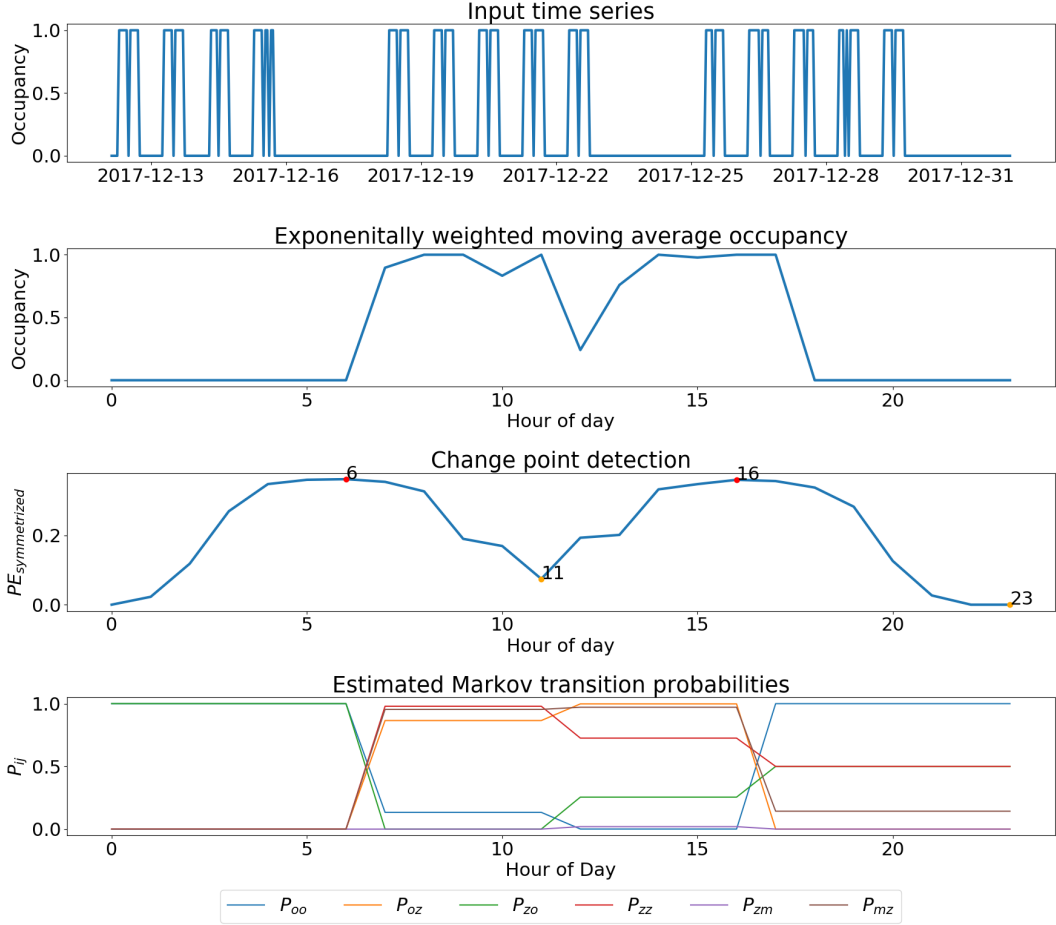


Figure 4.1: Input (top) and output of occupancy prediction model (bottom) showing exponentially weighted moving average daily occupancy profile (second from top) and changepoint scoring and detection (third from top).

4.3.1 Initialization

To start with the initialization parameters, Li and Hong [89] use a 10 day sliding window for step-ahead prediction and a month sliding window for day-ahead prediction. Here only synthetic data is used so any parameter tuning is not meaningful, such that wherever possible the parameters of [89] are used. The number of days, nd , used in the sliding window is 30 for up to day-ahead predictions. The time discretization is by hour so the number of time steps per day, ns , is set to 24.

4.3.2 Exponentially Weighted Daily Occupancy Profile

The occupancy data is binned by time step and day type (weekday or weekend) and an exponentially weighted average is computed within the sliding window of occupancy data OD . The common exponential moving average formula $(1-\lambda) \sum_{i=1}^{nd} OD_{s,i} \lambda^{i-1}$, where $1-\lambda$ is the converged value of $\frac{1}{\sum_{i=1}^{nd} \lambda^{i-1}}$, is given here using the explicit exponential weighting to avoid approximation error when nd is small (called wind-up for exponential weighting). This gives an exponentially weighted average W_s for each time step $s \in \{0, \dots, ns\}$. The exponential decay or forgetting parameter, λ , of 0.8 is used in the numeric simulations.

$$W_s = \frac{\sum_{i=1}^{nd} OD_{s,i} \lambda^{i-1}}{\sum_{i=1}^{nd} \lambda^{i-1}} \quad (4.3)$$

To allow the sliding window of the change point detection (within the sliding window of W) to move backwards from the first time step and forwards from the last the exponential weighted average dataset is extended in the forward and backward direction by appending an *offset* of half a day of time steps, $ns/2$, in either direction. This is equivalent to wrapping the sliding window values around the same exponentially weighted daily profile, thus extending its index range. The effect of doing so is later investigated in simulation.

4.3.3 RuLSIF Change Point Detection

The change point detection algorithm also uses a sliding window approach within its own sliding window. The relative density estimation is taken from this exponentially weighted daily profile with a forward, f , and backward, b , sliding window step size of 3 time steps each within a sliding window of 5 time steps. The RuLSIF change point score SC_s is computed for each point (i.e. a total sliding window of 5 steps in forward and backward direction, with three different points of evaluation for each data point W_s) in this extended range and then only the original range of the daily profile is extracted. The internal parameters of the RuLSIF method are fit using n-fold cross validation [90]. The local minima and maxima in the change point score time series are identified by taking the time step indexes when the first order difference changes sign to the change points, CP . The RuLSIF implementation is adapted from the work of Daisuke Motoki [105] based on the software distributed by the Sugiyama-Sato-Honda Lab at the University of Tokyo [167]. The first order peak detection algorithm used is from the freely available PeakUtils library [109].

4.3.4 Fitting Markov Transition Probabilities

Each change point specifies the time step at which the Markov transition matrix is predicted to change. Therefore, a first order Markov transition matrix can be fit on the occupancy data between each change point and the next change point (i.e. by computing the observed conditional probability). This creates an inhomogeneous Markov chain for the exponentially weighted average daily occupancy profile. Li and Hong propose an α smoothing factor to increase the transitions to previously unobserved states and reduce the occurrence of sink states [89]. In our case where the simulation data is generated with an inhomogeneous Markov chain this α factor may not improve prediction accuracy but is still included to represent more realistic predictions. An addition to this transition probability fitting method that aides in prediction on multiple states is using the base rate of all states (i.e. the total observed occurrence, unconditional on the previous state) for the transition probabilities when the occupant is in a previously unobserved state. This is instead of relying on the alpha parameter which will make a transition from the previously unobserved state to all other states equally likely.

Finally, leave-one-out cross validation (LOO-CV) is used in conjuncture with computing the conditional probabilities as mentioned above to select a cross validated Markov transition matrix. LOO-CV splits the data set by day and selects one day which is used for validation. The data for all other days is used as training data to compute the Markov transition probabilities and each Markov chain is used to generate one-step ahead predictions on the left-out validation data set. The Markov chain with the lowest squared error, ε , in prediction is selected for the change point.

This is performed between each change point independently to learn the full inhomogeneous Markov chain on-line.

Algorithm 2 Occupancy Prediction On-line Learning

```

1: Initialize:  $nd \leftarrow 30$  number of days in data set
2: Initialize:  $ns \leftarrow 24$  number of time steps per day
3: Initialize:  $np \leftarrow$  number of occupants
4: Initialize:  $\lambda \leftarrow 0.8$ 
5: Initialize:  $f \leftarrow 3$ 
6: Initialize:  $b \leftarrow 3$ 
7: Initialize:  $\alpha \leftarrow 0.1$ 
8:  $OD \leftarrow prior \in \mathbb{R}^{(nd)ns \times m}$ 
9: while on-line do
10:   for  $i$  in  $0:np$  do
11:      $OD \leftarrow O_{i,(k-ns \times nd):k} \in \mathbb{R}^{(nd)ns \times m}$ 
12:     for  $s$  in  $0:ns-1$  do
13:        $W_s \leftarrow \frac{\sum_{d=0}^{nd-1} OD_{d(ns)+s} \lambda^d}{\sum_{d=0}^{nd-1} \lambda^d}$ 
14:     end for
15:      $offset \leftarrow ns/2$ 
16:      $W \leftarrow [W_{ns-offset:ns}, W, W_{0:offset}]$ 
17:     for  $s$  in  $0:(ns \times 2 \times offset)$  do
18:        $SC_s \leftarrow PE_\alpha(P(W_{s-b:s}) \parallel P(W_{s:s+f})) + PE_\alpha(P(W_{s:s+f}) \parallel P(W_{s-b:s}))$  from [90]
19:     end for
20:      $SC \leftarrow SC_{offset:ns+offset}$ 
21:      $CP \leftarrow$  extract first order local minima and maxima of  $SC$ , from [109]
22:     for  $c$  in  $CP$  do
23:       for  $d$  in  $0:nd$  do
24:          $X \leftarrow [OD_{0:d \times ns}, OD_{(d+1) \times ns:nd \times ns}]$ 
25:          $V \leftarrow OD_{d \times ns:(d+1) \times ns}$ 
26:         for  $i$  in  $0:m$  do
27:           for  $j$  in  $0:m$  do
28:              $n_{ij} \leftarrow \sum_{k=0} X_{k+1} = j \wedge X_k = i$ 
29:             if  $\sum_{l=0}^m n_{il} > 0$  then
30:                $\hat{p}_{ij} \leftarrow \frac{n_{ij} + \alpha}{\sum_{l=0}^m n_{il} + \alpha}$  from [89]
31:             else
32:                $\hat{p}_{ij} \leftarrow \frac{\sum_{k=0} X_k = j}{\sum_{k=0} X_k}$ 
33:             end if
34:           end for
35:         end for
36:          $\hat{P}_{c,d} \leftarrow \begin{bmatrix} \hat{p}_{00} & \hat{p}_{01} & \dots & \hat{p}_{0m} \\ \hat{p}_{10} & \hat{p}_{11} & \dots & \hat{p}_{1m} \\ \vdots & \vdots & \ddots & \vdots \\ \hat{p}_{m0} & \hat{p}_{m1} & \dots & \hat{p}_{mm} \end{bmatrix}$ 
37:          $\varepsilon_d \leftarrow$  squared error predicting on  $V$ 
38:       end for
39:        $\hat{d} \leftarrow \underset{d}{\operatorname{argmin}}(\varepsilon_d)$ 
40:        $\hat{\mathbf{P}}_c \leftarrow \hat{P}_{c,\hat{d}}$ 
41:     end for
42:     return  $\hat{\mathbf{P}}_{i,k}$ 
43:   end for
44: end while

```

4.4 Simulation Analysis

To compare the applicability of the algorithm during on-line learning it is run for synthetic occupancy data for 42 days. The occupancy data is streamed by the on-line learning algorithm such that the sliding window shifts with each new occupancy state and the model updates for each new observed occupancy state. On initialization there is no pre-existing occupancy data so a prior needs to be generated. This is chosen to be a conservative occupancy schedule where the occupant is present in their office (a specific thermal zone) continuously from 6:00 to 20:00 on weekdays, and outside the building otherwise. The initialization parameters number of steps per day, $ns = 24$, and number of days in wieghted occupancy profile, $nd = 30$ are set for all simulations. This gives a hourly predictions based on hourly occupancy data. A shorter frequency (e.g. minute time steps) is likely desirable for real world applications. The underlying algorithm can accommodate shorter frequencies by changing the ns parameter and using input data at that frequency.

The analysis of simulation results is of importance for validating that adding the offset to the exponentially weighted daily average occupancy profile improves change point detection. This is evident upon comparing results for different step-ahead predictions with different offset time steps. As the prediction horizon grows (i.e. becomes greater than one-step ahead) the MAE shown in Figure 4.2 is minimal with an offset of $ns/2$ time steps ($ns/2 = offset = 12$ in this case) compared to no offset or other offset sizes. The same trend is observed with the root mean squared error (RMSE) shown in Figure 4.3). The improvement comes from correctly identifying when the Markov transition probabilities change. This allows for the correct data to be used to estimate the transition probabilities between the change points as well, which further improves the algorithm.

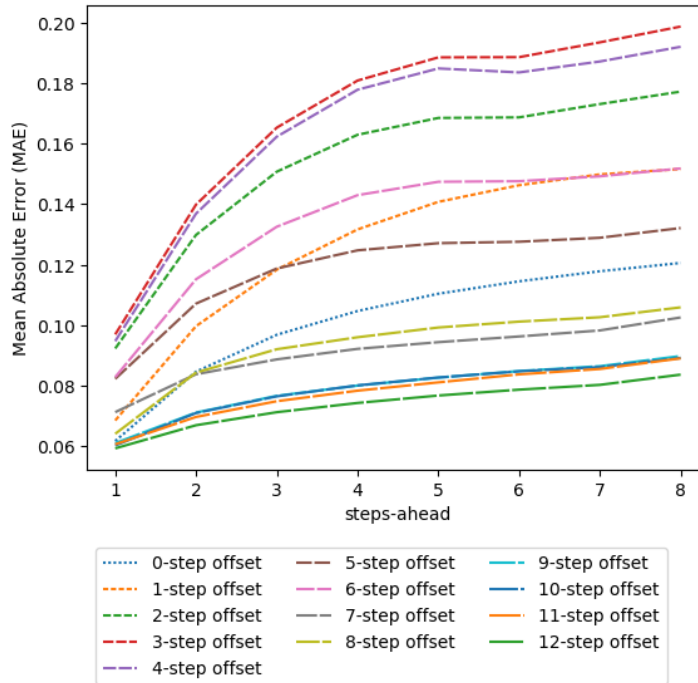


Figure 4.2: Occupancy n-step ahead prediction mean absolute error (MAE) for different offset time steps

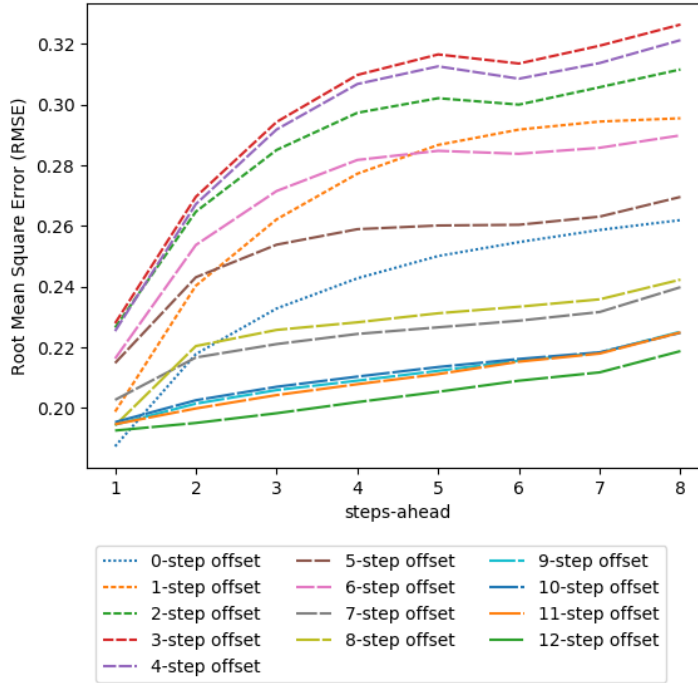


Figure 4.3: Occupancy n-step ahead prediction root mean squared error (RMSE) for different offset time steps

To check the convergence of the on-line learning algorithm from the prior to posterior (conditioned on the data) the log loss (logistic loss or cross-entropy) is computed for each time step prediction and true occupancy values. A daily (24 step) and weekly (168 step) moving average of the prediction log loss is computed for varying n-step ahead predictions to show how the predictions change with each iteration of the on-line learning algorithm. A moving average is chosen because the occupancy predictions were heavily dependent on the current state of occupancy and therefore noisy. The results are shown in Figure 4.4 for the daily moving average log loss and Figure 4.5 for the weekly moving average.

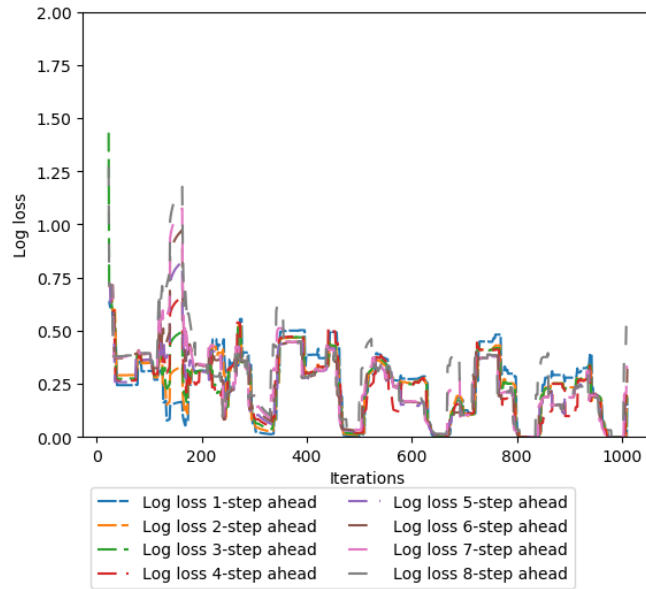


Figure 4.4: Occupancy prediction daily (24 time step) moving average log loss, 12-step offset

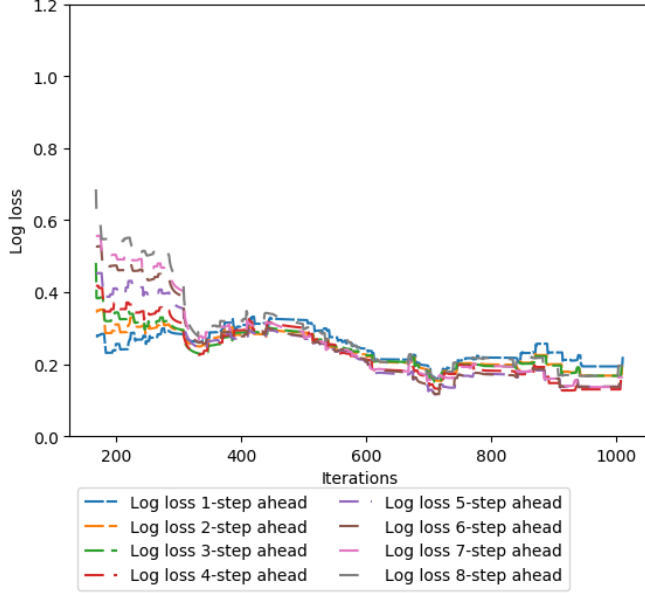


Figure 4.5: Occupancy prediction weekly (168 time step) moving average log loss, 12-step offset

There is a clear reduction in the log loss in the very beginning as more occupancy data is used to update the prediction model from the prior. As can be seen in the weekly moving average plot the log loss appears to converge after roughly four weeks (678 iterations). It is also worth mentioning that the log loss of the n-step ahead predictions becomes lower than one-step ahead. This is due to the scaling of the log loss being log scaled and the single step predictions possibly being potentially very wrong while the n-step ahead errors tend to become averaged with successive transition matrix multiplication. This can be seen in a simple example where $y_{true} = 1, 0, 0$, $y_{pred,1} = 0.95, 0.0, 0.95$, and $y_{pred,2} = 0.7, 0.5, 0.5$ which is more averaged. The log loss, which is defined by $-\log P(y_{true}|y_{pred}) = -(y_{true}\log(y_{pred}) + (1 - y_{true})\log(1 - y_{pred}))$, for $y_{pred,1}$ is 1.02 and for $y_{pred,2}$ is 0.58. However the MAE of $y_{pred,1}$ is lower than for $y_{pred,2}$. In any case the log loss is used simply to show the relative decrease in prediction errors as the on-line algorithm iterations increase.

Chapter 5

Controller Optimization

The optimal control problem (OCP) at the centre of MPC is the focus of this chapter. The formulation for discrete time MPC is given and a novel cost function for the MPC system is developed to approximate the expectation of thermal comfort costs to all occupants within all zones of the building combined with the predicted energy costs of producing a comfortable thermal environment. This tradeoff between comfort and energy is explored by approximating the probability function of each occupant individually having a preference to be warmer or cooler, or preferring no change at all, using the on-line model described in Chapter 3. These probabilities are also conditional on the occupancy probability of each occupant using the on-line model described in Chapter 4. The function is then able to value energy costs near the region of maximum comfort (or minimum discomfort) for all occupants in aggregate proportionally to the increased probability of occupants preferring to be warmer or cooler. This cost function is then optimized directly in discrete finite horizon MPC formulation to generate a control sequence approximating the optimal control sequence.

5.1 Discrete MPC formulation

Discrete time control is common for digitally controlled systems because the sampling of sensor measurements and computation between actuation signals happens in discrete time (i.e. at fixed intervals of continuous time). The discrete approximation of continuous time systems used in this work is the zero-order hold, which simply assumes the system is constant between measurements creating a piece-wise constant approximation of a given signal. For buildings that have slow dynamics the discretization frequency can be quite large without introducing large errors. The typical discrete time MPC formulation from Rawlings and Mayne [126] comprises of a stage cost $l(x(k), u(k))$ and terminal cost $l_N(x(N))$ and takes the sum over all time steps (or integral in continuous time) as

$$V(x(0), \mathbf{u}) = \sum_{k=0}^{N-1} l(x(k), u(k)) + l_N(x(N)), \text{s.t. } x^+ = Ax + Bu \quad (5.1)$$

With the states being measured through $y = Cx$ where C can be the identity matrix if the measurements are assumed to have no error, which is assumed in this work for simplicity. Possible extensions of this formulation for measurement errors and stochastic disturbances are introduced in Chapter 1 of [126]. There are several notable limitations with numerical solving of MPC

problems, which is typically the only possible solution method [126]. These limitations are 1) the real system dynamics are only approximated by the system model, 2) the horizon length is finite instead of infinite, 3) discretization of the system differential equations, and finally 4) the optimization problem is only solved to within some error tolerance (either due to solving method or finite precision of digital computation). With care these errors can be made insignificant and a tractable optimization problem can be constructed to solve for the optimal control sequence at each time step.

The discrete time optimal control problem can be formulated generally as in Chapter 8 of [126] for nonlinear systems as

$$\begin{aligned}
 & \underset{\mathbf{x}, \mathbf{u}}{\text{minimize}} \sum_{k=0}^{N-1} l(x_k, u_k) + V_f(x_N) \\
 & \text{s.t. } x_0 = x_0 \\
 & \quad x_{k+1} = f(x_k, u_k), \forall k = \{0, 1, \dots, N-1\} \\
 & \quad \{x_k, u_k\} \in \mathbb{Z}, \forall k = \{0, 1, \dots, N-1\} \\
 & \quad x_N \in \mathbb{X}_f
 \end{aligned} \tag{5.2}$$

where \mathbb{Z} is the feasible set representing constraints on x_k and u_k , and \mathbb{X}_f is the terminal set ($\mathbb{X}_f \in \mathbb{Z}$), the terminal cost V_f then approximating the infinite horizon cost of the state at the end of the finite horizon of N steps. One can now see that the state dynamics are no longer defined with linear transformation matrices and can be any arbitrary function, however complex functions may easily produce OCPs that are nonconvex and unsolvable given reasonable computation time. The dynamics in the RC building model are linear but have nonlinear terms for radiation in the boundary conditions (these could also be linearized). Most important to the optimization process is the choice of cost function which becomes the guiding function for the whole system.

5.2 MPC Cost Function

As mentioned the cost function for the MPC system has been chosen to approximate as closely as possible the thermal comfort costs to all occupants with all zones of the building combined with the heating and cooling energy costs. Weighting of the increased thermal preference probabilities caused by only expending energy to get close to the maximum comfort region gives a multi-objective optimization problem that adequately balances comfort and energy cost. The problem of deciding on an appropriate weighting is a subjective, cultural, and political endeavour that is beyond the scope of this project, however a first order estimate of the cost and a sensitivity analysis shows potential outcomes in the results presented in Chapter 7. It should also be noted that this model of a static cost for the event of preferring to be warmer or cooler is only effective near the maximum comfort region. Clearly if the temperature was extremely hot or cold the cost would be greater than just the occupants all having a thermal preference with a probability of 1.

At the building zone level the individual thermal preference profiles must be aggregated into an expectation to compute the zone cost function. This is done by summing the conditional probability that the occupant is also present in the zone. For example for the case of occupants

having a preference to be cooler ($c = 0$) at time k in zone z with state $X_{z,k}$ the probability is aggregated based on summing the conditional probability for each occupant i as follows.

$$\mathbb{E}_{z,k}[TP = \text{cooler} \parallel X_{z,k}, O_{i,k-1}] = \sum_{i=0}^N P_{i,k}(TP = \text{cooler} \parallel X_{z,k})P(O_{i,k} = z \parallel O_{i,k-1}) \quad (5.3)$$

The probability of occupant presence is considered to be independent of the thermal state and presence of other occupants so the conditional probability can be computed by multiplying the two probabilities as proposed. This produces the After normalization by the number of occupants the presence-weighted average preference probability distribution $\bar{P}_{z,k}(X_{z,k}, O_{i,k-1})$ is computed for each mutually exclusive preference class. The expectation however has a bias to condition zones that have more occupants closer to the maximum comfort region because the relative cost is lower. A simple way to remove this bias is to normalize by the expected zone occupancy to give an expected zone thermal profile.

$$\mathbb{E}[P_{z,k}(TP = \text{cooler} \parallel X_{z,k})] = \frac{\sum_{i=0}^N P_{i,k}(TP = \text{cooler} \parallel X_{z,k})P(O_{i,k} = z \parallel O_{i,k-1})}{\sum_{i=0}^N P(O_{i,k} = z \parallel O_{i,k-1})} \quad (5.4)$$

This is different than taking the average of each occupant comfort profile in that it puts no mass in regions that no individual occupant prefers. This is important because if a single occupant were to have a vastly different profile (i.e. that it did not overlap with any other occupant profiles), their profile would not change the maximum comfort region. This is because the profiles being logistic curves have a maximum of 1, so any portion of overlap between two curves giving a sum above 1 will always be greater than any single occupant profile. It is however incredibly unlikely that any true profile would have no overlap. A feedback mechanism allowing occupants to indirectly (or even directly) control their comfort profile would thus incentivize occupants to be truthful and not exaggerate their preferences to move the zone temperature towards their preferred temperature as this would cause their profile to be increasingly outside the maximum comfort region and therefore neglected from determining the maximum comfort region. An example of this aggregation for several occupant profiles derived from real world data can be seen in Figure 5.1 below, the individual profiles are shown in grey lines and the expected zone profile in black.

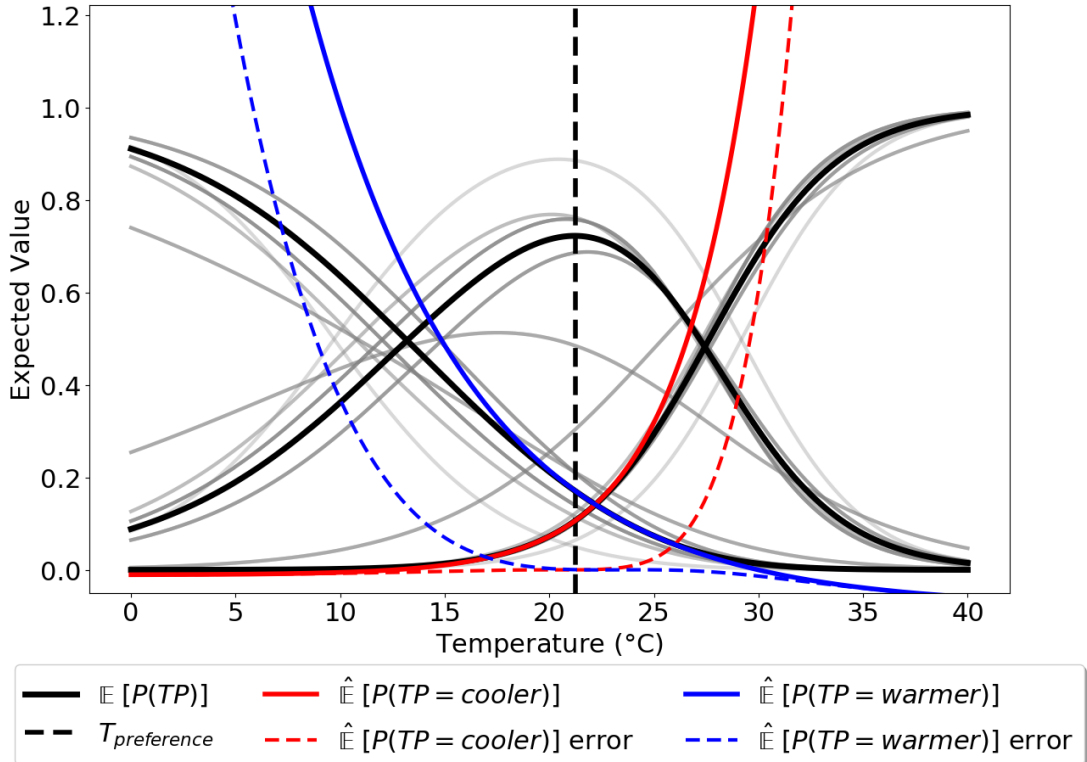


Figure 5.1: Expected zone thermal preference function (black lines) given the individual occupant preference functions conditional on their occupancy (grey lines). Also showing approximation with exponential functions (red and blue lines) and respective errors (dashed lines).

This zone profile is however not convex or guaranteed to be monotonic (in the case that comfort profiles are vastly different). An approximation of the curves for $E[P(TP = \text{cooler})]$ and $E[P(TP = \text{warmer})]$ each with an exponential curve of the form $e^{ax+b} + c$ is fit to the maximum comfort region (i.e. the region of the preference curves near the dashed black line). This is shown also in Figure 5.1 by the blue and red curves. There error of this approximation is also shown (dashed blue and red lines respectively), with an error of less than 0.05 for the comfort region (roughly 18 to 25 °C in this case). Crucially, outside of this region the approximation curves are exponentially higher than the expected profiles. This drives the system into the comfort region under all circumstances, solving the previously mentioned issues with having a constant thermal preference cost which is only valid within the comfort region (thus under valuing extreme conditions). Therefore this exponential approximation is not only a reasonable way to improve computational tractability, but can serve a role in valuing the cost of extreme conditions that are no longer governed by thermal preference.

The total stage cost can then be defined by summing the preference costs, given the exponential curves for each zone, and the energy costs over all thermal zones within the building and all time steps within the horizon as

$$\sum_{k=1}^{N_k} \sum_{z=1}^{N_z} C_c \mathbb{E}[P_{z,k}(TP = \text{cooler} \parallel X_{z,k})] + C_w \mathbb{E}[P_{z,k}(TP = \text{warmer} \parallel X_{z,k})] + C_E Q_z \quad (5.5)$$

Where C_c and C_w are the costs of preferring to be cooler and warmer in CHF/h, and C_E is the cost of energy in CHF/kWh respectively. This can then be augmented with weighting factors l_c ,

l_w , and l_E for sensitivity analysis. To give the full cost function $Q_k(\mathbf{u}_k, \mathbb{E}[P_{k+1}(TP)])$ for time step k to be

$$Q_k(\mathbf{u}_k, \mathbb{E}[P_{k+1}(TP)]) = \sum_{k=0}^{N_k} \sum_{z=1}^{N_z} l_c C_c \mathbb{E}[P_{z,k+1}(TP = \text{cooler} \parallel X_{z,k}, O_{i,k})] + \\ l_w C_w \mathbb{E}[P_{z,k+1}(TP = \text{warmer} \parallel X_{z,k}, O_{i,k})] + l_E C_E \mathbf{u}_{z,k} \quad (5.6)$$

This cost function is defined dynamically for each step, i.e. all preference curves are updated on-line, re-aggregated, and re-approximated for each zone. For the simulations in this work an order of magnitude estimate for the costs is given from an assumption that having a thermal preference carries a 0.5% decrease in productivity which is multiplied by the median monthly Swiss salary of 6235 CHF and median of 178 hours worked per month [114]. With the cost of preferring to be warmer and cooler assumed to be the same, $C_c = C_w = (6235 \text{ CHF/month})(178 \text{ hours/month})(0.5\%) = 0.175 \text{ CHF/hour}$ are the base thermal preference costs considered in this work. There is however no reason for these two costs to be equal in reality because each building and person has different physiological, behavioural, or psychological means to adapt to feeling warmer or cooler given a specific situation. For example an occupant during cold weather may have a sweater and be able to adapt to colder temperatures indoors (while preferring to be warmer), but in warm weather they would likely not have this sweater and therefore not be able to adapt to cooler indoor temperatures as effectively. Determining the relative costs C_w and C_c for a specific situation is considered future work. Some existing work in this area is presented in [45] to determining the cost of a temperature deviation for a specific occupant from a preferred temperature through direct compensation in a game theoretic formulation.

The final formulation of the OCP is given without terminal cost (or with a terminal cost of $V_f = Q_N(x_N, u_N)$) to be

$$\begin{aligned} & \underset{\mathbf{x}, \mathbf{u}}{\text{minimize}} \sum_{k=0}^N Q_k(x_k, u_k) \\ & \text{s.t. } x_0 = x_0 \\ & \quad x_{k+1} = f(x_k, u_k), \forall k = \{0, 1, \dots, N-1\} \\ & \quad \{x_k, u_k\} \in \mathbb{Z}, \forall k = \{0, 1, \dots, N-1\} \end{aligned} \quad (5.7)$$

A terminal cost that better approximates the infinite horizon could be formulated however given a reasonably long finite horizon this will have diminished effect on the first step actuation \mathbf{u}_0^* that is to be applied. There are no explicit constraints needed on the thermal state as the exponential cost function creates a relaxed constraint towards the comfort region. Temperature constraints could be useful in a real world system for defining a minimum unoccupied temperature, for example to prevent pipes from freezing or otherwise causing HVAC equipment and building damage. The constraints $\{x_k, u_k\} \in \mathbb{Z}, \forall k = \{0, 1, \dots, N-1\}$ are described in Section 7.1 and the building thermal dynamics $x_{k+1} = f(x_k, u_k), \forall k = \{0, 1, \dots, N-1\}$ is detailed in Chapter 6.

5.3 Optimization Framework

The resulting discrete time OCP is cast as a nonlinear program (NLP) by compiling the building thermal dynamics model and on-line learned cost functions with JModelica [4–6] and transferring the equations to CasADI [7]. The resulting NLP can be algorithmic differentiated by CasADI and solved with IPOPT [19, 153]. CasADI is a symbolic dynamic computation graph engine that implements forward and reverse mode algorithm differentiation to compute a sparse Hessian and Jacobian which is crucial for optimal control problems to be solved efficiently using IPOPT. CasADI is implemented in C++ but uses the Simplified Wrapper and Interface Generator (SWIG) [15] to provide a cross-language interface that allows Python code to be embedded in the CasADI computation graph. This optimization toolchain can thus handle a variety of dynamic optimization problems arising from nonlinear dynamics and cost functions. However if the building thermal dynamics model can be linearized and the cost function can be approximated with quadratics (instead of exponential functions used in this work) it would be solved more efficiently by a quadratic solver. To ensure model equations are twice continuously differentiable with respect to all of the variables by CasADI the model cannot contain integer variables or control flows (e.g. if statements or for loops) depending on the time-varying states. Creation of thermal dynamic models that meet this criteria is facilitated with a simple interface to Modelica described in Section 6.1.

The JModelica compiler has several preprocessing steps that reduce model complexity including model flattening, index reduction, and equation sorting [5]. This analytically propagates substitutions of known variables of the flattened model to obtain a Block-Lower-Triangle (BLT) representation of the systems of equations. Solving nonlinear MPC problems with JModelica has been addressed in [14] and [13]. In particular, the discretization, direct collocation, and piece-wise constant inputs. The JModelica optimization tool chain is described in detail in implements the direct local collocation method described by Magnusson in [92] and Chapter 3 of [91]. For direct local collocation discretization the system dynamics are only enforced at the collocation points. Radau collocation is the transcription method employed, which always places a collocation point at the beginning of each element. The other collocation points are chosen to maximize numerical accuracy. Radau collocation has superior stability properties compared to the alternatively implemented Lobatto or Gauss collocation. Lobatto collocation places points at both the start and end of each element, which can cause overdetermined equality constraints because of both DAE and continuity constraints.

Chapter 6

Building Simulation

There are three types of building models as previously mentioned, 1) physics-based (white box) models, 2) identification-based (black box) models, and 3) hybrid (or grey box) [144, 159]. The first are built from first-principles of physics including material properties, geometry, energy transfer, and knowledge of building systems. The second, also commonly referred to as machine learning methods, are built from measured input and output data and rely on statistics, function-fitting, and optimization. The key difference is that physics-based models enforce a specific and deliberate structure (e.g. conservation derived equations) and in many cases use parameters taken from available system knowledge. Identification-based methods have no imposed physical structure, which is generally considered to be part of the problem and is *learned* during the *training* (fitting of correlation function). Implementations can also be hybrids of the two (grey box models) which seek to reducing trade-offs between each model type [159]. For example in the case of physical models empirical data can be used to estimate parameters. The line between these two types of models is contextual, but generally a model can be considered physics-based if parameters have a physical interpretation and could in theory be measured [144].

The benefits associated with physics-based models are that they are generally well trusted because they are interpretable (at very least by experts) and can be more accurately extrapolated from. This is because one can reason about how other data or models would interact with conditions unobserved in the training dataset due to the physics [159]. Identification-based models however can have much simpler structures that approximate complex models, leading to faster computation time. Also the ability to learn structure allows for scalable deployment to problems on periphery of their design domain. In any case without a reasonably large and diverse data set of heating system inputs and thermal state measurements an identification-based approach cannot be investigated. For the additional reason of reducing the scope of this work a physics-based model is desired for both use as an MPC model and to emulate the building response.

For simulation experiments a Modelica based resistance-capacitance (RC) building model is chosen for implementation. This is because Modelica models have been developed within the IEA EBC Annex 60 project [163] (now continued in IBPSA Project 1) as the platform for development of new building simulation software. Specifically the Modelica Buildings Library [166] is used in this work, itself being based on the base implementation of the Modelica IBPSA Library. Modelica models also have integration through JModelica [4–6] and CasADi [7] with a variety of numerical solvers and in particular IPOPT [19, 153] as previously mentioned. An in-depth analysis of existing building simulation software is presented in Appendix B.1. The MPC building control is implemented through the MPCPy platform [22] which is a Python interface for JModelica and Modelica models. An additional tool for constructing the RC building models

and additional boundary equations has been developed to facilitate developing the simulations and is described in the next section. This tool also gives an easy way to compose models as non-linear programs (NLPs) that meet the first and second order derivative requirements of IPOPT.

6.1 Resistance Capacitance Building Model

The key purpose of the RC modeling tool is to correctly account for all boundary conditions of the RC building model and generate Modelica models that can be compiled by JModelica, differentiated algorithmically using CasAdi, and be simple enough to be solved by IPOPT much faster than real-time in MPC simulation experiments. The boundary conditions include: incident solar radiation (based on self-shading and surface angle), solar radiation through windows, long-wave radiation through windows (to sky), effective outdoor air temperature due to long-wave radiation, outdoor convection, and indoor convection. The thermal zones of the model were composed of exterior walls (with or without windows), roofs, and floors. Thermal zones could then be connected to each other using interior wall components. Each component is defined by simply specifying its physical parameters. A schematic RC network describing the boundary conditions is shown below in Figure 6.1.

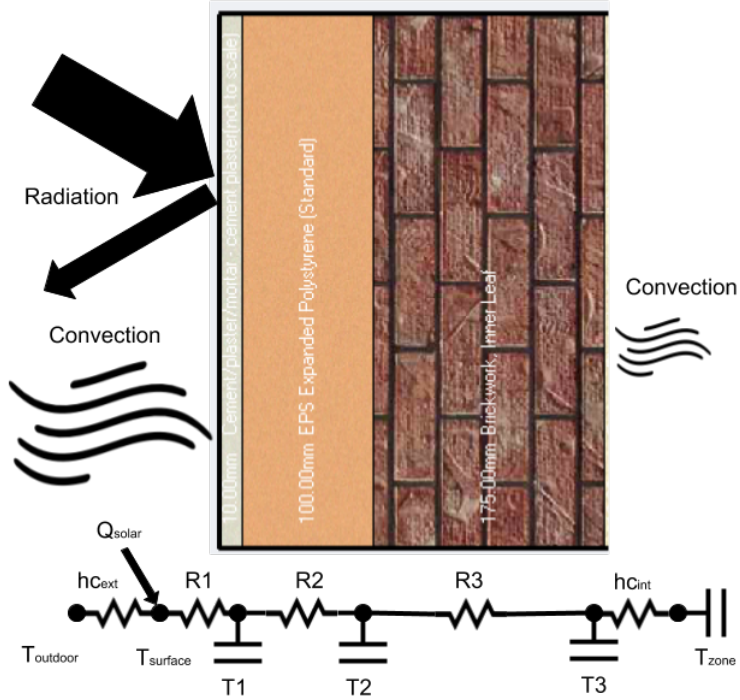


Figure 6.1: Building RC model exterior wall component showing boundary conditions and RC elements.

A similar solution for a Code Templating Tool (CoTeTo) for building models is presented in [151] that generates Modelica models from building data. This idea is attractive because existing data can be used to significantly reduce the modeling effort required to deploy MPC if the Modelica model can be utilized by the controller. The models generated by CoTeTo are however not suitable for use in the controller optimization as the models are not differentiable using CasADi. Similarly the RWTH-Teaser tool [127] generates Modelica models of building dynamics, yet these models also cannot be used for optimization for the same reason. To fill this need a building model

templating interface to Modelica has been implemented in Python to facilitate differentiable model generation. This templating interface uses a subset of the Modelica standard library and Modelica buildings library [166] (as not all Modelica language constructs are supported by automatic differentiation) to generate the building envelope components (exterior walls, roofs, floors, and interior walls) that can be simply composed into larger building models. The key to this implementation is the avoidance of integer variables and control flows depending on time varying states. The model equations can then be compiled through JModelica and algorithmically differentiated using CasADI to provide the first and second order derivatives for solving the resulting NLPs with IPOPT.

The boundary conditions of effective surface temperatures given short and long wave radiation and effective convections are calculated using the Verein Deutscher Ingenieure (VDI) 6007 guideline for calculation of transient thermal response of rooms and buildings as implemented in the Modelica buildings library [166]. Solar heat gain is calculated based on input weather data from an EnergyPlus Weather file (.EPW file format) and orientation angles of surfaces (tilt, azimuth, and latitude). This includes both direct normal radiation and diffuse horizontal radiation both given in hourly averaged W/m^2 . The exterior and interior convective heat transfer coefficients are taken from the literature for the context of low-rise buildings as described in the following section.

6.2 Parameters of Building Model for Simulation Experiments

The building model geometry consists of three thermal zones 10 m length by 5 m width by 3 m height comprising a single floor low-rise building. The geometry of the building is shown in Figure 6.2 below with a total floor area of 150 m^2 . The exterior wall area is 33% windows. The building has 15 unique occupants with a high density of 10 m^2 per occupant. The effect of doors is neglected and the windows are assumed to be inoperable. Crucially infiltration is neglected which significantly reduces the necessary heating requirement of the building, making the resulting case not representative of a real world building. Adding this could be quite simple, as it could be parametrized with a first order approximation of a thermal conductance. The goal of the simulation model is however to represent the dynamics of the occupants, each having unique occupancy and thermal preferences, all with the same averaged internal heat gains from metabolism of 83 W as mentioned in Section 2.3.

The building model uses parameters representative of relatively new construction within the existing building stock of Switzerland. The insulation thicknesses are taken to be for Swiss construction insulation after 1999 as reported in [119]. Each component is modelled thermally in one dimension with resistances and capacitances for each material layer of its construction. The physical parameters of each component are specified in two categories, 1) geometric properties: latitude (rad), azimuth (rad), tilt (rad), area (m^2), and thickness (m), and 2) thermal properties: thermal conductivity ($\text{W/m} \cdot \text{K}$), specific capacitance ($\text{W/kg} \cdot \text{K}$), density (kg/m^3), convection coefficient (exterior and interior in $\text{W/m}^2\text{K}$), and emissivity. The specific values for the thermal properties used in simulation experiments are given in Appendix Table B.6 from the ISO 10456 Building materials and products - Hygrothermal properties [23].

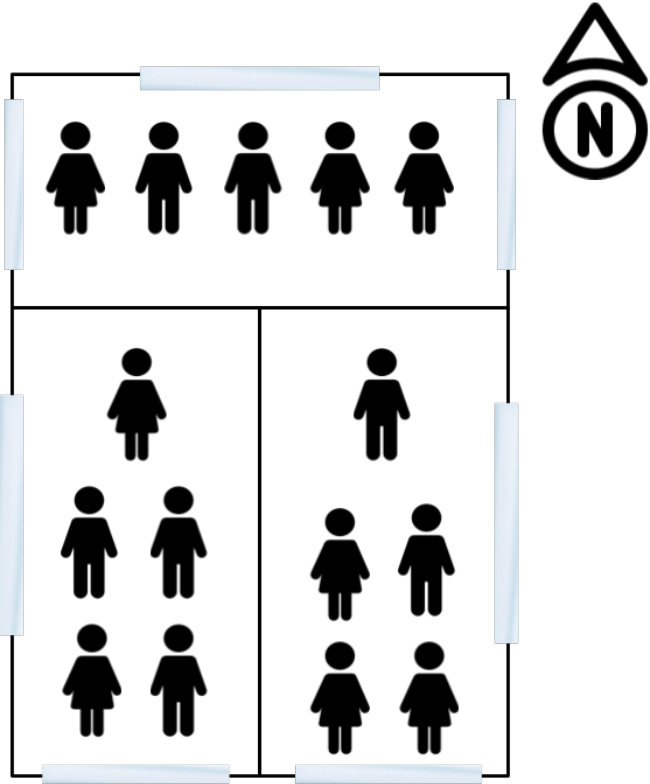


Figure 6.2: Building RC model exterior wall component showing boundary conditions and RC elements.

The windows are modelled after a double clear and low emissivity glazing shown in [55] to have a solar heat gain coefficient of 0.666 and thermal conductance of 1.99 W/m².K. This can be considered roughly typical for existing buildings in Switzerland [119]. The windows are parametrized as thermal resistors, assuming the heat capacity is negligible. This is a common assumption as even though glass has a relatively high heat capacity it is thin (e.g. two layers of 13mm) and therefore has relatively small mass. The additional infrared (long-wave) radiation is also considered in the effective outer surface temperature of the windows as computed using VDI 6007 as previously mentioned. The infrared emissivity of opaque exterior surfaces of asphalt (roofs) and plaster (exterior walls) are taken to be 0.9 [93].

External convective heat transfer coefficients are calculated for the average wind conditions (2.19 m s⁻¹ at 146 degrees clockwise from North) using the empirical correlations of free stream wind velocity for walls and flat roofs of low-rise buildings presented in [46] table 3, which compare well to existing methods. Given the respective surface-to-wind angles the convective heat transfer coefficients used are 7.4 W/m²K for North and West facing exterior walls, 6.5 W/m²K for South and East facing exterior walls, and 8.5 W/m²K for roofs. An extension would be to use the time series wind velocity to determine these coefficients for each time step in prediction.

The indoor convective heat transfer coefficients from natural convection due to the small temperature difference between an interior surface and zone air. Assuming this temperature difference to be less than 5K, and with a larger hydraulic radius than the data from [12], an upper bound can be taken from normalized charts. This gives approximate convective heat transfer coefficients of 2.7 W/m²K for interior wall surfaces (both surfaces of interior walls and the interior side of exterior walls), 0.5 W/m²K for ceilings (interior surface of roofs), and 3.2 W/m²K for floors.

Chapter 7

Simulation Experiments

Simulation experiments were run as proof of concept testing of the developed building control framework combining with the on-line predictive models of thermal preference and occupancy to implement MPC with human-in-the-loop feedback. Real thermal preference data has been used from the RP-884 database [37] as previously described. A meta-analysis of the RP 884 database is given in [40] showing distributions of variables within the different studies of the database. This variance between studies shows limitations of the dataset as a whole, however only small data sets of individual occupants, and all occupants from the same building (and therefore the same study), was used here. Specifically for developing ground truth occupant models preference models for on-line Bayesian updating of the posterior and initialization of models with an informed prior. These models infer probabilities which are then directly optimized over within the cost function of the MPC formulation. The results could be somewhat improved in a simulation scenario with greater variance in preferred temperatures by occupants. This chapter describes the specifics of the experiment implementation and discusses the results.

7.1 Simulation Setup

As mentioned in Section 5.1, a zero-order hold discretization scheme is used at a frequency of 3600 seconds (1 hour time steps). The weather data used is from the Geneva international weather files for energy calculations (IWEC). The experiments start on January 6th and have two unoccupied weekend days for the transient behavior from the initial temperature of all components to reach an appropriate thermal gradient from the interior zone air to the exterior. Comparisons are made between the proposed on-line learning controller to the perfect information controller and a standard comfort temperature (21°C) controller. The perfect information controller represents an upper bound (with best possible predictive models) while the standard comfort temperature (21°C) controller represents state of the art MPC (prescribed constant temperature set-point) with either perfect occupancy prediction or typical occupancy schedules. Each resulting time series is truncated when compared to other simulation results to allow for the same time frame of analysis as the minimal duration (roughly 20 days of simulation data). This difference in result timeseries length between experiments is due to a memory leak in the MPCPy interface with JModelica that causes simulations to crash after many iterations. Such a bug can be remedied with some effort but is an implementation detail that does not affect the results and conclusions presented here.

In MPCPy the number of finite elements for collocation (in JModelica) is set to the total experiment duration divided by the minimum sampling time. This ensures a sample point is at each

time step. The MPC horizon of 12 time steps each of one hour is used to ensure a horizon longer than the dynamics of the building which proved to be faster than desired when controlling for the air temperature in the zones. This causes pre-heating to be of negligible within the simulation experiments, forgoing much of the benefit MPC has over conventional set-point controllers. However the on-line MPC is only compared to other forms of MPC so this issue is reduced in the comparisons. Actuation is piece-wise constant between time steps as implemented using the *blocking_factors* CasADI option that only allows actuation switching at these predetermined time steps. The actuation was chosen to be an arbitrary heat source for each zone independently with the constraint $4000\text{W} \leq u_{z,k} \geq 0$. This could for example represent panel radiators on the interior surface of exterior walls below the windows as is common in many offices. As mentioned in Section 6.2 the building is modelled as a low-rise office building comprising three thermal zones, each of 50 m^2 (total 150 m^2) with 3 to 6 regular occupants.

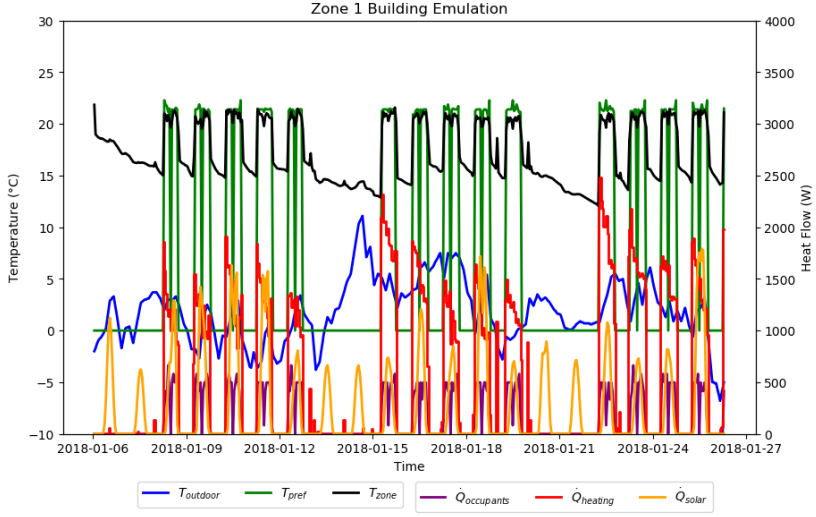
The on-line thermal preference and occupancy are initialized with prior data as described in Section 3.4 and Section 4.3 respectively. The lack of available data to build thermal preference models presents a limitation to the simulation results, with only five usable individual occupant longitudinal data sets in the RP-884 with a reasonable number of data points in each preference class. This includes four occupants from naturally ventilated buildings in Pakistan [112] and one occupant from a HVAC conditioned building in San Francisco [134]. With poor geographic and building type diversity (i.e. naturally ventilated) there is a clear lack of variation between the occupant data sets. Similarly the occupancy data for each occupant is simulated from the same Markov chain, only altering the office (thermal zone) which each occupant is to be present most of the time. With a greater variance in the thermal preferences and occupancy models the variance of the combined conditional distribution could be much larger. This would allow for further exploitation of predicted shifts to temperature preferences in a specific zone which would have allowed for greater energy savings and enhanced comfort (i.e. reduced preferences for change) with on-line learned individual thermal preference and occupancy models. The resulting simulation experiments were thus not favorable to exploitation with MPC using individualized thermal preference or occupancy models and should not be considered as representative of a real world scenario.

7.2 Simulation Results

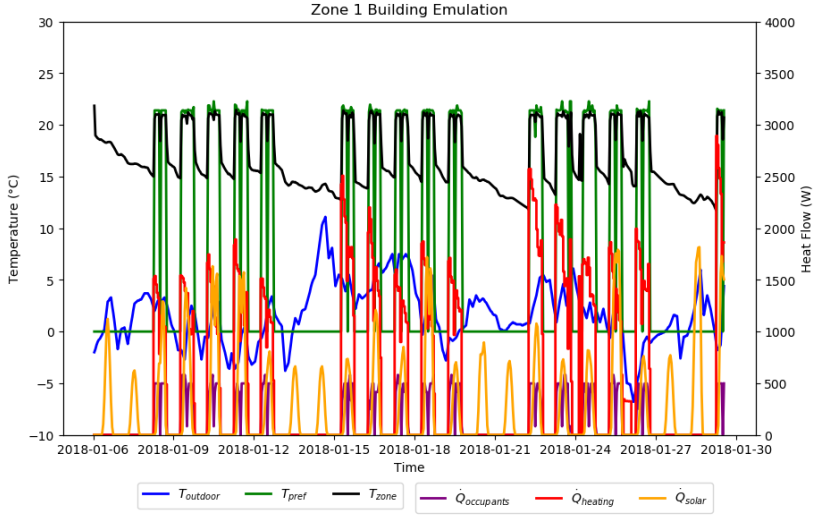
The resulting timeseries for the proposed on-line learning MPC controller for the first three weeks of operation in the first building zone are displayed in Figure 7.1 for on-line learning models of thermal preference and occupancy (a), perfect models of thermal preference and occupancy (b), and standard $21\text{ }^\circ\text{C}$ set-point with typical zone occupancy schedule (c). Emulation results for other building zones are displayed in Appendix C. The time series shows the outdoor temperature $T_{outdoor}$, preference temperature T_{pref} (the maximum comfort temperature given the zone occupancy and ground truth thermal preference models), and the resulting zone air temperature T_{zone} . One can see that (a) and (b) operate with T_{zone} just below T_{pref} , proportionally to the thermal preference probability, its cost, and its weighting ($l_c = l_w = 10$ are used in Figure 7.1).

Interestingly because of the neglected air infiltration heat losses the heat from occupants becomes quite similar to the input heat from actuation by the controller. Therefore the error in approximating each individual occupancy pattern causes considerable error to the disturbance predictions used by the controller, thus producing erratic zone temperatures with the on-line learned model. This actually works to the benefit of the standard model which over estimates the occupancy and thus slightly underheats the zone to just below $21\text{ }^\circ\text{C}$, which also happens to

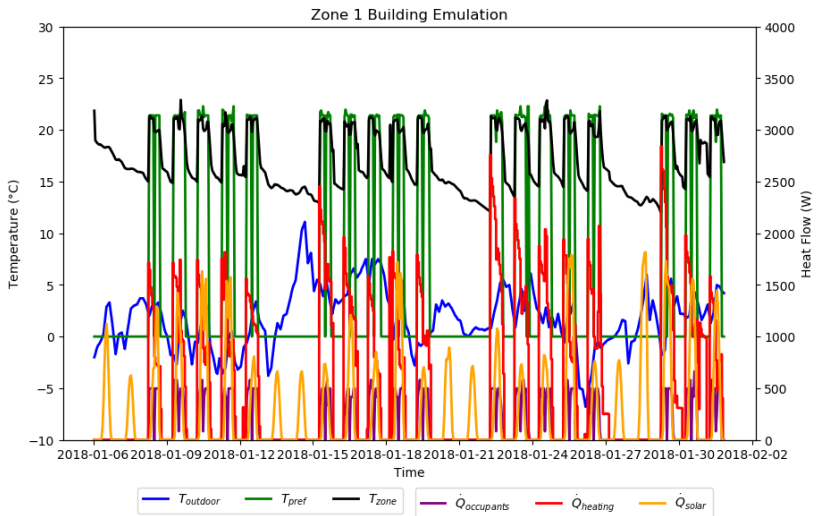
be the energy saving side near the zone optimal temperature. It is partly by coincidence that the occupant data used for the occupant thermal preference models has an the zone optimal temperature near 21 °C as recommended within Swiss norms as minimum for heating season. Clearly quite some thought has gone into these norms and in aggregate they are quite accurate. The nuance is that should specific situations arise where large variance from the norm exist the MPC framework is able to exploit it to either improve comfort, save energy, or do both. This is quite important when combining the occupancy and thermal preference models which allows for constructive interference of the variance between models to produce zone preference temperatures well below or above the values typically used for conditioning. This can be observed from the first, last and lunch hours of the simulations where due to variance in the occupancy the zone preference temperature changes.



(a) On-line learning models of thermal preference and occupancy.



(b) Perfect information models of thermal preference and occupancy.



(c) Standard model of minimum 21°C and schedule based occupancy model.

Figure 7.1: Simulation results with disturbances to building controlled with MPC using $l_c = l_w = 10$ with (a) on-line learning, (b) perfect information, and (c) standard comfort temperature (21°C) with schedule based occupancy, all for first zone of three zone building.

By varying the weighting of the thermal preference costs (l_c and l_w) a sensitivity analysis is performed to outline the pareto front representing the dominant strategies in the tradeoff between energy and thermal comfort (as measured by thermal preference hours) displayed in Figure 7.2. It is expected that as time progresses the on-line model methods (circles) would approach the perfect model costs plus some amount of error. Notably the on-line models may over take the standard constant set-point MPC controller, even with perfect occupancy models, as shown by the perfect model results (triangles) being superior to the standard model results (squares).

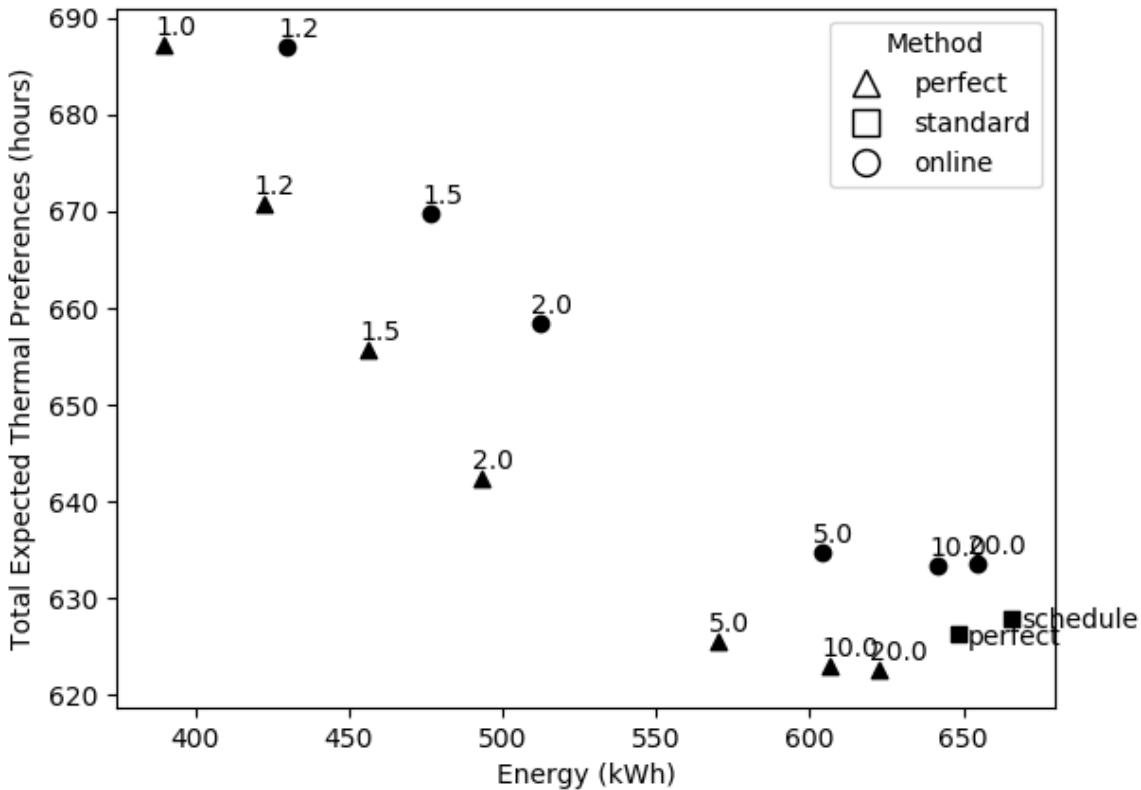


Figure 7.2: Pareto front of different model types with varied weighting of thermal preference (comfort). Standard models labeled with occupancy model (scheduled or perfect information) because they do not have a weighting and only track difference from 21°C.

In particular the weighting of $l_c = l_w = 5$ shows a nice trade off of comfort and energy, representing a total cost of thermal preference at 2.5% productivity decrease which is well within the figures mentioned in literature for thermal comfort. The cost comparison for this weighting is given in Figure 7.3 below.

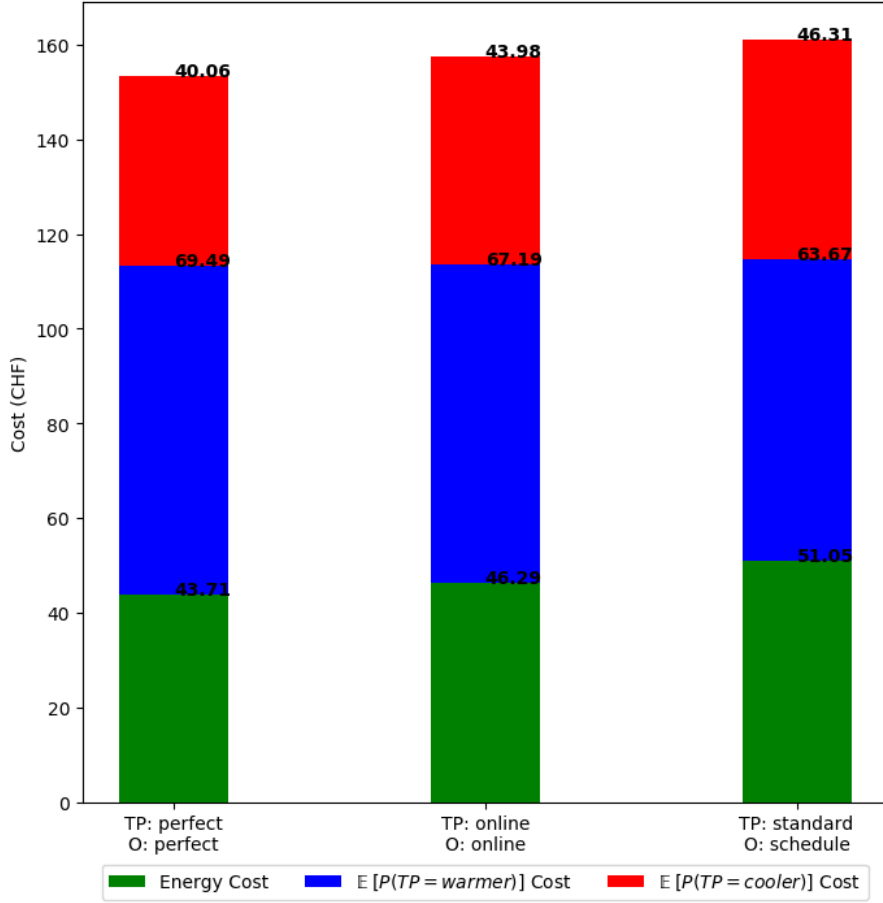


Figure 7.3: Cumulative cost (CHF) of energy and thermal preferences over first 20 days of simulation experiments for $l_c = l_w = 5$ with different thermal preference (TP) and occupancy (O) models.

Notably this weighting provides 14% energy savings over the constant temperature set-point MPC while providing an improved level of comfort with a slightly smaller expected number of thermal preference hours. This shows that both improving thermal comfort and reducing energy consumption is possible with this framework though is not indicative of possible savings in comparison to currently implemented controllers.

7.3 Conclusions

The concept of the *thermobile*, a building thermal conditioning controller that adapts to its environment and changing real thermal demands, has been implemented using MPC and investigated in simulation study showing promising proof of concept results for improving both energy savings and thermal comfort. The method uses human-in-the-loop feedback of direct thermal preference votes (e.g. collected from a mobile phone) and passive presence data from building occupants to update predictive Bayesian posterior models unique for each individual occupant. This novel feedback mechanism is a departure from the common consideration in building controls literature of thermal comfort as respecting prescribed temperature bounds by formulating determination of those bounds as a feedback loop with every occupant individually. This is done individually so that the combined variance of the inter-occupant models of thermal preference and occupancy can be exploited. As simple example, in a thermal zone with two occupants with different thermal preferences, if one occupant simply leaves for a significant time

this changes the comfort temperature because the preferences of the remaining occupant are modeled independently.

Similarly the consideration of the expected comfort cost within the MPC stage cost has been explored as means of explicitly confronting the tradeoff between energy cost and comfort. This should by all accounts favor occupant comfort for social and economic reasons and be represented in the cost weightings. Understanding the marginal costs and being able to optimize within the approximate comfort region additionally is crucial for defining energy efficient building conditioning systems. Notably it has been shown that aggregation of all preferences of occupants sharing a space through a thermal preference expectation function yields a tractable optimization problem and should align incentives of the occupants to providing truthful feedback to the on-line learning model representing their preferences. The core conceptual strategy of this controller being to not waste energy heating or cooling occupants who are unlikely to prefer it while keeping the occupants in the region where they are least likely in aggregate to have a preference to be warmer or cooler.

It remains future work to test this framework on larger datasets of real world thermal preferences and occupancy to quantify the opportunity for exploiting the variance between individual occupants thermal preferences and occupancy patterns. The lack of available data to build ground truth thermal preference models (with only five longitudinal data sets from the RP-884 database being usable) makes the quantitative results of the simulations of little consequence. It can however be seen qualitatively from these simulation experiments that should greater combined variance exist and cause situations of sustained shifts to the comfort temperature the proposed MPC control framework can indeed exploit them to achieve improved performance over a constant set-point temperature controller, even in MPC with the same predictive models for weather and occupancy. The implemented on-line learning models have reasonable convergence to near the ground truth models, however similar validation on larger real world data sets is required to make claims about performance. Development of new on-line learning algorithms and comparison to off-line methods is also important future work.

Bibliography

- [1] Abdul Afram and Farrokh Janabi-Sharifi. “Theory and applications of HVAC control systems—A review of model predictive control (MPC)”. In: *Building and Environment* 72 (2014), pp. 343–355.
- [2] Muhammad Aftab et al. “Automatic HVAC control with real-time occupancy recognition and simulation-guided model predictive control in low-cost embedded system”. In: *Energy and Buildings* 154 (2017), pp. 141–156.
- [3] Kaiser Ahmed, Jarek Kurnitski, Bjarne Olesen, et al. “Data for occupancy internal heat gain calculation in main building categories”. In: *Data in brief* 15 (2017), pp. 1030–1034.
- [4] Johan Åkesson, Magnus Gäfvert, and Hubertus Tummescheit. “Jmodelica—an open source platform for optimization of modelica models”. In: *6th Vienna International Conference on Mathematical Modelling*. 2009.
- [5] Johan Åkesson et al. “Modeling and optimization with Optimica and JModelica.org—Languages and tools for solving large-scale dynamic optimization problems”. In: *Computers & Chemical Engineering* 34.11 (2010), pp. 1737–1749.
- [6] Joel Andersson et al. “Integration of CasADI and JModelica.org”. In: *Proceedings of the 8th International Modelica Conference; March 20th-22nd; Technical University; Dresden; Germany*. 063. Linköping University Electronic Press. 2011, pp. 218–231.
- [7] Joel AE Andersson et al. “CasADI- a software framework for nonlinear optimization and optimal control”. In: *Mathematical Programming Computation* (2018), pp. 1–36.
- [8] Christophe Andrieu, Arnaud Doucet, and Roman Holenstein. “Particle markov chain monte carlo methods”. In: *Journal of the Royal Statistical Society: Series B (Statistical Methodology)* 72.3 (2010), pp. 269–342.
- [9] M Sanjeev Arulampalam et al. “A tutorial on particle filters for online nonlinear/non-Gaussian Bayesian tracking”. In: *IEEE Transactions on signal processing* 50.2 (2002), pp. 174–188.
- [10] ASHRAE Standard ASHRAE. “Standard 55-2013”. In: *Thermal environmental conditions for human occupancy* (2013), p. 12.
- [11] Ercan Atam. “Current software barriers to advanced model-based control design for energy-efficient buildings”. In: *Renewable and Sustainable Energy Reviews* 73 (2017), pp. 1031–1040.
- [12] Hazim B Awbi and A Hatton. “Natural convection from heated room surfaces”. In: *Energy and buildings* 30.3 (1999), pp. 233–244.
- [13] Magdalena Axelsson. “Nonlinear Model Predictive Control in JModelica.org”. In: (2015).

- [14] Magdalena Axelsson, Fredrik Magnusson, and Toivo Henningsson. “A framework for non-linear model predictive control in jmodelica.org”. In: *Proceedings of the 11th International Modelica Conference, Versailles, France, September 21-23, 2015*. 118. Linköping University Electronic Press. 2015, pp. 301–310.
- [15] David M Beazley et al. “SWIG: An Easy to Use Tool for Integrating Scripting Languages with C and C++.” In: *Tcl/Tk Workshop*. 1996.
- [16] R Becker and M Paciuk. “Thermal comfort in residential buildings—failure to predict by standard model”. In: *Building and Environment* 44.5 (2009), pp. 948–960.
- [17] Zsofia Belafi, Tianzhen Hong, and Andras Reith. “Smart building management vs. intuitive human control—Lessons learnt from an office building in Hungary”. In: *Building Simulation*. Vol. 10. 6. Springer. 2017, pp. 811–828.
- [18] Willy Bernal et al. “MLE+: a tool for integrated design and deployment of energy efficient building controls”. In: *Proceedings of the Fourth ACM Workshop on Embedded Sensing Systems for Energy-Efficiency in Buildings*. ACM. 2012, pp. 123–130.
- [19] Lorenz T Biegler and Victor M Zavala. “Large-scale nonlinear programming using IPOPT: An integrating framework for enterprise-wide dynamic optimization”. In: *Computers & Chemical Engineering* 33.3 (2009), pp. 575–582.
- [20] David M Blei, Alp Kucukelbir, and Jon D McAuliffe. “Variational inference: A review for statisticians”. In: *Journal of the American Statistical Association* 112.518 (2017), pp. 859–877.
- [21] Torsten Blochwitz et al. “Functional mockup interface 2.0: The standard for tool independent exchange of simulation models”. In: *Proceedings of the 9th International MODELICA Conference; September 3-5; 2012; Munich; Germany*. 076. Linköping University Electronic Press. 2012, pp. 173–184.
- [22] David Blum and Michael Wetter. “MPCpy: An open-source software platform for model predictive control in buildings”. In: *IBPSA Build. Simul. Conf.* Vol. 2017. 2017.
- [23] *Building materials and products - Hygrothermal properties - Tabulated design values and procedures for determining declared and design thermal values*. Standard. Geneva, CH: International Organization for Standardization, Jan. 2007.
- [24] C Buratti, P Ricciardi, and M Vergoni. “HVAC systems testing and check: a simplified model to predict thermal comfort conditions in moderate environments”. In: *Applied Energy* 104 (2013), pp. 117–127.
- [25] Davide Cali et al. “Analysis of occupants’ behavior related to the use of windows in German households”. In: *Building and Environment* 103 (2016), pp. 54–69.
- [26] Thomas A Catanach and James L Beck. “Bayesian Updating and Uncertainty Quantification using Sequential Tempered MCMC with the Rank-One Modified Metropolis Algorithm”. In: *arXiv preprint arXiv:1804.08738* (2018).
- [27] Chien-fei Chen, Xiaojing Xu, and Julia K Day. “Thermal comfort or money saving? Exploring intentions to conserve energy among low-income households in the United States”. In: *Energy Research & Social Science* 26 (2017), pp. 61–71.
- [28] Yuanda Cheng, Jianlei Niu, and Naiping Gao. “Thermal comfort models: A review and numerical investigation”. In: *Building and Environment* 47 (2012), pp. 13–22.
- [29] Jianye Ching and Yi-Chu Chen. “Transitional Markov chain Monte Carlo method for Bayesian model updating, model class selection, and model averaging”. In: *Journal of engineering mechanics* 133.7 (2007), pp. 816–832.

- [30] Nicolas Chopin, Pierre E Jacob, and Omiros Papaspiliopoulos. “SMC2: an efficient algorithm for sequential analysis of state space models”. In: *Journal of the Royal Statistical Society: Series B (Statistical Methodology)* 75.3 (2013), pp. 397–426.
- [31] Andrew Cowie et al. “Usefulness of the obFMU module examined through a review of occupant modelling functionality in building performance simulation programs”. In: *IBPSA Building Simulation Conference*. 2017.
- [32] Cristiana Croitoru et al. “Thermal comfort models for indoor spaces and vehicles-Current capabilities and future perspectives”. In: *Renewable and Sustainable Energy Reviews* 44 (2015), pp. 304–318.
- [33] Georgios Darivianakis et al. “A stochastic optimization approach to cooperative building energy management via an energy hub”. In: *Decision and Control (CDC), 2015 IEEE 54th Annual Conference on*. IEEE. 2015, pp. 7814–7819.
- [34] Georgios Darivianakis et al. “Scalability through decentralization: A robust control approach for the energy management of a building community”. In: *IFAC-PapersOnLine* 50.1 (2017), pp. 14314–14319.
- [35] Georgios Darivianakis et al. “The Power of Diversity: Data-Driven Robust Predictive Control for Energy-Efficient Buildings and Districts”. In: *IEEE Transactions on Control Systems Technology* (2017).
- [36] Richard De Dear and Gail Schiller Brager. “Developing an adaptive model of thermal comfort and preference”. In: (1998).
- [37] Richard J De Dear. “A global database of thermal comfort field experiments”. In: *ASHRAE transactions* 104 (1998), p. 1141.
- [38] R.J. De Dear et al. “Progress in thermal comfort research over the last twenty years”. In: *Indoor air* 23.6 (2013), pp. 442–461.
- [39] Richard de Dear. “Recent enhancements to the adaptive comfort standard in ASHRAE 55-2010”. In: *Proceedings of the 45th annual conference of the Architectural Science Association. Sydney, Australia: ANZAScA*. 2011.
- [40] Harimi Djamilia. “Indoor thermal comfort predictions: Selected issues and trends”. In: *Renewable and Sustainable Energy Reviews* 74 (2017), pp. 569–580.
- [41] Simona D’Oca et al. “Human-building interaction at work: Findings from an interdisciplinary cross-country survey in Italy”. In: *Building and Environment* 132 (2018), pp. 147–159.
- [42] Bing Dong et al. “Impact of Occupancy-Based Buildings-to-Grid Integration on Frequency Regulation in Smart Grids”. In: *2018 Annual American Control Conference (ACC)*. IEEE. 2018, pp. 5399–5405.
- [43] Bing Dong et al. “Modeling occupancy and behavior for better building design and operation-A critical review”. In: *Building Simulation*. Springer, pp. 1–23.
- [44] Arnaud Doucet, Nando De Freitas, and Neil Gordon. “An introduction to sequential Monte Carlo methods”. In: *Sequential Monte Carlo methods in practice*. Springer, 2001, pp. 3–14.
- [45] Annika Eichler, Georgios Darivianakis, and John Lygeros. “Humans in the loop: a stochastic predictive approach to building energy management in the presence of unpredictable users”. In: *IFAC-PapersOnLine* 50.1 (2017), pp. 14471–14476.
- [46] Marcelo G Emmel, Marc O Abadie, and Nathan Mendes. “New external convective heat transfer coefficient correlations for isolated low-rise buildings”. In: *Energy and Buildings* 39.3 (2007), pp. 335–342.

- [47] Bundesamt fur Energie. *Analyse des schweizerischen Energieverbrauchs 2000 - 2016 nach Verwendungszwecken*. http://www.bfe.admin.ch/themen/00526/00541/00542/02167/index.html?dossier_id=02169&lang=en. 2017.
- [48] Diana Enescu. "A review of thermal comfort models and indicators for indoor environments". In: *Renewable and Sustainable Energy Reviews* 79 (2017), pp. 1353–1379.
- [49] Omid Esmaili, Lisa Grant Ludwig, and Farzin Zareian. "Improved performance-based seismic assessment of buildings by utilizing Bayesian statistics". In: *Earthquake Engineering & Structural Dynamics* 45.4 (2016), pp. 581–597.
- [50] P Ole Fanger and Jørn Toftum. "Extension of the PMV model to non-air-conditioned buildings in warm climates". In: *Energy and buildings* 34.6 (2002), pp. 533–536.
- [51] Poul O Fanger et al. "Thermal comfort. Analysis and applications in environmental engineering." In: *Thermal comfort. Analysis and applications in environmental engineering*. (1970).
- [52] William J Fisk and Arthur H Rosenfeld. "Estimates of improved productivity and health from better indoor environments". In: *Indoor air* 7.3 (1997), pp. 158–172.
- [53] Daniel Fernández González and Luis J Yebra. "Comparison case between Modelica and specialized tools for building modelling". In: *IFAC-PapersOnLine* 48.1 (2015), pp. 874–879.
- [54] Siddharth Goyal, Herbert A Ingle, and Prabir Barooah. "Occupancy-based zone-climate control for energy-efficient buildings: Complexity vs. performance". In: *Applied Energy* 106 (2013), pp. 209–221.
- [55] Christian A Gueymard et al. "Spectral effects on the transmittance, solar heat gain, and performance rating of glazing systems". In: *Solar Energy* 83.6 (2009), pp. 940–953.
- [56] H Burak Gunay, William OBrien, and Ian Beausoleil-Morrison. "A critical review of observation studies, modeling, and simulation of adaptive occupant behaviors in offices". In: *Building and Environment* 70 (2013), pp. 31–47.
- [57] H Burak Gunay et al. "Modelling and analysis of unsolicited temperature setpoint change requests in office buildings". In: *Building and Environment* 133 (2018), pp. 203–212.
- [58] E Halawa and Joost van Hoof. "The adaptive approach to thermal comfort: A critical overview". In: *Energy and Buildings* 51 (2012), pp. 101–110.
- [59] Frédéric Haldi and Darren Robinson. "The impact of occupants' behaviour on building energy demand". In: *Journal of Building Performance Simulation* 4.4 (2011), pp. 323–338.
- [60] Frédéric Haldi et al. "Modelling diversity in building occupant behaviour: a novel statistical approach". In: *Journal of Building Performance Simulation* 10.5-6 (2017), pp. 527–544.
- [61] W Keith Hastings. "Monte Carlo sampling methods using Markov chains and their applications". In: (1970).
- [62] David B Hitchcock. "A history of the Metropolis–Hastings algorithm". In: *The American Statistician* 57.4 (2003), pp. 254–257.
- [63] Trong Nghia Hoang et al. "Collective Online Learning via Decentralized Gaussian Processes in Massive Multi-Agent Systems". In: *arXiv preprint arXiv:1805.09266* (2018).
- [64] Tianzhen Hong et al. "Advances in research and applications of energy-related occupant behavior in buildings". In: *Energy and Buildings* 116 (2016), pp. 694–702.
- [65] Tianzhen Hong et al. "An occupant behavior modeling tool for co-simulation". In: *Energy and Buildings* 117 (2016), pp. 272–281.

- [66] Tianzhen Hong et al. “An ontology to represent energy-related occupant behavior in buildings. Part I: Introduction to the DNAs framework”. In: *Building and Environment* 92 (2015), pp. 764–777.
- [67] Tianzhen Hong et al. “Occupant behavior models: A critical review of implementation and representation approaches in building performance simulation programs”. In: *Building Simulation*. Springer. 2017, pp. 1–14.
- [68] Tianzhen Hong et al. “Ten questions concerning occupant behavior in buildings: The big picture”. In: *Building and Environment* 114 (2017), pp. 518–530.
- [69] Michael A Humphreys and Mary Hancock. “Do people like to feel ‘neutral’?: Exploring the variation of the desired thermal sensation on the ASHRAE scale”. In: *Energy and Buildings* 39.7 (2007), pp. 867–874.
- [70] ISO ISO. “Standard 7730”. In: *Moderate Thermal Environments-Determination of the PMV and PPD Indices and Specification of the Conditions for Thermal Comfort* (1984).
- [71] Achin Jain et al. “Learning and Control using Gaussian Processes”. In: (2017).
- [72] Gareth James et al. *An introduction to statistical learning*. Vol. 112. Springer, 2013.
- [73] Ruoxi Jia and Costas Spanos. “Occupancy modelling in shared spaces of buildings: a queueing approach”. In: *Journal of Building Performance Simulation* 10.4 (2017), pp. 406–421.
- [74] Byron W Jones. “Capabilities and limitations of thermal models for use in thermal comfort standards”. In: *Energy and Buildings* 34.6 (2002), pp. 653–659.
- [75] Filip Jorissen and Lieve Helsen. “Towards an Automated Tool Chain for MPC in Multi-zone Buildings”. In: (2016).
- [76] M Jradi et al. “ObepME: An online building energy performance monitoring and evaluation tool to reduce energy performance gaps”. In: *Energy and Buildings* 166 (2018), pp. 196–209.
- [77] Nikolas Kantas et al. “On particle methods for parameter estimation in state-space models”. In: *Statistical science* 30.3 (2015), pp. 328–351.
- [78] M Killian and M Kozek. “Ten questions concerning model predictive control for energy efficient buildings”. In: *Building and Environment* 105 (2016), pp. 403–412.
- [79] Joyce Kim, Stefano Schiavon, and Gail Brager. “Personal comfort models—A new paradigm in thermal comfort for occupant-centric environmental control”. In: *Building and Environment* 132 (2018), pp. 114–124.
- [80] Joyce Kim et al. “Personal comfort models: predicting individuals’ thermal preference using occupant heating and cooling behavior and machine learning”. In: *Building and Environment* 129 (2018), pp. 96–106.
- [81] K Konis and M Annavararam. “The occupant mobile gateway: a participatory sensing and machine-learning approach for occupant-aware energy management”. In: *Building and Environment* 118 (2017), pp. 1–13.
- [82] Steven Lamb and Kenny CS Kwok. “A longitudinal investigation of work environment stressors on the performance and wellbeing of office workers”. In: *Applied ergonomics* 52 (2016), pp. 104–111.
- [83] Mathieu GA Lapotre, Bethany L Ehlmann, and Sarah E Minson. “A probabilistic approach to remote compositional analysis of planetary surfaces”. In: *Journal of Geophysical Research: Planets* 122.5 (2017), pp. 983–1009.

- [84] Adrian Leaman and Bill Bordass. "Assessing building performance in use 4: the Probe occupant surveys and their implications". In: *Building Research & Information* 29.2 (2001), pp. 129–143.
- [85] Donghwan Lee et al. "Approximate Dynamic Programming for Building Control Problems with Occupant Interactions". In: (2018).
- [86] Donghwan Lee et al. "Simulation-based policy gradient and its building control application". In: *2018 Annual American Control Conference (ACC)*. IEEE. 2018, pp. 5424–5429.
- [87] Seungjae Lee et al. "A Bayesian approach for probabilistic classification and inference of occupant thermal preferences in office buildings". In: *Building and Environment* 118 (2017), pp. 323–343.
- [88] Zhaoxuan Li and Bing Dong. "A new modeling approach for short-term prediction of occupancy in residential buildings". In: *Building and Environment* 121 (2017), pp. 277–290.
- [89] Zhaoxuan Li and Bing Dong. "Short term predictions of occupancy in commercial buildings—Performance analysis for stochastic models and machine learning approaches". In: *Energy and Buildings* 158 (2018), pp. 268–281.
- [90] Song Liu et al. "Change-point detection in time-series data by relative density-ratio estimation". In: *Neural Networks* 43 (2013), pp. 72–83.
- [91] Fredrik Magnusson. "Numerical and symbolic methods for dynamic optimization". In: (2016).
- [92] Fredrik Magnusson and Johan Åkesson. "Dynamic optimization in jmodelica.org". In: *Processes* 3.2 (2015), pp. 471–496.
- [93] Concetta Marino, Francesco Minichiello, and William Bahnfleth. "The influence of surface finishes on the energy demand of HVAC systems for existing buildings". In: *Energy and Buildings* 95 (2015), pp. 70–79.
- [94] Julien F Marquant et al. "A holarchic approach for multi-scale distributed energy system optimisation". In: *Applied Energy* 208 (2017), pp. 935–953.
- [95] Kathryn J McCartney and J Fergus Nicol. "Developing an adaptive control algorithm for Europe". In: *Energy and buildings* 34.6 (2002), pp. 623–635.
- [96] DA McIntyre. *Indoor climate*. Elsevier, 1980.
- [97] Nicholas Metropolis et al. "Equation of state calculations by fast computing machines". In: *The journal of chemical physics* 21.6 (1953), pp. 1087–1092.
- [98] Bert Metz et al. *Climate change 2007: mitigation of climate change*. Cambridge Univ. Press, 2007.
- [99] Clayton Miller et al. "Urban and building multiscale co-simulation: case study implementations on two university campuses". In: *Journal of Building Performance Simulation* 11.3 (2018), pp. 309–321.
- [100] SE Minson, M Simons, and JL Beck. "Bayesian inversion for finite fault earthquake source models I - Theory and algorithm". In: *Geophysical Journal International* 194.3 (2013), pp. 1701–1726.
- [101] Amin Mirakhori and Bing Dong. "Market and behavior driven predictive energy management for residential buildings". In: *Sustainable Cities and Society* 38 (2018), pp. 723–735.

- [102] Amin Mirakhori and Bing Dong. “Model predictive control for building loads connected with a residential distribution grid”. In: *Applied Energy* 230 (2018), pp. 627–642.
- [103] Amin Mirakhori and Bing Dong. “Occupancy behavior based model predictive control for building indoor climate-A critical review”. In: *Energy and Buildings* 129 (2016), pp. 499–513.
- [104] Asit Kumar Mishra and Maddali Ramgopal. “Field studies on human thermal comfort an overview”. In: *Building and Environment* 64 (2013), pp. 94–106.
- [105] Daisuke Motoki. *Github - change point detector*. 2017.
- [106] D Müller et al. “AixLib–An Open-Source Modelica Library within the IEA-EBC Annex 60 Framework”. In: *BauSIM 2016* (2016), pp. 3–9.
- [107] Tapsya Nayak et al. “Prediction of Human Performance Using Electroencephalography under Different Indoor Room Temperatures”. In: *Brain sciences* 8.4 (2018).
- [108] Sophie Naylor, Mark Gillott, and Tom Lau. “A review of occupant-centric building control strategies to reduce building energy use”. In: *Renewable and Sustainable Energy Reviews* 96 (2018), pp. 1–10.
- [109] Lucas Hermann Negri and Christophe Vestri. *lucashn/peakutils: v1.1.0*. Sept. 2017.
- [110] Fergus Nicol and Michael Humphreys. “Derivation of the adaptive equations for thermal comfort in free-running buildings in European standard EN15251”. In: *Building and Environment* 45.1 (2010), pp. 11–17.
- [111] Fergus Nicol, Michael Humphreys, and Susan Roaf. *Adaptive thermal comfort: Foundations and analysis*. Routledge, 2015.
- [112] Fergus Nicol, Gal Najam Jamy, and Oliver Sykes. *A Survey of Thermal Comfort in Pakistan: Toward New Indoor Temperature Standards; Final Report*. School of Architecture, Oxford Brookes Univ., 1994.
- [113] William O’Brien et al. “International survey on current occupant modelling approaches in building performance simulation”. In: *Journal of Building Performance Simulation* 10.5-6 (2017), pp. 653–671.
- [114] Federal Statistical Office. *Wage levels - Switzerland*.
- [115] Frauke Oldewurtel, David Sturzenegger, and Manfred Morari. “Importance of occupancy information for building climate control”. In: *Applied energy* 101 (2013), pp. 521–532.
- [116] Frauke Oldewurtel et al. “Use of model predictive control and weather forecasts for energy efficient building climate control”. In: *Energy and Buildings* 45 (2012), pp. 15–27.
- [117] Nigel A Oseland. “Predicted and reported thermal sensation in climate chambers, offices and homes”. In: *Energy and Buildings* 23.2 (1995), pp. 105–115.
- [118] Antonio Paone and Jean-Philippe Bacher. “The Impact of Building Occupant Behavior on Energy Efficiency and Methods to Influence It: A Review of the State of the Art”. In: *Energies* 11.4 (2018), p. 953.
- [119] Agis M Papadopoulos. “State of the art in thermal insulation materials and aims for future developments”. In: *Energy and Buildings* 37.1 (2005), pp. 77–86.
- [120] Theis Heidmann Pedersen and Steffen Petersen. “Investigating the performance of scenario-based model predictive control of space heating in residential buildings”. In: *Journal of Building Performance Simulation* (2017), pp. 1–14.
- [121] Theis Heidmann Pedersen and Steffen Petersen. “Investigating the performance of scenario-based model predictive control of space heating in residential buildings”. In: *Journal of Building Performance Simulation* 11.4 (2018), pp. 485–498.

- [122] Yuzhen Peng et al. “Using machine learning techniques for occupancy-prediction-based cooling control in office buildings”. In: *Applied Energy* 211 (2018), pp. 1343–1358.
- [123] Luis Pérez-Lombard, José Ortiz, and Christine Pout. “A review on buildings energy consumption information”. In: *Energy and buildings* 40.3 (2008), pp. 394–398.
- [124] Nikolina Pivac, Sandro Nizetic, and Vlasta Zanki. “The Current State of Research on Thermal Comfort Prediction Models”. In: *2018 3rd International Conference on Smart and Sustainable Technologies (SpliTech)*. IEEE. 2018, pp. 1–6.
- [125] Gilles Plessis, Aurélie Kaemmerlen, and Amy Lindsay. “BuildSysPro: a Modelica library for modelling buildings and energy systems”. In: *Proceedings of the 10 th International Modelica Conference; March 10-12; 2014; Lund; Sweden*. 96. Linköping University Electronic Press. 2014, pp. 1161–1169.
- [126] James B Rawlings, David Q Mayne, and Moritz M Diehl. “Model predictive control: Theory, Computation, and Design 2nd Edition”. In: (2017).
- [127] Peter Remmen et al. “TEASER: an open tool for urban energy modelling of building stocks”. In: *Journal of Building Performance Simulation* 11.1 (2018), pp. 84–98.
- [128] M Robillart et al. “Model reduction and model predictive control of energy-efficient buildings for electrical heating load shifting”. In: *Journal of Process Control* (2018).
- [129] Peter Rockett and Elizabeth Abigail Hathway. “Model-predictive control for non-domestic buildings: a critical review and prospects”. In: *Building Research & Information* 45.5 (2017), pp. 556–571.
- [130] Nancy C Ruck. “Building design and human performance”. In: (1989).
- [131] Ricardo Forgiarini Rupp, Natalia Giraldo Vásquez, and Roberto Lamberts. “A review of human thermal comfort in the built environment”. In: *Energy and Buildings* 105 (2015), pp. 178–205.
- [132] John Salvatier, Thomas V Wiecki, and Christopher Fonnesbeck. “Probabilistic programming in Python using PyMC3”. In: *PeerJ Computer Science* 2 (2016), e55.
- [133] Roozbeh Sangi et al. “A platform for the agent-based control of HVAC systems”. In: *Proceedings of the 12th International Modelica Conference, Prague, Czech Republic, May 15-17, 2017*. 132. Linköping University Electronic Press. 2017, pp. 799–808.
- [134] Gall Schiller et al. “A field study of thermal environments and comfort in office buildings”. In: (1988).
- [135] Georg Ferdinand Schneider, Georg Ambrosius Peßler, and Simone Steiger. “Modelling and Simulation of Standardised Control Functions from Building Automation”. In: *Proceedings of the 12th International Modelica Conference, Prague, Czech Republic, May 15-17, 2017*. 132. Linköping University Electronic Press. 2017, pp. 209–218.
- [136] Steffen Schütte, Stefan Scherfke, and Michael Sonnenschein. “Mosaik-smart grid simulation API”. In: *Proceedings of SMARTGREENS* (2012), pp. 14–24.
- [137] Torsten Schwan, René Unger, and Jörg Pipiorke. “Aspects of FMI in Building Simulation”. In: *Proceedings of the 12th International Modelica Conference, Prague, Czech Republic, May 15-17, 2017*. 132. Linköping University Electronic Press. 2017, pp. 73–78.
- [138] Marcel Schweiker and Andreas Wagner. “A framework for an adaptive thermal heat balance model (ATHB)”. In: *Building and Environment* 94 (2015), pp. 252–262.
- [139] Marcel Schweiker and Andreas Wagner. “Influences on the predictive performance of thermal sensation indices”. In: *Building Research & Information* 45.7 (2017), pp. 745–758.

- [140] Marcel Schweiker et al. “Challenging the assumptions for thermal sensation scales”. In: *Building Research & Information* 45.5 (2017), pp. 572–589.
- [141] Christian Schweizer et al. “Indoor time–microenvironment–activity patterns in seven regions of Europe”. In: *Journal of Exposure Science and Environmental Epidemiology* 17.2 (2007), p. 170.
- [142] Sally Shahzad et al. “A study of the impact of individual thermal control on user comfort in the workplace: Norwegian cellular vs. British open plan offices”. In: *Architectural Science Review* 60.1 (2017), pp. 49–61.
- [143] Pervez Hameed Shaikh et al. “A review on optimized control systems for building energy and comfort management of smart sustainable buildings”. In: *Renewable and Sustainable Energy Reviews* 34 (2014), pp. 409–429.
- [144] David Sturzenegger. “Model predictive building climate control: Steps towards practice”. PhD thesis. ETH Zurich, 2014.
- [145] David Sturzenegger et al. “BRCM Matlab toolbox: Model generation for model predictive building control”. In: *American Control Conference (ACC), 2014*. IEEE. 2014, pp. 1063–1069.
- [146] David Sturzenegger et al. “Model predictive climate control of a swiss office building: Implementation, results, and cost–benefit analysis”. In: *IEEE Transactions on Control Systems Technology* 24.1 (2016), pp. 1–12.
- [147] Mohammad Taleghani et al. “A review into thermal comfort in buildings”. In: *Renewable and Sustainable Energy Reviews* 26 (2013), pp. 201–215.
- [148] Shin-ichi Tanabe, Masaoki Haneda, and Naoe Nishihara. “Workplace productivity and individual thermal satisfaction”. In: *Building and Environment* 91 (2015), pp. 42–50.
- [149] Marko Tanaskovic et al. “Robust adaptive model predictive building climate control”. In: *IFAC-PapersOnLine* 50.1 (2017), pp. 1871–1876.
- [150] Hélène Thieblemont et al. “Predictive control strategies based on weather forecast in buildings with energy storage system: A review of the state-of-the art”. In: *Energy and Buildings* 153 (2017), pp. 485–500.
- [151] Matthias Thorade et al. “An open toolchain for generating Modelica code from Building Information Models”. In: *Proceedings of the 11th International Modelica Conference, Versailles, France, September 21-23, 2015*. 118. Linköping University Electronic Press. 2015, pp. 383–391.
- [152] Michal Vesely and Wim Zeiler. “Personalized conditioning and its impact on thermal comfort and energy performance—A review”. In: *Renewable and Sustainable Energy Reviews* 34 (2014), pp. 401–408.
- [153] Andreas Wächter and Lorenz T Biegler. “On the implementation of an interior-point filter line-search algorithm for large-scale nonlinear programming”. In: *Mathematical programming* 106.1 (2006), pp. 25–57.
- [154] Andreas Wagner, William O’Brien, and Bing Dong. *Exploring occupant behavior in buildings: methods and challenges*. Springer, 2017.
- [155] Chuang Wang, Da Yan, and Yi Jiang. “A novel approach for building occupancy simulation”. In: *Building simulation*. Vol. 4. 2. Springer. 2011, pp. 149–167.
- [156] Kunpeng Wang, Peer-Olaf Siebers, and Darren Robinson. “Towards Generalized Co-simulation of Urban Energy Systems”. In: *Procedia Engineering* 198 (2017), pp. 366–374.

- [157] Wei Wang, Jiayu Chen, and Tianzhen Hong. “Modeling occupancy distribution in large spaces with multi-feature classification algorithm”. In: *Building and Environment* 137 (2018), pp. 108–117.
- [158] Wei Wang et al. “Occupancy prediction through Markov based feedback recurrent neural network (M-FRNN) algorithm with WiFi probe technology”. In: *Building and Environment* 138 (2018), pp. 160–170.
- [159] Zeyu Wang and Ravi S Srinivasan. “A review of artificial intelligence based building energy use prediction: Contrasting the capabilities of single and ensemble prediction models”. In: *Renewable and Sustainable Energy Reviews* 75 (2017), pp. 796–808.
- [160] Paweł Wargocki and David P Wyon. “Ten questions concerning thermal and indoor air quality effects on the performance of office work and schoolwork”. In: *Building and Environment* 112 (2017), pp. 359–366.
- [161] Michael Wetter, Marco Bonvini, and Thierry S Nouidui. “Equation-based languages—A new paradigm for building energy modeling, simulation and optimization”. In: *Energy and Buildings* 117 (2016), pp. 290–300.
- [162] Michael Wetter and Christoph Haugstetter. “Modelica versus TRNSYS—A comparison between an equation-based and a procedural modeling language for building energy simulation”. In: *Proceedings of SimBuild 2.1* (2006).
- [163] Michael Wetter and Christoph van Treeck. “IEA EBC Annex 60: New Generation Computing Tools for Building and Community Energy Systems”. In: *The Regents of the University of California and RWTH Aachen University* (2017).
- [164] Michael Wetter, Christoph van Treeck, and Jan Hensen. “New generation computational tools for building and community energy systems”. In: *Energy in Buildings and Communities Programme. IEA EBC Annex 60* (2013).
- [165] Michael Wetter et al. “IEA EBC annex 60 modelica library—an international collaboration to develop a free open-source model library for buildings and community energy systems”. In: *Proceedings of building simulation 2015*. 2015.
- [166] Michael Wetter et al. “Modelica buildings library”. In: *Journal of Building Performance Simulation* 7.4 (2014), pp. 253–270.
- [167] Makoto Yamada. *Sugiyama-Sato-Honda Lab at the University of Tokyo*.
- [168] Makoto Yamada et al. “Relative density-ratio estimation for robust distribution comparison”. In: *Neural computation* 25.5 (2013), pp. 1324–1370.
- [169] Da Yan and Tianzhen Hong. *EBC Annex 66 Final Report - Definition and simulation of occupant behavior in buildings*. May 2018.
- [170] Da Yan et al. “IEA EBC Annex 66: Definition and simulation of occupant behavior in buildings”. In: *Energy and Buildings* 156 (2017), pp. 258–270.
- [171] Rui Yang and Lingfeng Wang. “Development of multi-agent system for building energy and comfort management based on occupant behaviors”. In: *Energy and Buildings* 56 (2013), pp. 1–7.
- [172] Rui Yang and Lingfeng Wang. “Multi-objective optimization for decision-making of energy and comfort management in building automation and control”. In: *Sustainable Cities and Society* 2.1 (2012), pp. 1–7.
- [173] Xin Zhang, Qiang Miao, and Zhiwen Liu. “Remaining useful life prediction of lithium-ion battery using an improved UPF method based on MCMC”. In: *Microelectronics Reliability* 75 (2017), pp. 288–295.

- [174] Yan Zhang et al. “Rethinking the role of occupant behavior in building energy performance: A review”. In: *Energy and Buildings* (2018).
- [175] Yi Zhang and Jonathan Koren. “Efficient bayesian hierarchical user modeling for recommendation system”. In: *Proceedings of the 30th annual international ACM SIGIR conference on Research and development in information retrieval*. ACM. 2007, pp. 47–54.
- [176] Jie Zhao et al. “Occupant individual thermal comfort data analysis in an office”. In: *Sustainable Human-Building Ecosystems*. 2015, pp. 108–116.

Appendix A

Thermal Comfort Methods

A.1 Steady-State Heat Balance

The steady-state heat balance from the PMV method [51], or heat load (L) in W is given below as a function of: air dry-bulb temperature (T_{air}) in K, mean radiant temperature (MRT) in K, air velocity (V_{air}) in m/s², relative humidity RH , metabolic rate M and work W in W, and clothing insulation I_{cl} in clo (1 clo = 0.155 Km²W⁻¹ or R-SI).

$$\begin{aligned}
 L &= (M - W) - h_{loss} \\
 h_{loss} &= h_{radiation} + h_{convection} + h_{evaporation} + h_{respiration} + h_{sweat} \\
 h_{radiation} &= 3.96 \times 10^{-8} \cdot f_{cl} \cdot (T_{cl}^4 - MRT^4) \\
 h_{convection} &= f_{cl} \cdot h_c \cdot (T_{cl} - T_{air}) \\
 h_{evaporation} &= 3.05 \cdot (5.73 - 0.007 \cdot (M - W) - p_a) \\
 h_{respiration} &= 0.0014 \cdot M \cdot (34 - (T_{air} - 273.15)) + 0.0173 \cdot M \cdot (5.87 - p_a) \\
 h_{sweat} &= 0.42 \cdot (M - W - 58.15) \\
 h_c &= \max(2.38 \cdot (T_{cl} - T_{air})^{0.25}, 12.1 \cdot \sqrt{V_{air}}) \\
 f_{cl} &= \begin{cases} 1.0 + 0.2 \cdot I_{cl}, & \text{if } I_{cl} < 0.5 \text{clo} \\ 1.05 + 0.1 \cdot I_{cl}, & \text{otherwise} \end{cases} \\
 p_a &= RH \cdot 10 \cdot e^{-((16.6536 - 4030.183)/(T_{air} - 273.15 + 235))} \\
 T_{cl} &= T_{skin} - 0.155 \cdot I_{cl} \cdot (h_{radiation} + h_{convection}) \\
 T_{skin} &= 308.7 - 0.0275 \cdot (MET - W)
 \end{aligned} \tag{A.1}$$

A.2 Adaptive Thermal Comfort

The adaptive thermal comfort standard, which has been introduced in the ASHRAE 55-2004 and EN15251 standards, uses a linear correlation between a prescribed indoor comfort temperature and the running mean outdoor temperature [110]. The EN15251 standard developed for free-running buildings by Nicol and Humphreys gives the following relation for the comfort temperature and outdoor running mean temperature.

Category	Application	Limit
1	Spaces occupied by very sensitive and fragile persons	± 2 K
2	New buildings and renovations	± 3 K
3	Existing buildings	± 4 K
4	Only acceptable for a limited periods	$\pm >4$ K

Table A.1: EN15251 standard categories of acceptable temperature ranges in free-running mode, from [110].

$$T_{comf} = 0.33T_{rm} + 18.8 \quad (\text{A.2})$$

The running mean outdoor temperature is defined in [110] as $T_{rm} = (1 - \alpha) \sum_{i=0}^n \alpha^i T_{od-i}$, where T_{od} is the outdoor mean temperature for indexed for each day. The recommended decay rate α is 0.8 [110]. In this work each previous 24 hour period from the current time is considered instead of calendar date to allow for the temperature of the current day to be considered in a continuous fashion. In the EN15251 standard the difference from this comfort temperature separates the level comfort into different categories. The best being category 1 with a difference of +/- 2K. The categories are given in table X below from the standard.

The ASHRAE scale is used to generate these correlations rather than the MCI considered in this present work. There are additional caveats about applicability in cold climates where the linear correlation would prescribe low indoor temperatures. The adaptive thermal comfort standard implementation has been used in this work as a baseline comparison for predicting thermal comfort. However because it is only valid for cooling mode (and not in heating mode) the results are not reported here.

Appendix B

Building Simulation

B.1 Building Simulation Software

This chapter compares building simulation platforms in 1) ability to simulate whole building dynamics, 2) ability to integrate third-party models (for occupant behaviour), and 3) capability for optimization within MPC framework. Notably, co-simulation environments are increasingly favoured for 2) and 3) that can use the tried and tested methods developed meeting criteria in 1) with open interfaces such as the Functional Mock-up Interface (FMI) standard [21]. For this reason three types of simulation software are discussed: whole building simulation programs, building component models, and co-simulation environments.

B.2 Whole Building Simulation Software

Whole building simulation software is typically used in building design for energy performance assessment. Use in control design or building operations is not often considered. However these developed models are generally described as being the most accurate in terms of building dynamics despite recognized performance gaps. The most widely adopted software packages are compared in table B.1.

As shown in [67] every whole building simulation analysed has a different native input file format (either text or binary based) making interoperability with other simulation software difficult. Additionally, proprietary closed source software (e.g. IES VE) only distribute compiled binaries which dissuade third party model integration or optimization. The modular FMI approach has been proposed for fixing the interoperability issues [67] yet few packages support it. In co-simulation one strength of the FMI is that it allows for each model to be evaluated with its own solver and time constants, thus avoiding stiff ODE systems in coupling and allowing fine grain performance optimization [137]. The FMI itself is a tool independent standard to support both model exchange (ME) and co-simulation (CS) of dynamic models using a common API for specifying the exchange of data during co-simulation. This is implemented with a combination of XML-files, C-header files, and C-code or just compiled binaries [21].

EnergyPlus is the most common simulation package used in research. It is also quite well known in industry as well. The BRCM interfaces with EnergyPlus via the Input Data Files (IDF) and is able to import the thermal model of the building to create a discretized state matrix (A),

Software	Developer	FMI support	Summary
EnergyPlus ¹	DoE BTO, NREL, Lawrence Berkely Lab	FMI CS 1.0 ²	Most common building simulation tool. Free and open source ³ . GUIs available, e.g. OpenStudio ⁴ and DesignBuilder ⁵ .
IDA ICE ⁶	EQUA Simulation AB	None	Commercial closed source
IES VE ⁷	Integrated Environmental Solutions Ltd	None	Commercial closed source
TRNSYS ⁸	TRNSYS Developers Group	FMI CS 2.0 ⁹	Commercial semi-open source
TRACE 700 ¹⁰	Trane	None	Commercial closed source
ESP-r ¹¹	Energy Systems Research Unit (ESRU) University of Strathclyde	Co-Simulation	Primarily used in research, free open source ¹²

Table B.1: Whole building simulation software packages

although the actuation characteristics cannot be imported directly from the EnergyPlus model and must be specified by hand (i.e. the B matrix).

B.3 Building Component Models

Another way to simulate a whole building is with component models that can be connected together. One point of potential confusion is that these component models can be co-simulated with some whole building energy simulations, notably EnergyPlus allows this level of integration through the FMI standard where one defines which variables are exposed through the EnergyPlus FMU, as used in [99] to co-simulate with CitySim on an urban scale. Table B.2 shows a list of existing component models.

Co-simulation is becoming increasingly common when simulating large systems such as urban energy systems [156] and smaller systems that are being modelled with increasing complexity such as building energy models (BEM). A strong proponent of this has been the the IEA EBC Annex 60, now continued 2017 to 2022 as IBPSA Project 1¹³, which implements physical equation based models for building components written in Modelica [164]. These equation based models

¹<https://energyplus.net/>

²<https://github.com/lbl-srg/EnergyPlusToFMU>

³<https://github.com/NREL/EnergyPlus>

⁴<https://github.com/NREL/OpenStudio>

⁵<https://designbuilder.co.uk/>

⁶<https://www.equa.se/en/>

⁷<https://www.iesve.com/software>

⁸<http://www.trnsys.com/>

⁹<https://sourceforge.net/projects/trnsys-fmu/>

¹⁰<https://www.trane.com>

¹¹<http://www.esru.strath.ac.uk/Programs/ESP-r.htm>

¹²<https://github.com/ESP-rCommunity/ESP-rSource>

¹³<https://ibpsa.github.io/project1/index.html>

Software	Developer	FMI support	Summary
Modelica Buildings library [165]	IBPSA Project 1 affiliates	FMI ME/CS 1.0 and 2.0	Equation based modelica models for thermal characteristics and HVAC systems. Free open source ¹⁸ .
BRCM Matlab Toolbox[145]	Automatic Control Lab, ETH Zurich	None	Simulates building with equation based component models for thermal characteristics and HVAC systems based on bilinear resistance-capacitance, Free and open source ¹⁹ .
Radiance ²⁰	Lawrence Berkeley Lab	None	Lighting simulation with ray tracing. Can couple with EnergyPlus in OpenStudio. Free and open source ²¹
obFMU[65]	Lawrence Berkeley Lab	FMI	Designed for co-simulation, can be implemented with obXML schema. Free and open source ²² .

Table B.2: List of building component models

when composed together into larger hierarchical system simulations can be optimized within a Modelica simulation environment with symbolic manipulation and use of application specific solvers [161]. There have also been reports showing that the development of these models is less time consuming and easier to debug [162]. An accuracy comparison between a small EnergyPlus building model and Modelica model in [53] shows less than 1% difference at maximum for indoor air temperature. A similar comparison of a BRCM and EnergyPlus model shows a difference within 0.5°C over a 5 day test simulation [145].

It should be noted that the Modelica Buildings Library with the support of IEA EBC Annex 60 is the base of several other open source research-driven modelica building modeling libraries together including: AixLib¹⁴ from RWTH Aachen University[106], BuildingSystems¹⁵ from UdK Berlin, IDEAS¹⁶ from KU Leuven, and BuildSysPro¹⁷ from EDC[125]. As previously mentioned the obXML and obFMU following the FMI standard are presented to solve interoperability issues for simulation [65]. However, the modelling capabilities are extremely limited.

B.4 Hierarchical Simulation Environments

Beyond building simulation is the simulation environment, also sometimes called simulation manager or master, that must co-simulate the building, additional disturbances (such as occupant behaviour), and the control system. In our case the control system includes additional actuation models for the building for MPC. The building model can also be a whole building simulation

¹⁴<https://github.com/RWTH-EBC/AixLib>

¹⁵<https://github.com/UdK-VPT/BuildingSystems>

¹⁶<https://github.com/open-ideas/IDEAS>

¹⁷<https://github.com/edf-enerbat/buildsyspro>

¹⁸<https://github.com/lbl-srg/modelica-buildings>

¹⁹<http://www.brcm.ethz.ch/doku.php>

²⁰<http://radsite.lbl.gov/radiance/HOME.html>

²¹<https://github.com/NREL/Radiance>

²²<https://behavior.lbl.gov/?q=node/4>

package coupled with component models. Defining the input and output couplings between simulation sub-models in a hierarchical way makes use of modern software developments to give greatest flexibility in simulation design. A list of available simulation environments is given in table B.3.

The Building Control Virtual Test Bed (BCVTB) has unique interfaces for FMI ME/CS 1.0 and 2.0 as well as EnergyPlus, Matlab, Simulink, Modelica models, and hardware protocols such as BACnet. However the BCVTB project is not actively developed with the latest activity from 2016. The same development team is now working on the Modelica Buildings Library which has had recent major releases and is actively developed. Similarly, Spawn of EnergyPlus (SOEP)³⁵ is planned as successor to BCVTB and is in specification development. The MLE+ Toolbox serves a similar function as BCVTB and allows for greater use of Matlab, however has been inactive for longer and is not as full featured. In any case simulation of occupant behavior would need to be implemented separately.

B.5 Discussion of Building Modelling Platforms

In practice there are many possible solutions to scalable and extensible building simulation. When considering applications in model-based building control design a good account is given in [11], the authors here note only Modelica based modeling has the capability for advanced control design and rich building thermodynamics models. With consideration to occupant behaviour models in building simulation programs another account is given in [67], the authors of which also propose the obFMU using the FMI standard. Driven largely by the IEA EBC Annex 60 (now IBPSA Project 1) there have been many recent building modeling software development projects with Modelica and other FMI compliant models. Modelica models provide the greatest support for stand-alone components within a building model and also interfaces for non-linear solvers. For these reasons a JModelica, which focuses on Modelica equation based models, based modeling platform is investigated further for implementation. Some other notable examples of building simulation and optimal control software are mentioned here. EnergyPlus and Matlab coupled within the BCVTB in [120] and [149]. EnergyPlus coupled with the Matlab GPML library used in [71]. The authors in [75] show how Modelica can be used to simplify creation of linear HVAC models for MPC using the Modelica Buildings Library. Also, [14] shows a method to reduce the average computation time for numerically solving nonlinear MPC problems. Using Dymola [135] present implementations for standardised building control functions using existing building component modelica models. Finally [133] uses HVAC models built using the Modelica Buildings Library can be solved using multi-agent systems.

²³<https://simulationresearch.lbl.gov/bcvtb>

²⁴<https://github.com/lbl-srg/bcvtb>

²⁵<http://www.jmodelica.org/>

²⁶<https://www.3ds.com/products-services/catia/products/dymola/>

²⁷<https://openmodelica.org/>

²⁸<https://github.com/OpenModelica>

²⁹<http://bauklimatik-dresden.de/nandrad/>

³⁰<https://github.com/lbl-srg/MPCPy>

³¹<https://sourceforge.net/p/fmipp/code/ci/master/tree/>

³²<https://bitbucket.org/account/user/mosaik/projects/PROJ>

³³<https://ch.mathworks.com/products/simulink.html>

³⁴https://github.com/mlab-upenn/mlep_v1.1

³⁵<https://lbl-srg.github.io/soep/>

Software	Developer	FMI support	Summary
BCVTB ²³	DoE BTO, LBL	FMI ME/CS 1.0 and 2.0	Middleware based on the Ptolemy II framework. EnergyPlus, Radiance, Matlab, and Modelica interfaces. Free open source ²⁴ .
JModelica[4]	Modelon AB and Department of Automatic Control, Lund University	FMI ME/CS 1.0 and 2.0	Free and open source ²⁵ , Python interface for Modelica and FMI simulation, linked to multiple solvers.
Dymola ²⁶	Dassault Systèmes	FMI ME/CS 1.0 and 2.0	Proprietary closed source, multiple language interfaces for Modelica and FMI simulation.
OpenModelica ²⁷	Open Source Modelica Consortium	FMI ME/CS 1.0 and 2.0	Free and open source ²⁸ , multiple language interfaces for Modelica and FMI simulation.
NANDRAD ²⁹	Institute for Building Climatology, TU Dresden	FMI ME/CS 2.0	Developed for large building simulation and compatibility with Modelica models. In experimental development. Closed source.
MPCPy[22]	Lawrence Berkeley National Laboratory	FMI ME/CS 1.0 and 2.0	Lightweight python API for MPC using FMI. Based on JModelica PyFMI core for FMI interface, free and open source ³⁰
Mosaik[136]	Oldenburg Institute for Information Technology	FMI ME/CS 1.0	Python based API for co-simulation developed for energy grids. FMI interface through FMI++ ³¹ . Free and open source ³² .
Simulink ³³	The MathWorks, Inc.	FMI ME/CS 1.0 and 2.0 (import only)	Model-based design and simulation. Supports Matlab, legacy for C and C++. Proprietary closed source.
MLE+ Toolbox [18]	mLAB, University of Pennsylvania	FMI ME/CS 1.0 and 2.0	Couples EnergyPlus with Matlab in a Matlab run-time environment. Free and open source ³⁴ .

Table B.3: List of available simulation environments

B.6 Building Material Properties

Component	Material	Thickness (mm)	Density (kg/m ³)	Thermal conductivity (W/mK)	Heat Capacity (J/kgK)
Roofs	Asphalt	10	2100	0.70	1000
	Expanded Polystyrene	150	30	0.035	1450
	Concrete	240	2000	1.35	1000
External walls	Plaster	10	1600	0.80	1000
	Expanded Polystyrene	120	30	0.035	1450
	Brickwork	180	1600	0.70	840
Internal walls	Brickwork	120	1600	0.70	840
Ground floor	Hardwood	20	700	0.17	1600
	Expanded Polystyrene	140	30	0.035	1450
	Concrete	200	2000	1.35	1000

Table B.4: Building model thermal properties, material layers listed outer surface to inner surface. Thermal properties from ISO-10456[23].

Appendix C

Additional Simulation Results

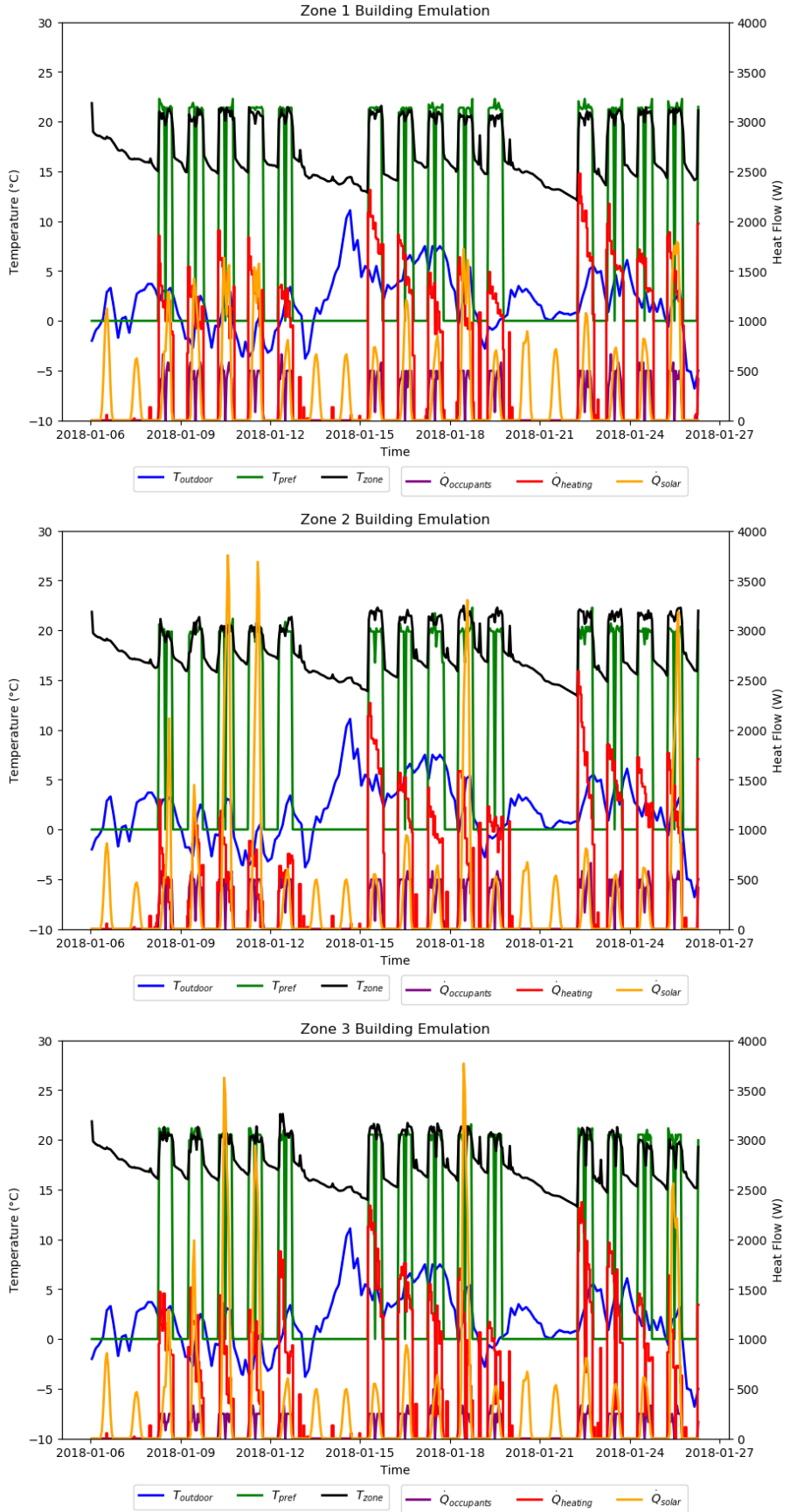


Figure C.1: Simulation results with on-line learned occupancy and thermal preference models for 15 occupants in three zone building, $l_c = l_w = 10$. From top to bottom zone 1, zone 2, and zone 3.

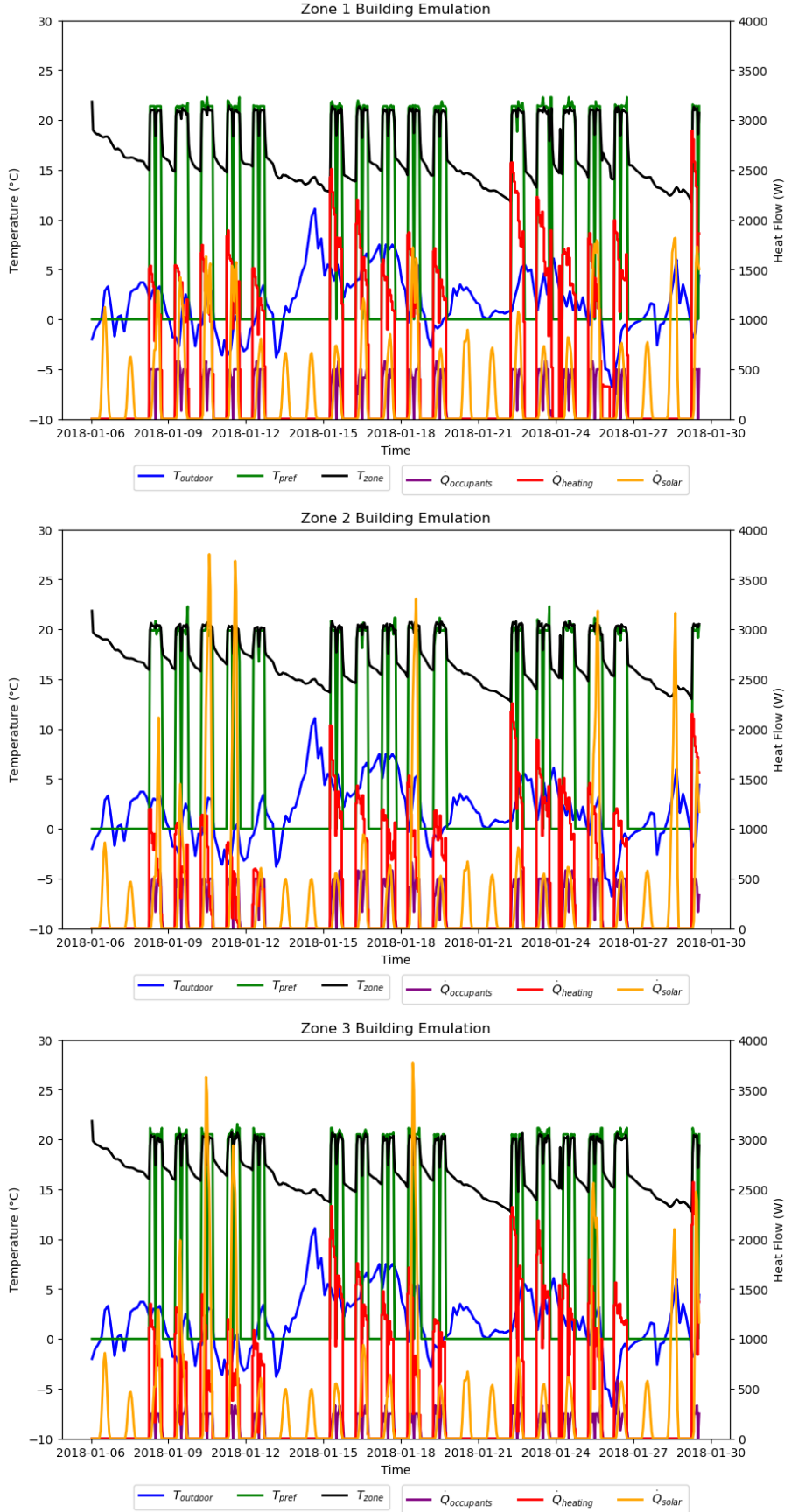


Figure C.2: Simulation results with perfect occupancy and thermal preference models for 15 occupants in three zone building, $l_c = l_w = 10$. From top to bottom zone 1, zone 2, and zone 3.

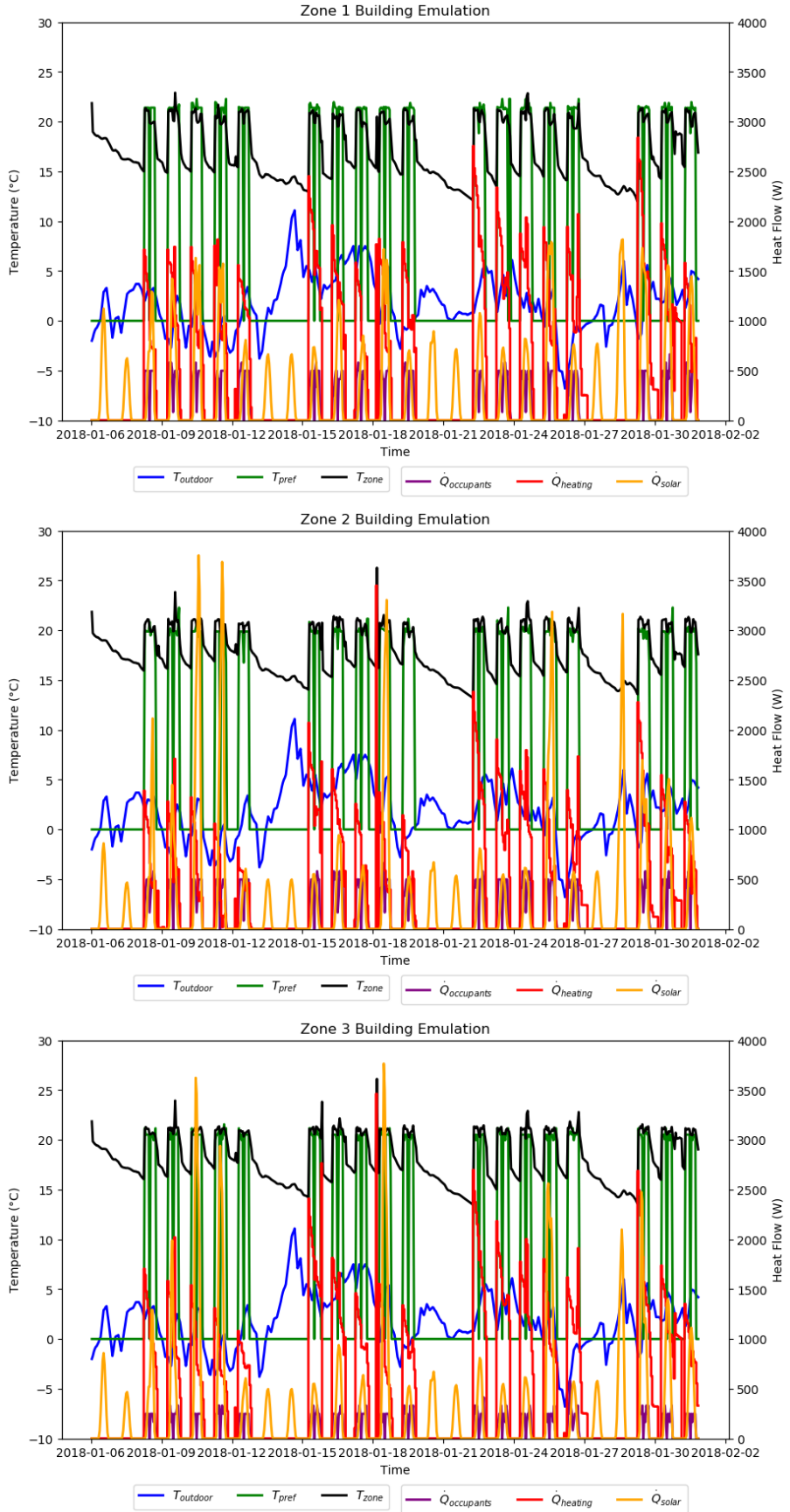


Figure C.3: Simulation results with constant 21°C comfort temperature and schedule based occupancy model for 15 occupants in three zone building. From top to bottom zone 1, zone 2, and zone 3.

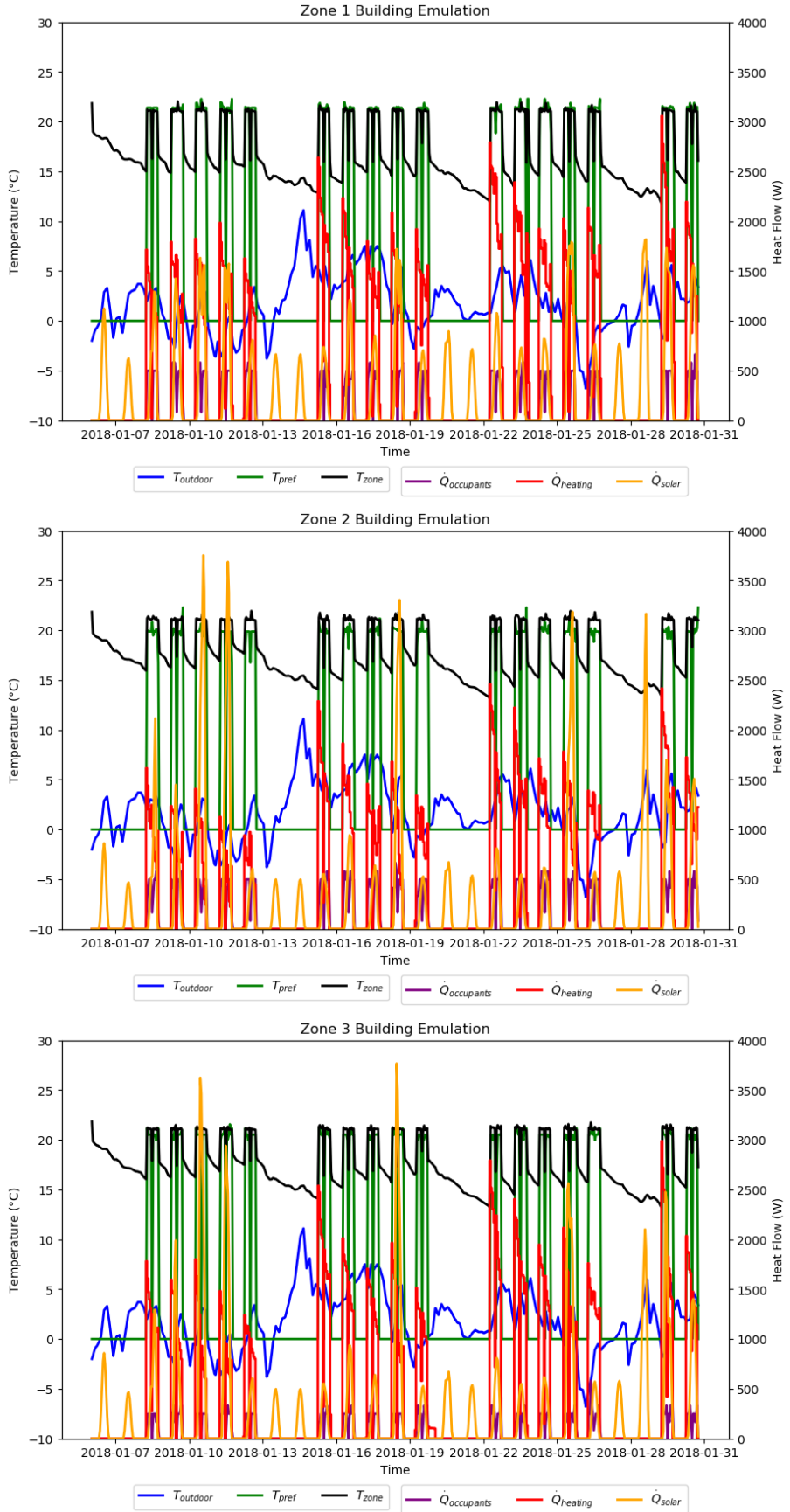


Figure C.4: Simulation results with constant 21 $^{\circ}\text{C}$ comfort temperature and perfect occupancy model for 15 occupants in three zone building. From top to bottom zone 1, zone 2, and zone 3.